AUTO-INHIBITORY MECHANISM FOR THE REGULATION OF A P4-ATPASE

by

Tessy Tereas Sebastian

Dissertation

Submitted to the Faculty of the

Graduate School of Vanderbilt University

in partial fulfillment of the requirements

for the degree of

DOCTOR OF PHILOSOPHY

in

Biological Sciences

May, 2014

Nashville, Tennessee

Approved

Todd R. Graham, PhD

Katherine R. Friedman, PhD

Ela W. Knapik, PhD

Melanie D. Ohi, PhD

James G. Patton, PhD

+JMJ

Ad majorem Dei gloriam

For my beloved family –
Mom, Dad, and Arun

ACKNOWLEDGEMENTS

I've been blessed, over the years, to have had many wonderful individuals who have shaped my love for science and learning. I thank all of these wonderful teachers who have shaped me into the scientist, student, and teacher, that I am today – Mrs. Joyce Schoeneberg, Mr. Tom Cradick, Mr. Paul Trinklein, Mr. David Lay, Mr. Nichols, Dr. Bowman, Mr. Wehling, and Dr. Ron Modras, who gave a shy and timid kid confidence as well as the courage to find her own voice; Dr. Susan Spencer and Dr. John Tavis, who taught me the basic lab skills I use everyday, and introduced me to bench science.

I would also like to thank Dr. Todd Graham, for giving me the opportunity to join his lab and train under him during my time at Vanderbilt. His support, encouragement and enthusiasm for science was key in shaping me into the scientist I am today. I am also grateful to the many colleagues I've had the opportunity to work with, and learn from, during my years at Vanderbilt, especially Dr. Paramasivam Natarajan, Dr. Baby-Periyanayaki Muthusamy, Dr. Xiaoming Zhou, Dr. Peng Xu, and Dr. Ryan Baldridge.

My dissertation committee members, Dr. Jim Patton, Dr. Kathy Friedman, Dr. Ela Knapik and Dr. Melanie Ohi, have given me so much of their time, support, encouragement, and direction over the years; for this I thank them. I've been fortunate, during my graduate career to have collaborated with many excellent scientists, thanks to whom I've expanded my scholarship and technical abilities. Special thanks to Melanie Ohi and Melissa Chambers for direction, help with, and use of electron microscopy; Anne Kenworthy and Charles Day, as well as Lisa Theorin, Gerdi Kemmer, and Thomas

Günther-Pomorski, for collaborating with, and aiding in, the development of protocols for formation of proteo-GUVs.

Funding from the National Institutes of Health has supported all the work described in this thesis, and the Vanderbilt Discovery Grant provided partial funding for me during my graduate career. I was able to attend many national and international conferences, and work in the lab of Thomas Günther-Pomorski (University of Copenhagen, Frederiksberg, Denmark) as a visiting scientist (February, 2012), thanks to funding received from the Gisela Mosig Travel Fund.

I am so appreciative of my wonderful circle of friends, both at Vanderbilt and in Nashville, who have given me so much love, encouragement, support and room to vent; you have become my sisters and brothers. My Uncle Joyce, Aunt Asha, Rose, and Jon – my Nashville family – thank you for your love and care. Over the years, we have become so close. You have made me a member of your family and I will never forget our times together. Finally, I want to thank my family – Mom, Dad and Arun – for being mine. Mom and Dad – you always support and never doubt me. You have made me the woman I am today and I thank God for you everyday. Arun – how can I even begin to describe how much you mean to me, little brother? We have grown up together and been through so much together. You are my best friend. Thank you for being you.

TABLE OF CONTENTS

LIST OF FIGURES

LIST OF TABLES

Table

LIST OF ABBREVIATIONS

TGN	*trans*-Golgi Network
ER	Endoplasmic Reticulum
PM	Plasma Membrane
P4-ATPase	Type IV P-type ATPase or Flippase
TM	Transmembrane Domain
C-tail	C-terminal Tail of Drs2p
R domain	Regulatory Domain
GEF	Guanine Nucleotide Exchange Factor
PS	Phosphatidylserine
PC	Phosphatidylcholine
PE	Phosphatidylethanolamine
SM	Sphingomyelin
PI(4)P or PI4P	Phosphatidylinositol 4-phosphate
TAP_N-Drs2p	N-terminal TAP-tagged Construct of Drs2p
Drs2p-TAP_C	C-terminal TAP-tagged Construct of Drs2p
CBP	Calmodulin-Binding Peptide
TEV protease	Tobacco Etch Virus Protease
C12E8	Polyoxyethylene (8) Dodecyl Ether
C12E9	Polyoxyethylene (9) Dodecyl Ether
CHAPS	3-[(3-Cholamidopropyl)Dimethylammonio]-1-Propanesulfonate
DOPC	1,2-Dioleoyl-*sn*-Glycero-3-Phosphocholine
DOPS	1,2-Dioleoyl-*sn*-Glycero-3-Phosphoserine
NBD-PC	1-Palmitoyl-2-[6-(NBDamino)hexanoyl]-*sn*-glycero-3-Phosphocholine
C6 NBD-PS	1-Palmitoyl-2-[6-(NBD-amino)hexanoyl]-*sn*-glycero-3-Phosphoserine
C12 NBD-PS	1-Palmitoyl-2-[12-(NBD-amino)dodecanoyl]-*sn*-glycero-3-Phosphoserine
Rho-PE	Headgroup labeled Phosphoethanolamine (Lissamine Rhodamine B)
ATP, ATPγS	Adenosine triphosphate, adenosine 5′-*O*-(thiotriphosphate)
WT	Wild-type

CHAPTER I

INTRODUCTION

The plasma membrane of eukaryotes has evolved to be important in its function as a barrier to the outside world. It creates an interface between the interior of the cell and the external environment, and protects the cell against pathogens. Within organisms, the plasma membrane functions as a site of cell signaling some of which is due to the asymmetric nature of its composition. Normally, within the membrane bilayer, phosphatidylserine (PS) and phosphatidylethanolamine (PE) are sequestered to the cytosolic leaflet. Ablation of plasma membrane asymmetry and exposure of these phospholipids can serve as a signal for various biological and regulatory mechanisms, such as platelet activation, apoptosis, and recruitment of macrophages.

Maintenance of the membrane asymmetry of phospholipids in the plasma membrane is of vital importance. A class of proteins called the type-IV P-type ATPases or flippases maintains this asymmetry. These proteins function by flipping phospholipids from one side of the membrane bilayer to the other side in an energy-dependent manner. Furthermore, these flippases play vital roles in vesicle-mediated protein transport (Sebastian, Baldridge, Xu, & Graham, 2012). This introductory chapter will seek to introduce flippases, their family of proteins, trace the origins of their discovery, understand the important roles they play within a cell and in organisms, how they work, and how they're regulated.

The Family of P-type ATPases

P-type ATPases are a large family of membrane proteins that pump heavy metal ions, cations, and phospholipids across a membrane bilayer against their concentration gradient using the energy of ATP hydrolysis. According to the Axelsen and Palmgren nomenclature, they are divided into five groups based on their phylogenetic relationships (sequence alignments) (Axelsen & Palmgren, 1998; Kuhlbrandt, 2004). Type I (or P1) ATPases are heavy metal pumps (ex. K^+ ATPase, Cu^{+2} ATPase), while Type II (or P2) ATPases are cation transporters (ex. sarcoplasmic reticulum Ca^{+2} ATPase (SERCA), Na^+/K^+ ATPase). Type III (or P3) ATPases include the proton pumps (ex. H^+ ATPase, Mg^+ ATPase) and Type V (or P5) ATPases have unknown substrate specificity. Meanwhile, Type IV (or P4) ATPases (ex. Drs2p, ATP8A1) flip phospholipids across the membrane bilayer, are called flippases, and are of primary interest to the work presented in this thesis (Kuhlbrandt, 2004). Figure 1-1 shows the phylogenetic relationships between the P4-ATPases found in yeast (*Saccharomyces cerevisiae*), plants (*Arabidopsis thaliana*), worms (*Caenorhabditis elegans*), and humans (*Homo sapiens*).

Structure and Function

Several of the P-type ATPases have had crystal structures reported, including P1-, P2- and the P3-ATPases (Gourdon et al., 2011; Morth et al., 2007; Pedersen, Buch-Pedersen, Morth, Palmgren, & Nissen, 2007). From these structures, it has become evident that the P-type ATPases have high levels of similarity in their structure and domain organization

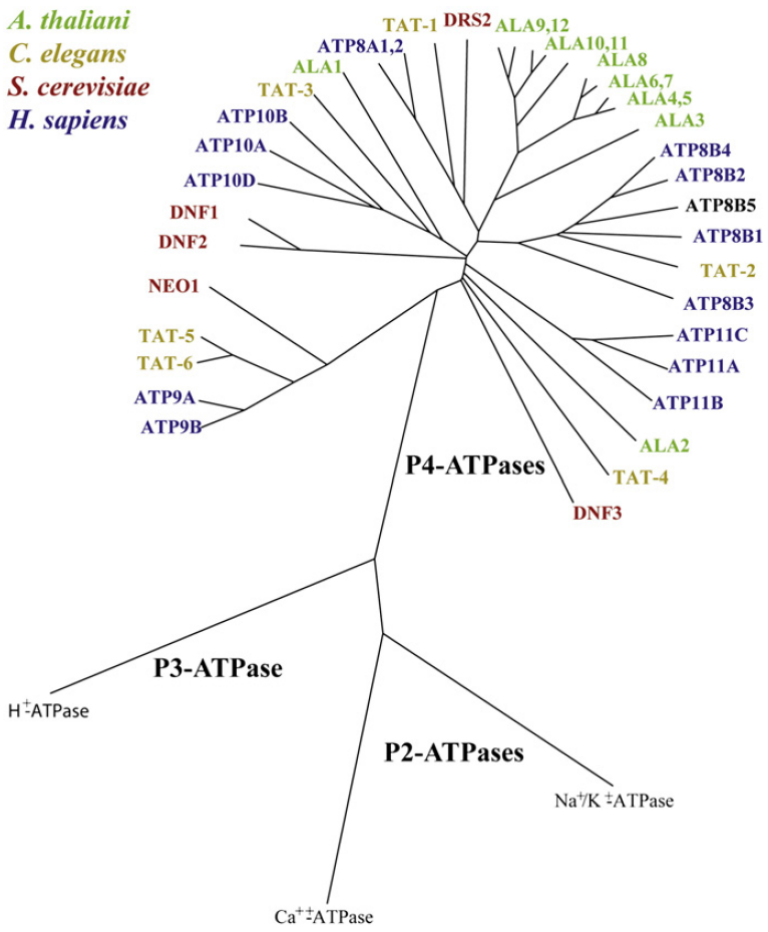

Figure 1-1. Phylogenetic tree showing the relationship between the P4-ATPases of yeast (*S. cerevisiae*), worms (*C. elegans*), plants (*A. thaliana*) and humans (*H. sapiens*). *Image from (Sebastian et al., 2012).*

(Fig. 1-3). The P-type ATPases have four structural domains – the actuator (A) domain, the phosphorylation (P) domain, the nucleotide binding (N) domain and the transmembrane (TM) domain (Fig. 1-2A). The A domain is formed by the N-terminal tail and the cytosolic loop between transmembrane segments 2 and 3. There is a large cytosolic loop between TM 4 and 5, which forms both the P and N domains (Toyoshima, 2009; Toyoshima, Nakasako, Nomura, & Ogawa, 2000). Most P-type ATPases, especially the P4-ATPases (based on homology modeling) have 10 transmembrane segments. Additionally, several of these proteins have long N- and C-terminal extensions that can

form additional regulatory R-domains (Au, 1987; Hwang, Harper, Liang, & Sze, 2000; P. James et al., 1988; Palmgren, Larsson, & Sommarin, 1990; Palmgren, Sommarin, Serrano, & Larsson, 1991; Portillo, de Larrinoa, & Serrano, 1989; Rasi-Caldogno, Carnelli, & De Michelis, 1992, 1993, 1995). The influence of an R-domain (the C-terminal tail) on Drs2p will be the focus of Chapter 2 of this thesis.

A

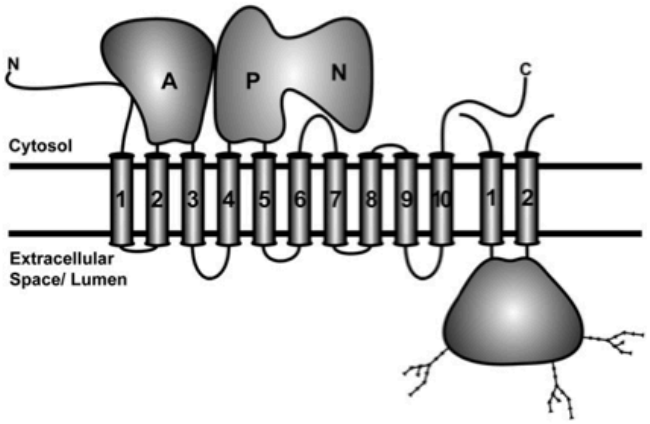

B

α subunit	β subunit	Reference
Drs2	Cdc50	[4]
Dnf1	Lem3 (Ros3)	[4]
Dnf2	Lem3 (Ros3)	[20]
Dnf3	Crf1	[20]
Neo1	None detected	
TAT-1	CHAT-1	[10]
ALA2	ALIS1, ALIS3, ALIS5	[21]
ALA3	ALIS1, ALIS3, ALIS5	[11]
ATP8A1	CDC50A (also CDC50B?)	[5, 6]
ATP8A2	CDC50A	[6]
ATP8B1	CDC50A, CDC50B	[22]
ATP8B2	CDC50A, CDC50B	[5, 6]
ATP8B4	CDC50A (also CDC50B?)	[5, 6]
ATP9A	None detected	[24]
ATP9B	None detected	[24]
ATP10A	CDC50A	[24]
ATP10B	CDC50A	[24]
ATP10D	CDC50A	[24]
ATP11A	CDC50A	[24]
ATP11B	CDC50A	[24]
ATP11C	CDC50A	[24]
LdMT	LdRos3	[23]

Figure 1-2. Structure of P4-ATPase (A) and association with Cdc50 family members (B). *Image from ((Sebastian et al., 2012).*

SERCA was the first of the ATPases to be crystallized (Fig. 1-3) and structures have been reported in nine different conformations representing most, if not all, of the

conformations of the protein during its catalytic reaction cycle (Toyoshima & Mizutani, 2004; Toyoshima et al., 2000; Toyoshima & Nomura, 2002; Toyoshima, Nomura, & Tsuda, 2004). This has led to a clearer understanding of the reaction cycle in which these proteins are involved. During their catalytic cycle, the P-type ATPases form an aspartyl-phosphate intermediate, which has led to their being called "P-type". The catalytic cycle is called the Post-Albers cycle, after Robert Post and R. Wayne Albers, who were the first to describe this mechanism (Albers, Fahn, & Koval, 1963; Charnock & Post, 1963; Post, Hegyvary, & Kume, 1972; Post & Jolly, 1957; Post & Sen, 1965; Post, Sen, & Rosenthal, 1965). Although Post and Albers initially described the mechanism of action of the Na^+/K^+ ATPase, this description has since been extended to other P-type ATPases as well.

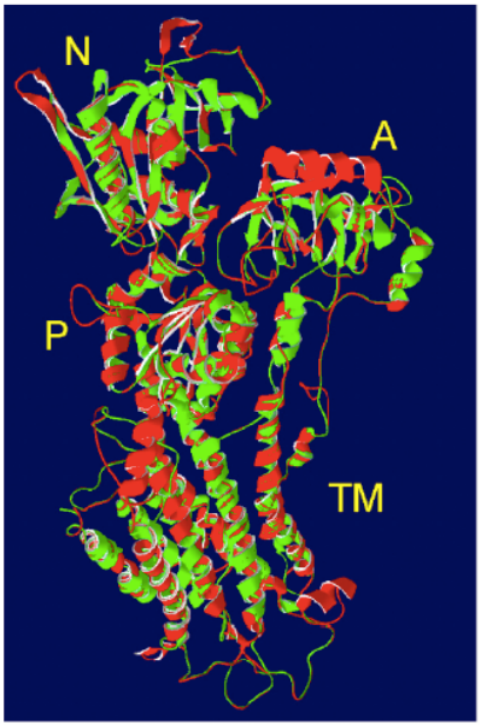

Figure 1-3. Sequence of Drs2p threaded onto crystal structure of SERCA1p. Drs2p is a yeast P4-ATPase, and SERCA1p is a cation pump of the P2-ATPase family. A, P, N, TM indicate the different structural domains of the protein. *Image from Zhou, et al. (Book chapter, Wiley).*

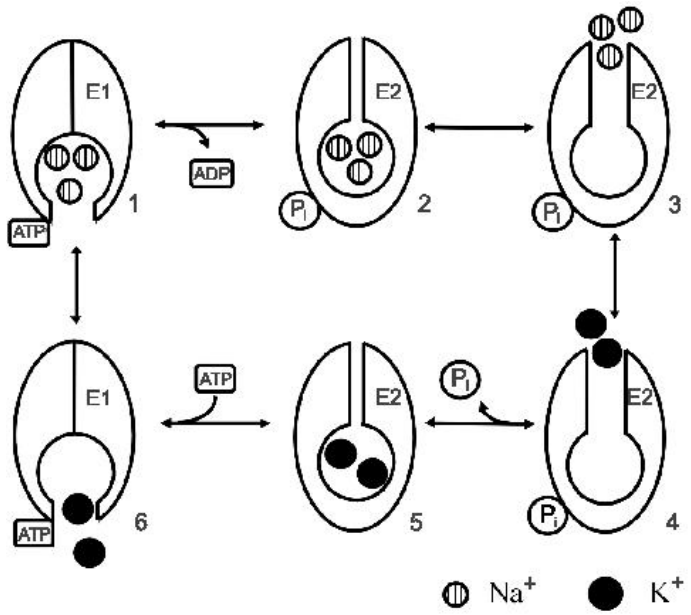

Figure 1-4. Model of the Post-Albers cycle. This image shows the taking up and release of 3 Na^+ ions to the lumen and the taking up and release of 2 K^+ ions to the cytosol. The different steps of the cycle, and ATP hydrolysis are also indicated. *Image from http://aups.org.au/Proceedings/42/19-28/.*

The pump cycles between two main conformations, E1 and E2, that are controlled by substrate and nucleotide binding, along with the addition and release of a phosphate group (Fig. 1-4). In the E1-ATP step, three Na^+ ions, from the cytosol, bind a high affinity site within the transmembrane domain of the protein (specifically, a binding pocket surrounded by TM segments 4, 5, 6, 7, and 9). The interaction of the Na^+ ions with this site induces the N domain, which interacts with a molecule of Mg^{+2}-ATP, to undergo a conformational change that brings the γ-phosphate to closer proximity with the phosphorylation site in the P-domain. This allows transfer of the γ-phosphate, from the ATP to the conserved aspartate residue (Asp369). At this point of the cycle, i.e. E1P-ADP, the substrate binding sites (within the transmembrane domain) are oriented so that they are not accessible from either side of the membrane. Furthermore, the Na^+ ions are in an occluded state. Then, the A domain rotates to bring the TGES motif, located within the actuator domain, closer to the phosphorylated aspartate. At the same time,

ADP is released. This step produces the E2P conformation, and also involves the opening of the membrane domain to the extracellular (or lumenal) side of the membrane and the loss of the high affinity Na^+ binding sites. At this point, the three Na^+ ions are quickly released, against their concentration gradient, and 2 K^+ ions quickly take their place within the open substrate binding site that has now acquired high affinity for K^+. The aspartyl phosphate residue is hydrolyzed by the TGES motif, access from either side of the membrane to the substrate binding site is obstructed, and this moves the ATPase from the E2-P to the E2 state. Finally, re-orientation of the A and N domains, as well as dissociation of the Mg^{+2} and an inorganic phosphate molecule, resets the protein back to the E1 state. Subsequently, the K^+ ions are released to the cytosol (against the gradient) because the substrate binding site is now open and reorients into the Na^+-binding conformation (Toyoshima, 2009).

While the other members of the P-type ATPase family have conserved binding pockets that can easily translocate small ions, the major question remained – how can P4-ATPases translocate large phospholipid molecules? Recent work, from the Graham lab, has posited new insight into the mechanism by which P4-ATPases are able to translocate phospholipids during their catalytic cycle. Rather than using the canonical substrate-binding site defined for cation pumps, the P4-ATPases have evolved the use of a new translocation pathway using the first four TM segments. In addition to identifying the residues, within TM4, responsible for substrate specificity, a novel two-gate mechanism for phospholipid flip was proposed (Baldridge & Graham, 2012; Baldridge & Graham, 2013). Over 20 residues have been identified as sites that aid in the translocation of the phospholipid at the two gates. This mechanism suggests that the binding of the

phospholipid (from the exofacial leaflet), at the entry gate, likely occurs during the transition of the protein from E1-P to E2-P. The phospholipid is then loaded into the exit gate at E2-P. Dephosphorylation, and transition back to the E1 conformation would eject the phospholipid into the cytosolic leaflet (Baldridge & Graham, 2013).

Dnf1p and Drs2p are both yeast flippases that cycle between the *trans*-Golgi network (TGN), plasma membrane and early endosomes. Drs2p is usually found in the TGN and early endosomes while Dnf1p has primarily plasma membrane and early endosomal localization. While they are quite similar in overall structure, cellular localization and mechanism of function, they differ in their phospholipid (substrate) preferences. Dnf1p preferentially flips PC while Drs2p preferentially flips PS. To identify residues that would confer substrate specificity for each of these P4-ATPases, several Dnf1p chimeras were created with sections of the Drs2p protein swapped into the Dnf1p structure (Baldridge & Graham, 2012). Swapping TM segments 3 and 4 from Drs2p into Dnf1p conferred PS substrate preference to Dnf1p. Further analysis of these segments revealed that a single mutation, Tyr618 to Phe (in TM4) is sufficient to confer a change in substrate preference in Dnf1p. The complementary mutation (Phe511 to Tyr) in TM4 of Drs2p also altered the substrate specificity of Drs2p from PS to PC (Baldridge & Graham, 2012).

Moreover, through additional genetic screens and directed mutagenesis experiments, many residues that further contribute to substrate preference and specificity were identified. It was discovered that these residues group at two interfacial regions that flank TM segments 1-4. These data suggest there are two regions of importance that

determine substrate specificity and allow for the flip of a bulky phospholipid substrate during the catalytic cycle of the protein; these are called the entry and exit gates. The phospholipid is initially selected at the entry gate and is transferred to the exit gate to allow the head group to exit to the opposing leaflet (Baldridge & Graham, 2013).

The Family of P4-ATPases and the Cdc50 family of proteins

The first P4-ATPase sequence to be published was Drs2p (from yeast). From sequence comparisons, performed at that time, it was thought to be a Ca^{+2} ATPase (Ripmaster, Vaughn, & Woolford, 1993). Soon afterwards, the sequence for bovine ATPase II (ATP8A1) was published and found be almost 50% identical to the sequence of Drs2p (Tang, Halleck, Schlegel, & Williamson, 1996). As a result, Drs2p and ATP8A1 were recognized as the founding members of a new family of P-type ATPases (Axelsen & Palmgren, 1998). While they are not found in prokaryotes, the P4-ATPases have several members in each of the sequenced eukaryotic genomes. Yeast have five P4-ATPases. They are Drs2p (Defect in Ribosome Synthesis), Dnf1p, Dnf2p and Dnf3p (Drs2p Neo1p Family ATPases), and Neo1p (Neomycin resistance). Meanwhile, *C. elegans* has six, designated TAT-1 through TAT-6 (for Transbilayer Amphipath Transporter). Mammals have at least 14 (ATP8A1 to ATP11C, also see Fig. 1-1 and 1-2). Many of these proteins (considered the α subunit) associate with a β subunit (Bryde et al., 2010; B. Chen et al., 2010; Furuta, Fujimura-Kamada, Saito, Yamamoto, & Tanaka, 2007; Lopez-Marques et al., 2010; Paulusma et al., 2008; Perez-Victoria, Sanchez-Canete, Castanys, & Gamarro, 2006; Poulsen et al., 2008; Saito et al., 2004; Takatsu et al., 2011; van der Velden et al., 2010).

Much work has shown that P4-ATPases require co-chaperones for proper exit from the endoplasmic reticulum (ER) (Saito et al., 2004). These co-chaperones, members of the Cdc50p family of proteins (Cdc50p, Lem3p, and Crf1p), are considered to be β subunits to P4-ATPases. In yeast, there are three members of this family – Cdc50p (which associates with Drs2p), Lem3p/Ros3p (which associates with Dnf1p and Dnf2p), and Crf1p (which associates with Dnf3p). Both mammalian and worm P4-ATPases also have 3 CDC50 members – CDC50A, CDC50B, and CDC50C in mammals, W03G11.2, R08C7.2a (CHAT-1), and F20C5.4 in *C. elegans* (Fig. 1-2). There may be several reasons why there are so few β subunits compared to the α subunits. The first is likely functional redundancy; i.e. several α subunits can share a single β subunit. Another reason is that some P4-ATPases (like Neo1p in yeast) do not have a β subunit associated with it (Bryde et al., 2010; S. Chen et al., 2006; Paulusma et al., 2008; Poulsen et al., 2008; Saito et al., 2004; Takatsu et al., 2011; van der Velden et al., 2010).

The β subunits for the yeast P4-ATPases were initially discovered in genetic screens looking at defects in phospholipid translocation and membrane asymmetry (Radji, Kim, Togan, Yoshikawa, & Shirahige, 2001). More recently, these findings have been extended to *C. elegans*. A forward genetic screen, based on the loss of PS asymmetry, uncovered mutations in both CHAT-1 and TAT-1, which are Cdc50p and Drs2p homologs respectively (B. Chen et al., 2010). Furthermore, parallels have been drawn between the Drs2p-Cdc50p complexes and the Na^+/K^+ and H^+/K^+ ATPases, which, also possesses β (and in some cases γ) subunits (Geering, 2001; Kuhlbrandt, 2004).

The CDC50 family of proteins has two transmembrane segments, as well as a large glycosylated extracellular domain (Fig. 1-2). The essential interaction between the P4-ATPases and their co-chaperones was discovered by the Tanaka lab; they showed that absence of the β subunit, Cdc50p, caused ER accumulation of Drs2p. Similarly, the deletion of Lem3p, caused ER accumulation of Dnf1p and Dnf2p. This interaction is also reciprocal - deletion of Drs2p caused Cdc50p accumulation in the ER. In addition to co-localizing with their respective α subunits, co-immunoprecipitation experiments have shown that the Cdc50p chaperones physically interact with the P4-ATPases. The Tanaka group also observed similar phenotypes in mutants of the P4-ATPases and mutants of Cdc50 family proteins (S. Chen et al., 2006; Furuta et al., 2007; Saito et al., 2004). This suggests functionally essential interactions exist between the α and β subunits. Conditional mutants of Cdc50p have also been identified. These mutants maintain their ability to bind Drs2p, but lose function *in vivo* at non-permissive temperatures. From these experiments, it was discovered that, when Cdc50p mutants lose activity, the Cdc50p-Drs2p heterodimer is functionally defective (Takahashi, Fujimura-Kamada, Kondo, & Tanaka, 2011). This implies that Cdc50 proteins play important roles in the catalytic cycles of P4-ATPases.

When the yeast P4-ATPase, Drs2p, was purified and reconstituted into liposomes, it was discovered that there was a sub-stoichiometric amount of Cdc50p present in these samples (Zhou & Graham, 2009). An argument was made that the low levels of flippase activity detected in these preparations was due to the small amounts of Cdc50p. The assessment was that higher levels of Drs2p-Cdc50p complexes within a sample would generate higher levels of activity because it is thought that Cdc50p plays a major role in

Drs2p activity. When the Molday lab used a dual affinity approach to purify ATP8A2 complexed with CDC50A (using monoclonal antibodies which recognized each of these proteins), they obtained samples that had a robust ATPase and flippase activity – especially when compared to the values obtained for Drs2p (Coleman & Molday, 2011). However, since they didn't assay the ATP8A2 monomer (in the absence of CDC50A), it is still uncertain how much of a role CDC50A plays in the activity of the P4-ATPase.

While recent evidence from plants and human P4-ATPase experiments suggest that the β subunit is not essential for substrate specificity or proper localization of the flippase, it has been shown that, in both yeast and human complexes, β subunits prefer to bind the E2-P form of the P4-ATPases. Furthermore, the Molday group, created chimeras between CDC50A and CDC50B which enabled them to map regions (both the TM and exocytoplasmic domains) on CDC50A that were: (a) critical for association with ATP8A2 and, (b) essential for creating a functional complex. They also discovered that the N-terminal cytosolic segment of CDC50A is important in the reaction cycle of the P4-ATPase (Coleman & Molday, 2011). As more evidence is being uncovered, it is obvious that the Cdc50 family of proteins plays important roles in the activity of P4-ATPases. However, the extent to which these proteins influence flippase activity and play regulatory roles, especially interactions with other proteins during vesicular trafficking, is still open for discussion.

Impact of P4-ATPases on Physiology

While P4-ATPases are essential for yeast cell viability (Hua, Fatheddin, & Graham, 2002), there are also several biological processes and disorders that have been linked to P4–type ATPases. On an organ and organismal level, this protein class plays a major role in promoting and maintaining optimal health. For example, mutations in human ATP8B1 (or FIC1) cause progressive familial intrahepatic cholestasis (PFIC) or benign recurrent intrahepatic cholestasis (BRIC) (Bull et al., 1998; Folmer, Elferink, & Paulusma, 2009). These severe diseases cause liver failure due to defects in bile secretion, and patients often need liver transplants to stay alive. The liver cells lose phospholipid asymmetry and canalicular membranes become more sensitive to bile salts. The loss of resistance enhances the extraction of cholesterol from the cells, which eventually leads to cholestasis. This is one example of a disease directly attributed to a defect in P4-ATPase expression or function. Meanwhile, several other diseases states and defects are linked to mutations in P4-ATPases. For example, deficiencies in *Atp8b1* are associated with progressive hearing loss due to cochlear hair cell degeneration (Stapelbroek et al., 2009).

As mentioned, P4-ATPases are responsible for creating and maintaining membrane asymmetry – especially at the plasma membrane. Exposure of PS (which is normally sequestered in the cytosolic leaflet of the plasma membrane) to the extracellular leaflet is critical as a signaling mechanism in apoptosis and blood clotting reactions (Zwaal, Comfurius, & Bevers, 2005). Phagocytes recognize exposed PS and proceed to engulf and kill the cell. At an organismal level, experiments demonstrating this were performed in *C. elegans* (Darland-Ransom et al., 2008). When the ATP8A1 ortholog, TAT-1, is

ablated, PS is exposed to the cell surface and these cells are removed by mechanisms dependent on proteins responsible for the recognition and engulfment of PS-exposing cells. Mutations in ATP8A2, which has high expression levels in the brain, retina, and testes, have been implicated in axonal degeneration (and thus, neurodegenerative diseases) in mice (Cacciagli et al., 2010; Coleman, Kwok, & Molday, 2009). These observations have also been made in human patients.

P4-ATPases are also linked to B-cell development (Atp11c) (Siggs et al., 2011; Yabas et al., 2011), neuronal growth and maturation (Atp8a2) (Q. Xu et al., 2012), hippocampal-dependent learning (Atp8a1) (Levano et al., 2012), cell migration (Atp8a1) (Kato et al., 2013), and spermatogenesis (Atp8b5/FetA) (P. Xu et al., 2009). In mice, mutations in Atp10a (also known as Atp10c) are implicated in obesity and type II diabetes phenotype (M. Dhar et al., 2000). Atp10a-deficient mice also display hyperinsulinemia and are insulin-resistant (M. S. Dhar et al., 2004). Recently, *ATP10D* has been linked to lipid metabolism deficiencies, and this association has been extended to suggest risks for myocardial infarction (Flamant et al., 2003; Hicks et al., 2009). In *C. elegans*, *tat-2* through *tat-4* become essential for worm reproduction during periods of sterol starvation (Lyssenko, Miteva, Gilroy, Hanna-Rose, & Schlegel, 2008).

In plants, MgPDE1 and MgAPT2, which are P4-ATPases of the rice blast fungus, *M.grisea*, are required for its pathogenicity, especially root infectivity by the fungus (Balhadere & Talbot, 2001). Knockdown of *Arabidopsis thaliana* ALA1 is associated with cold resistance of the plant and these plants are much smaller than wild-type plants (Gomes, Jakobsen, Axelsen, Geisler, & Palmgren, 2000). Mutations in *ALA3* are

responsible for malformation of roots, pollen tubes and trichome patterning. Basically, trafficking defects cause the root cells to be unable to secrete the appropriate proteins and establish proper border cells to successfully interact with the soil environment.

The mechanism underlying the correlation between these biological phenomena and P4–ATPases is yet to be elucidated, but the impact of this class of proteins on life is unquestionable. Physiologically, defects in P4-ATPases can cause many disease conditions. But, the two main functions of the P4-ATPases, at a cellular level, include their role in the creation and establishment of membrane asymmetry as well as their influence in vesicle-mediated protein trafficking. These topics will be further explored in the following sections.

Function of P4-ATPases in Cells – Membrane Asymmetry and Membrane Curvature

The plasma membrane, Golgi, and endosomal membranes of eukaryotic cells are asymmetric structures composed of different phospholipids on each of its two membrane monolayers. Phosphatidylserine (PS), and phosphatidylethanolamine (PE) are mostly sequestered to the cytosolic or inner membrane, while phosphatidylcholine (PC) and sphingolipids are sequestered to the extracellular or lumenal (outer) membrane. The unique feature of this asymmetry is that each of the two membrane surfaces provide differing environments, both chemical and electric (net charge), which allow for varying protein functions at the membrane. The plasma membrane is the site of important cell-cell interactions, and the site of interactions for soluble signaling proteins with the membrane surfaces. Many important signaling cascades are initiated at the plasma

membrane. Disruption of plasma membrane asymmetry, as previously described, is a hallmark of physiological process such as apoptosis and blood clotting. There is also evidence that controlled loss of plasma membrane asymmetry plays a role in cellular process such as host-pathogen interactions and cytokinesis (Emoto et al., 1996; Mercer & Helenius, 2008; Zwaal & Schroit, 1997).

Phospholipids are amphiphilic molecules with a hydrophilic head group and hydrophobic tails. Due to this chemical structure, they are able to freely diffuse within a membrane bilayer, but very rarely flip-flop spontaneously between membrane leaflets. The reason is that the energy needed for the hydrophilic head group to traverse the hydrophobic environment that exists between the membrane leaflets is great. Therefore, this is a phenomenon that occurs rarely (Kornberg & McConnell, 1971). Normal maintenance of the asymmetry of phospholipids in the plasma membrane is extremely important. So the question remains – how is membrane asymmetry, present in most eukaryotic membranes, created and maintained?

At the ER, the site of phospholipid synthesis, the lipid bilayer is symmetric, due to the presence of a scramblase – an energy-independent protein that allows for non-specific bidirectional movement of lipids. Recent work has identified one of the scramblases involved in phospholipid scrambling (and PS exposure) at the plasma membrane. This protein, called TMEM16F, was identified in a mouse B-cell line as displaying Ca^{+2}-dependent scramblase activity (Suzuki, Umeda, Sims, & Nagata, 2010). Mutations in this scramblase were identified in patients with Scott's syndrome (a rare bleeding disorder where there is a lack of scramblase activity) (Castoldi, Collins, Williamson, & Bevers,

2011; Suzuki et al., 2010). When TMEM16F was reconstituted and assayed for activity, it was found that, as a result of a Ca^{+2} influx, scramblase activity was initiated. Furthermore, two other proteins from the TMEM16 family, also purified and reconstituted, failed to show such scramblase activity (Malvezzi et al., 2013). Meanwhile, in genetic studies, TMEM16C, TMEM16D, TMEM16G, and TMEM16J were also implicated in having phospholipid scramblase activity, while the other TMEM16 family members were identified as Cl^- channels (Suzuki et al., 2013). Thus, scramblases are one protein class that mediates phospholipid transfer, however they are not involved in the creation of membrane asymmetry.

Floppases and flippases are the other two protein classes involved in the creation of membrane asymmetry. The difference is that these proteins mediate energy-dependent, unidirectional movement of phospholipids. While floppases "flop" lipids from the cytosolic to the extracellular (or lumenal) leaflet, flippases (the P4-ATPases) "flip" lipids from the extracellular to the cytosolic leaflet. The class of proteins responsible for floppase activity is the ABC transporters, and they are found both in prokaryotic and eukaryotic membranes (Juliano & Ling, 1976). In eukaryotes, ABCA1, ABCA2, ABCB4, and ABCG1 are all capable of flopping PC and cholesterol across the membrane, while ABCG5 and ABCG8 displays substrate specificity for sterol movement. Another class of ABC transporters are involved in multi-drug resistance and bile secretion (MDR proteins) (Doerrler & Raetz, 2002; Dong, Yang, & McHaourab, 2005). MsbA is an ABC transporter (closely related to the MDR family) and found in *E.coli*. It is responsible for translocating lipidA moieties of lipopolysaccharides from the cytosolic to the

periplasmic membrane (Dean & Annilo, 2005). Overall, the ABC transporters are capable of translocating a wider range of substrates compared to the P4-ATPases.

Flippases, meanwhile, have more specific substrate specificities and move PS and PE unidirectionally towards the cytosolic leaflet (Alder-Baerens, Lisman, Luong, Pomorski, & Holthuis, 2006; Gomes et al., 2000; Natarajan, Wang, Hua, & Graham, 2004; Pomorski et al., 2003; Tang et al., 1996). Initially, it was unclear if flippases played a direct role in the translocation of phospholipids at membranes. Deletion of *DRS2* caused defects in PS translocation (Tang et al., 1996), although later reports suggested this influence was minimal (Marx et al., 1999; Siegmund et al., 1998). Furthermore, discovery of trafficking deficiencies in these mutants also suggested that P4-ATPases had indirect roles in phospholipid translocation. Subsequent work showing that inactivation of Drs2p causes an ablation in flippase activity in purified Golgi membranes (Natarajan et al., 2009; Natarajan et al., 2004), as well as genetic studies demonstrating a function for Dnf1p and Dnf2p in flippase activity (towards NBD-labeled PC and PE) at the plasma membrane (Pomorski et al., 2003), cemented the idea that these proteins were likely flipping phospholipids. Plasma membrane flippase activity, meanwhile, was also demonstrated in several plant (ALA1, ALA2, and ALA3), and mammalian (FetA, Atp8b1) ATPases (Poulsen et al., 2008; P. Xu et al., 2009).

Another mechanism for concentrating PS in the cytosolic leaflet of the plasma membrane is by direct transfer of PS, from its site of synthesis (at the ER), to the PM. New evidence has been presented for the role of oxysterol-binding proteins (OSBP's) in this lipid translocation of PS. In yeast, Osh6 and Osh7 (oxysterol-binding protein homologs) have

been discovered to have specificity for PS and participate, *in vivo*, in transporting PS from the ER to the plasma membrane, as well as maintaining PS homeostasis. This is some of the first evidence of non-vesicular transport of a phospholipid. Additionally, ORP5 and ORP10 (human OSBPs) have been identified as sharing a similar preference for PS (Maeda et al., 2013). Because of the role of PS sequestration as a hallmark membrane asymmetry (the loss of which serves as an important signaling mechanism), this discovery opens new avenues of research into several disease states and associated therapies, including cancer and metabolic diseases.

The first evidence that a protein was responsible for translocating phospholipids between the two leaflets of a membrane bilayer and that this action was responsible for the asymmetric composition of membranes came with the discovery of the aminophospholipid translocase (APLT) by Seigneuret and Devaux (Seigneuret & Devaux, 1984). When different phospholipids were added exogenously, to human red blood cells, it was observed that PS and PE were preferentially translocated to the cytosolic leaflet of the red blood cell, which resulted in shape changes to the cell (Fig. 1-5). For instance, when spin-labeled PC was added to the extracellular membrane, there was an increase in the surface area of the extracellular membrane (echinocyte shape) and the membrane appears swollen. However, when a spin-labeled PS was added to the extracellular membrane, the red blood cells went from the normal discocyte shape to the echinocyte shape (due to addition of exogenous phospholipid to the outer leaflet) and the quickly to a crenated stomatocyte shape (Fig. 1-5) (Daleke & Huestis, 1985; Seigneuret & Devaux, 1984). This second change was due to the flipping of PS, by the

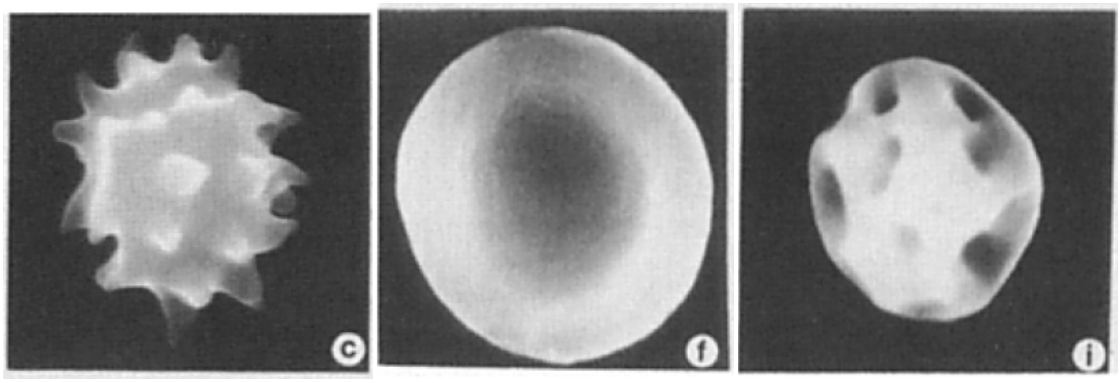

Figure 1-5. Red blood cell membranes change shape in response to exogenously added phospholipids and phospholipid translocation. The left panel (c) shows echinocyte shape (after addition of exogenous phospholipids). The center panel (f) shows discocyte shape of a normal red blood cell. The right panel (i) shows crenated stomatocyte shape which occurs when the exogenously added phospholipid is translocated across the membrane bilayer. *Image from Daleke & Huestis, 1989.*

APLT, to the cytosolic leaflet. There is a concurrent increase in the surface area of the cytosolic leaflet, while the extracellular leaflet bends inward to maintain the association between the membrane bilayers. Thus, it seems that the change in cell shapes correlates with the differences in the number of phospholipids between the two leaflets of a membrane bilayer.

This idea – that, when there is an increase in the phospholipid number of one layer of a tightly coupled membrane bilayer, it expands and the other layer contracts to maintain this coupling – is called the Bilayer Couple Hypothesis (Sheetz & Singer, 1974), and was first conceived by Sheetz and Singer in 1974. It serves as the foundation upon which most of the hypotheses that address the role of proteins and their role in the creation of membrane curvature has been built. One example relevant to this hypothesis is the influence of phosphatidic acid translocation across liposome membranes (driven by a pH gradient), which induces curvature as predicted by the hypothesis (Eastman, Hope,

& Cullis, 1991). Shape changes in red blood cells (see section on APLT discovery by Seigneuret and Devaux) induced by additional phospholipid being added to the extracellular leaflet and then flipped to the cytosolic leaflet is another example.

There are several hypotheses on how membrane curvature is formed and captured by proteins in order to bud transport vesicles from the plasma membrane or organelles. The textbook view of vesicle budding suggests that the assembly of clathrin triskelia and associated adaptor proteins onto a membrane causes localized curvature of the membrane due to the intrinsic curved structure of the polyhedral clathrin coat and its ability to self-assemble into baskets (Kirchhausen, 2000a, 2000b). Clathrin-coated vesicles have been shown to form from protein-free liposomes, *in vitro* (Takei et al., 1998). However, calculations on the energy required for membrane deformation versus the energy used by clathrin to self-assemble into polyhedral baskets suggests that this clathrin may be insufficient for driving the dynamic levels of membrane curvature needed for vesicle formation in cells (Nossal, 2001). Other labs have argued for the "Brownian ratchet" mechanism which claims that since biological membranes are extremely fluid structures, momentary curvature is created due to natural fluid fluctuations in the membrane (Hinrichsen, Meyerholz, Groos, & Ungewickell, 2006). Various proteins, including clathrin subunits, are able to sense and capture this curvature and, as a result, recruit the proteins necessary to build a functional vesicle.

Proteins that possess specialized domains (such as BAR-domains, ENTH- and ANTH-domains, and ALPS domains) have also been implicated in sensing, capturing, or

causing membrane curvature (Ford et al., 2002; Graham & Kozlov, 2010; Itoh & De Camilli, 2006; Ren, Vajjhala, Lee, Winsor, & Munn, 2006). It has also been hypothesized that proteins with amphipathic helices, such as Arf, or lysolipids, can generate positive membrane curvature by inserting their helix (or acyl chain) into the outer leaflet of the membrane bilayer. There has been much work done in artificial membranes to show that cytosolic proteins, such as Arf, COPI, and epsins, are capable of tubulating membranes (Beck et al., 2011; Beck et al., 2008). However, it has been argued that these effects are a result of protein-protein crowding (Stachowiak et al., 2012). Furthermore, the quantity of protein added to the membranes in these experiments is not representative of the protein levels found normally in a cell. Also, the rate of membrane curvature formation by these proteins is not typical in cells. Finally, lipid-modifying enzymes, lysophospholipid acyltransferases (LPATs), sphingomyelinase, and dynamin are other proteins implicated in the creation of membrane curvature (Graham & Kozlov, 2010).

P4-ATPases, due to their ability to translocate phospholipids between membrane leaflets, and their association with protein trafficking defects, are yet another group of proteins deemed to have a function in membrane curvature formation. The favored model for how flippases contribute to membrane asymmetry and vesicle budding is based on the bilayer couple hypothesis by Sheetz and Singer. This hypothesis states that the expansion of one leaflet relative to the other will cause membrane bending because the two leaflets are physically coupled to each other (Sheetz & Singer, 1974).

In addition to the creation and maintenance of membrane asymmetry, flippases also play important roles in vesicle-mediated protein transport. More specifically, it is hypothesized that flippases are involved in the creation of transport vesicles. How is this achieved? The ability of flippases to flip phospholipids creates asymmetry in the membrane composition. Additionally, this unidirectional flip, from the cytosolic leaflet to the extracellular or lumenal leaflet, creates an imbalance in the number of phospholipids in each membrane. As the number of phospholipids in the cytosolic leaflet increases, the surface area of that leaflet increases and positive membrane curvature is attained (Fig. 1-6) (Graham & Kozlov, 2010). The decrease in the number of phospholipids in the lumenal leaflet, coupled with the close association between the two membrane layers, results in membrane invagination towards the cytosolic side. The resulting positive membrane curvature, bending into the cytosol, is then captured by coat proteins, adaptor proteins and other factors responsible for the formation of a mature transport vesicle. Flippase activity by P4-ATPases should, as a result, induce positive membrane curvature (bending of the membrane towards the cytosol). However, we have no direct evidence that the flippase activity of P4-ATPases causes membrane bending. Drs2p, we hypothesize, causes flipping of phospholipids from one leaflet to the other, expands the outer leaflet causing membrane bending since the two leaflets are coupled. This curvature is captured by curvature-sensing proteins that are able to recruit AP-1 and clathrin onto the membrane (Graham & Kozlov, 2010). In Chapter 3 of this thesis, I outline experiments and assays designed and developed to test the role of Drs2p on membrane curvature and its influence in vesicle budding.

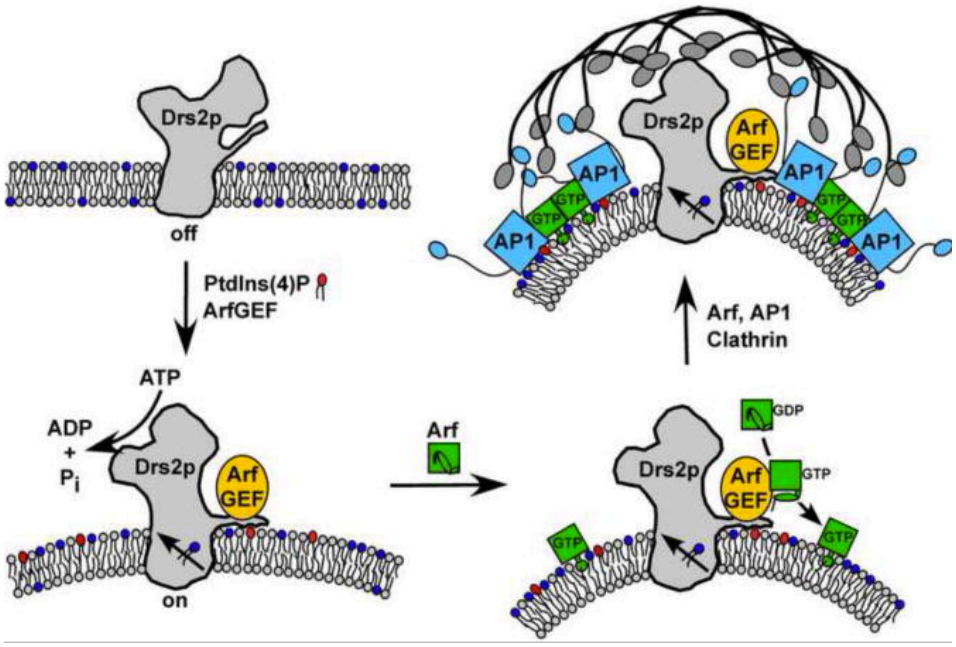

Figure 1-6. Potential mechanism by which Drs2p creates membrane curvature and works to create transport vesicles. *Image from (Graham & Kozlov, 2010).*

Function of P4-ATPases in Cells – Vesicle-Mediated Protein Transport*

** This section has been modified from the BBA Review: (Sebastian et al., 2012).*

P4-ATPases were first linked to protein trafficking when Drs2p, and its chaperone, Cdc50p, were discovered to genetically interact with Arf (C. Y. Chen & Graham, 1998; C. Y. Chen, Ingram, Rosal, & Graham, 1999; S. Chen et al., 2006; Sakane, Yamamoto, & Tanaka, 2006). Arf (ADP-ribosylation factor) is a small G-protein that cycles between GTP- and GDP-bound form through the action of several guanine nucleotide exchange factors (ArfGEFs) and GTPase activating proteins (ArfGAPs). In the GTP-bound form, Arf mediates the binding of adaptor proteins and coat proteins, such as COPI and clathrin, to sites of vesicle formation (Bonifacino & Glick, 2004). The synthetic lethal

interaction between Drs2p and Cdc50p with Arf suggested that these proteins were important players in vesicle budding pathways. *drs2Δ* is also synthetically lethal with clathrin temperature-sensitive alleles, but not COPI or COPII mutations, which implicated Drs2p in clathrin-mediated protein trafficking pathways (C. Y. Chen et al., 1999).

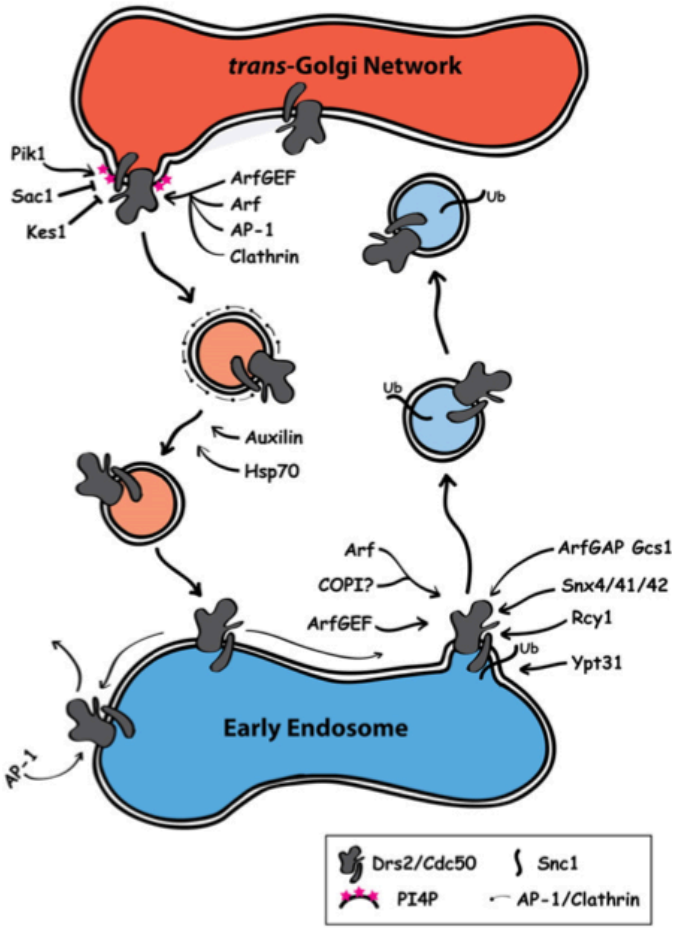

Figure 1-7. Drs2p trafficking pathways and players. Image from (Sebastian et al., 2012).

Drs2p primarily localizes to the *trans*-Golgi network (TGN) and this is one of the sites from which clathrin-coated vesicles bud. The phenotypes exhibited by *drs2Δ* cells are similar to the defects observed in cells deficient in clathrin. Both mutants accumulate enlarged Golgi cisternae and late Golgi enzymes involved in proteolytically processing

pro-α-factor are mislocalized in both *drs2Δ* and clathrin mutants. Furthermore, the *drs2Δ* cells are markedly deficient in clathrin-coated vesicles (CCVs) that can be purified from these cells (C. Y. Chen et al., 1999). The screen for mutants defective in ribosome synthesis that first identified *DRS2* may seem at odds with the roles described here in protein trafficking and membrane asymmetry. However, many mutants that exhibit defects in vesicle-mediated protein transport create membrane stress, which is sensed by the cell integrity pathway to down regulate ribosome production and attenuate translation (Deloche, de la Cruz, Kressler, Doere, & Linder, 2004; Li, Moir, Sethy-Coraci, Warner, & Willis, 2000). The defect in ribosome synthesis only appears after shifting *drs2Δ* cells to cold temperatures (below 20 °C) for a few hours (Ripmaster et al., 1993), while most of the Golgi defects are observed at any temperature (C. Y. Chen et al., 1999; Muthusamy, Raychaudhuri, et al., 2009). The localization of Drs2p to the TGN and observation that temperature-sensitive for function alleles of *DRS2* (*drs2–12* or *drs2–31*) cause a loss of vesicle formation within 30 minutes of temperature shift imply a direct role for Drs2p in vesicle budding (Gall et al., 2002).

There are many co-factors involved in the formation, budding and uncoating of clathrin-coated vesicles (Kirchhausen, 2000a). Most notably, adaptor proteins are essential in cargo selection and organizing the coat at sites of vesicle formation. In yeast, AP-1 (adaptor protein-1), a heterotetrameric complex composed of γ, β1, μ1, and σ1 adaptin subunits, is recruited by Arf and functions at the TGN and early endosomes (Fig. 1-7). Another set of adaptor proteins, Gga1 and Gga2 (Golgi-localized, Gamma-ear containing, Arf-binding) bud clathrin-coated vesicles from the TGN that are targeted to the late endosome. The AP-3 tetrameric adaptor (composed of δ, β3, μ3 and σ3 adaptin subunits)

also appears to bud from the TGN in an Arf-dependent, but clathrin independent manner (Muthusamy, Natarajan, Zhou, & Graham, 2009). After a clathrin-coated vesicle buds, the yeast auxilin (Swa2) and Hsp70 (Ssa proteins) are required for clathrin disassembly and uncoating (Fig. 1-7) (Gall et al., 2000; Xiao, Kim, & Graham, 2006).

Drs2p and Cdc50p are required for bi-directional transport between the TGN and the early endosome in pathways mediated by AP-1/clathrin and an F-box protein called Rcy1p (Fig. 1-7) (Furuta et al., 2007; Hua et al., 2002; Liu, Surendhran, Nothwehr, & Graham, 2008). The phenotypes associated with loss of Drs2p or AP-1 function within cells are very similar. For example, chitin synthase III (Chs3p) is thought to cycle between the TGN and early endosome and is exported to the plasma membrane at certain times in the cell cycle (Valdivia, Baggott, Chuang, & Schekman, 2002). Mutation of exomer subunit genes, such as *CHS6*, prevents transport of Chs3p to the plasma membrane. But, when *chs6Δ* is combined with either *drs2Δ* or AP-1 subunit mutations, Golgi-endosomal trafficking is disrupted and Chs3p redirects to the plasma membrane and late endosome or vacuole (Liu et al., 2008; Valdivia et al., 2002). These results suggest that Drs2p, AP-1 and clathrin mediate both anterograde and retrograde transport of this cargo between the TGN and early endosome (Liu et al., 2008).

Drs2p also appears to cycle between the TGN and early endosomes (Fig. 1-7). Occasionally, some Drs2p molecules find their way to the plasma membrane, but multiple endocytosis signals ensure a quick return to the early endosome and TGN system (Liu, Hua, Nepute, & Graham, 2007). When AP-1 is disrupted, wholesale re-routing of Drs2p to the plasma membrane is observed and Drs2p can be held at this

location with an endocytosis block. However, upon lifting the endocytosis block, Drs2p recycles through the endocytic pathway back to the TGN in the absence of AP-1 (Liu et al., 2008). The role of AP-1, it seems, is to traffic Drs2p and Chs3p from the TGN to the early endosome, but unlike Chs3p, Drs2p does not need AP-1 for the return trip. Because Drs2p is required to support Chs3p trafficking in AP-1 pathways, it seemed possible that the flippase activity may be required to support Drs2p's own transport by AP-1. In fact, inactivation of Drs2p activity (by shifting a GFP-tagged temperature sensitive form of Drs2p to the nonpermissive temperature) caused re-routing of Drs2p to the plasma membrane, comparably to what was observed by inactivation of AP-1 (Liu et al., 2008).

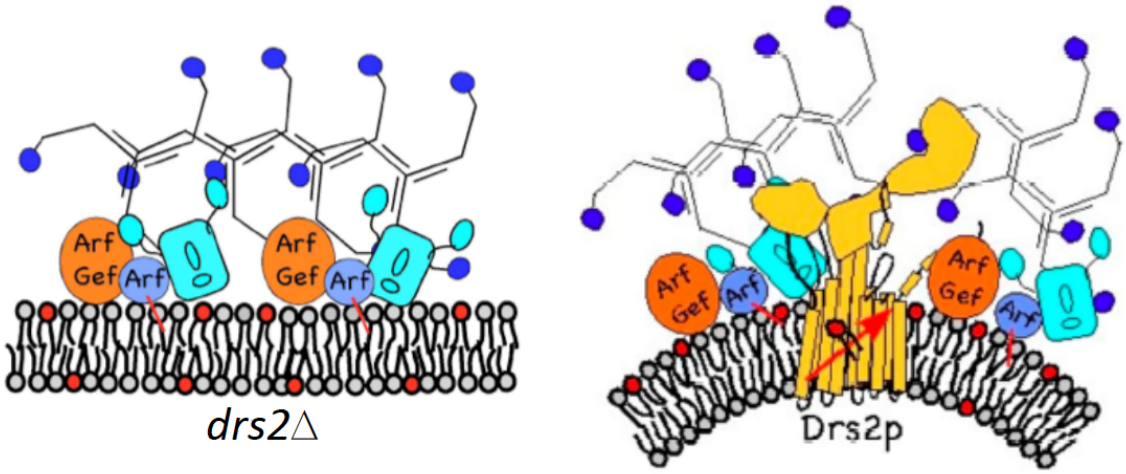

Figure 1-8. Enzymatically active Drs2p is required for the budding of AP-1/clathrin-coated vesicles. *Image from Liu, et al., 2008.*

These observations support the idea that the formation of AP-1/clathrin-coated vesicles requires Drs2p flippase activity. Remarkably, however, the Arf-dependent recruitment of AP-1 and clathrin to the TGN is not perturbed in *drs2Δ* cells (Fig. 1-8) (Liu et al., 2008). Moreover, the enlarged Golgi cisternae that accumulate in *drs2Δ* cells lack budding

profiles or highly curved tubular elements (C. Y. Chen et al., 1999; Gall et al., 2002), even though the coat proteins are present on the membrane. Thus, a simple model that Drs2p facilitates coat recruitment to drive vesicle budding is incorrect. It seems more likely that Drs2p imparts curvature to the membrane by pumping phospholipid to the cytosolic leaflet, thereby producing a surface that the clathrin coat can more easily deform (Graham, 2004).

Drs2p and Cdc50p are also critical for directing cargo from the early endosome back to the TGN in the "Rcy1p pathway" (Fig. 1-7) (Furuta et al., 2007; Hua et al., 2002). The F-box protein Rcy1p can form a Skp1-cullin-F-box (SCF-Rcy1) complex (Kus, Caldon, Andorn-Broza, & Edwards, 2004) and Rcy1p is required for the early endosome to TGN trafficking of Snc1p, an exocytic SNARE protein that cycles between the early endosome, TGN and plasma membrane (Galan et al., 2001; Lewis, Nichols, Prescianotto-Baschong, Riezman, & Pelham, 2000). The SCF Rcy1p complex is an effector of the Rab proteins Ypt31p and Ypt32p, and is proposed to ubiquitinate Snc1p to generate a signal for recycling out of the endosome (S. H. Chen, Shah, & Segev, 2011). Trafficking of Snc1p is unaffected by AP-1 disruption (Liu et al., 2008) and there is some indication that COPI might influence the Rcy1p pathway, although the vesicle coat acting in this pathway is unclear (Robinson et al., 2006). The sorting nexin complex Snx4/41/42p and the ArfGAP Gcs1p are also linked to this recycling pathway (Hettema, Lewis, Black, & Pelham, 2003; Sakane et al., 2006). The *drs2Δ* and *cdc50Δ* mutations disrupt retrograde trafficking of Snc1p from the early endosome to the TGN comparably to the *rcy1Δ* mutation. In addition, Cdc50p accumulates in the early endosomes of Rcy1p mutants and so Drs2p–Cdc50p also appears to travel the Rcy1p pathway back to the TGN (Furuta et al., 2007).

In fact, growth defects associated with *rcy1Δ* can be suppressed by overexpression of Drs2p/Cdc50p and Snc1p, implying that these proteins are the critical cargos in the Rcy1p pathway (Furuta et al., 2007). While Rcy1p interacts with Drs2p–Cdc50p (Furuta et al., 2007), it is not known if Rcy1p ubiquitinates this flippase to facilitate retrieval or acts by another mechanism.

The *C. elegans tat-1* and *chat-1* mutants (potentially orthologous to Drs2p–Cdc50p) also show a strong defect in cargo recycling through endosomes (B. Chen et al., 2010; Ruaud et al., 2009), indicating that this function in protein trafficking is well-conserved through evolution. TAT-1 and CHAT-1 co-localize within intestinal cells to the plasma membrane (apical and basolateral) along with early/recycling endosomes. In fact, CHAT-1 decorates tubules on recycling endosomes that require RAB-10 for formation, and these tubules are exaggerated in an *rme-1* mutant (Eps15 homology domain (EHD) protein required for tubule scission) (B. Chen et al., 2010). Intestinal cells of the *tat-1* or *chat-1* mutants accumulate large vacuolated structures bearing markers for late endosomes and lysosomes (B. Chen et al., 2010; Ruaud et al., 2009). In addition, several markers for the early and late endosomes, recycling endosomes and late Golgi show aberrant co-localization to aggregated vesicles. A number of proteins that normally recycle from the early endocytic pathway back to the plasma membrane, including human transferrin receptor, human IL-2 receptor α-chain and glucose transporter 1 (GLUT-1), are all trapped in abnormal endosomal intermediates in the mutants (B. Chen et al., 2010). Moreover, the recycling endosome tubular extensions appear to be completely lost in the *tat-1* and *chat-1* mutants (B. Chen et al., 2010). These data suggest that TAT-1 and CHAT-1 help drive the tubular membrane extensions from recycling

endosomes that enrich cargo for delivery back to the plasma membrane.

In addition to bidirectional transport between the TGN and early endosome, and recycling from endosomes back to the plasma membrane, P4-ATPases may also contribute to budding of exocytic vesicles from the TGN (Gall et al., 2002). Budding yeast produce at least two classes of exocytic vesicles distinguished by density and cargo (Harsay & Bretscher, 1995). Inactivation of either Drs2p or clathrin prevents formation of the denser class that accumulates when actin assembly is perturbed (Gall et al., 2002). It remains unclear if these Drs2p-dependent exocytic vesicles actually bud from the TGN or an early endosome, and it is possible that they are analogous to the tubular carriers produced by recycling endosomes in *C. elegans*.

However, phenotypes exhibited by *A. thaliana ala3* mutants suggest a defect in forming exocytic secretory vesicles directly from the TGN (Poulsen et al., 2008). The peripheral columnella cells in the root tip of wild-type plants display TGN cisternae with large, bulbous extensions filled with electron translucent slime polysaccharide. Secretory vesicles containing the slime polysaccharide derived from the Golgi are easily detected in the cytoplasm prior to their fusion to the plasma membrane. In contrast, the ala3 columella cells have a complete absence of the distended TGN cisternae and a marked deficiency of secretory vesicles in the cytoplasm (Poulsen et al., 2008). ALA3 also plays a critical role in trichome formation on leaves, which is a wonderful model for directional membrane growth and complex cell patterning (Zhang & Oppenheimer, 2009). The trichome branch elongation defect in *ala3* plants may result from defects in membrane trafficking and/or regulation of the actin cytoskeleton. This is reminiscent of the

polarized growth defects reported for *lem3Δ* mutants in budding yeast (Saito et al., 2007), and the loss of microvilli from the apical membrane of Caco-2 cells deficient for Atp8b1 (Verhulst et al., 2010).

Thus far, only Atp8b5 has been shown to have a role in protein trafficking in mammalian cells (P. Xu et al., 2009). RNA interference of Atp8b5 in murine mastocytoma P815 cells causes the distension of Golgi cisternae and abrogates constitutive secretion. Interestingly, these secretory pathway defects are only observed at lower temperatures (33°C), perhaps because other P4-ATPases can compensate for the Atp8b5 deficiency at 37°C (P. Xu et al., 2009). Alternatively, it is possible that Golgi membranes in Atp8b5 deficient cells are more sensitive to changes in membrane fluidity associated with reduced temperature.

In the budding yeast system, there is clear evidence for both overlapping and non-overlapping functions for the P4-ATPases (Hua et al., 2002). The defects in bidirectional transport between the TGN and endosomes and exocytosis are observed in *drs2Δ* single mutants, in spite of the presence of four other P4-ATPases in these cells. Dnf1p is also unable to replace the function of Drs2p in AP-1/clathrin-coated vesicle formation or the formation of Snc1 retrograde vesicles. Thus, Neo1p and the Dnf P4-ATPases cannot replace the critical function of Drs2p in these pathways. However, growth and protein trafficking defects associated with *drs2Δ* become more severe as additional DNF genes are knocked out. For example, neither a *drs2Δ* nor a *dnf1Δ* single mutant displays a defect in the AP-3-dependent transport of cargo to the vacuole. However, the *drs2Δ dnf1Δ* double mutant exhibits a substantial defect in sorting AP-3 cargo (Hua et al., 2002). Thus,

it appears that Drs2p and Dnf1p are interchangeable in this pathway. Furthermore, Dnf1-N550S, a mutant form of Dnf1p that preferentially translocates PS, has been shown to replace Drs2p in transport between the TGN and early endosomes. It is also able to recruit the downstream effector, Gcs1p (an Arf-GAP) to sites of increasing membrane curvature and anionic charge. This anionic charge is often imparted to the membrane due to the translocation of phosphatidylserine to the cytosolic leaflet (P. Xu, Baldridge, Chi, Burd, & Graham, 2013). Neo1p and Dnf1p may also compensate for loss of Drs2p in delivering cargo from the Golgi to the late endosome, which is a GGA-dependent pathway (Hua & Graham, 2003; Singer-Kruger et al., 2008; Wicky, Schwarz, & Singer-Kruger, 2004). In addition, the *dnf1Δ dnf2Δ* cells show a cold-sensitive endocytosis defect that is exacerbated by addition of *drs2Δ (Pomorski et al., 2003)*. While cells are viable until all four *DRS2 DNF* genes are knocked out, the single *neo1Δ* mutation is lethal (Hua et al., 2002). Thus, Neo1p has an essential role that cannot be replaced by Drs2p or Dnf proteins.

Neo1p appears to localize to both Golgi and endosomes and has been implicated in the COPI-dependent retrograde transport of cargo from the Golgi to the ER (Hua & Graham, 2003; Singer-Kruger et al., 2008; Wicky et al., 2004). For example, the Rer1p protein rapidly cycles between the ER and Golgi, but COPI inactivation causes mislocalization of Rer1p to downstream compartments (Sato, Sato, & Nakano, 2001). Similarly, Neo1p inactivation causes the same Rer1p mislocalization phenotype (Hua & Graham, 2003). Additionally, Neo1p has been implicated in GGA dependent trafficking of cargo from the TGN to the late endosome. GGA is recruited to the TGN membrane by associations with both Arf and the Arf-like protein Arl1p, which forms a complex with Mon2 (a large

scaffold protein) and Neo1p (Singer-Kruger et al., 2008). In *C. elegans*, TAT-5 has been implicated in the budding of extracellular vesicles. Loss of TAT-5 causes loss of PE asymmetry which then leads to wide-scale shedding of these vesicles. Worm embryos, then, have defects in cell adhesion and morphogenesis (Wehman, Poggioli, Schweinsberg, Grant, & Nance, 2011).

Regulation of P4-ATPases

Thus, the role of flippases in a cell is an important one. And, as such, it is closely regulated by a variety of mechanisms in the cell. Flippase protein kinases (FPK) are a class of proteins that were discovered, in a genetic screen, as positive regulators of Dnf1p and Dnf2p (Nakano, Yamamoto, Kishimoto, Noji, & Tanaka, 2008). In addition to directly phosphorylating the P4-ATPase, a double mutant of these proteins (*fpk1Δ fpk2Δ*) has similar phenotypic defects as *dnf1Δ dnf2Δ* – they have defects in their flippase activity (as measured by inability to translocate fluorescent derivatives of the Dnf substrates, PC or PE), and have protein trafficking defects (similar to a loss of Dnf1p-Lem3p or Dnf2p-Lem3p phenotype) (Nakano et al., 2008). Additional work has identified other protein kinases, such as Ypk1p, that play a role in regulating Fpk activity at the membrane, and it is the organization of and changes to the membrane composition that tightly regulates the influence of these kinases, and the resulting activity of the flippase (Roelants, Baltz, Trott, Fereres, & Thorner, 2010).

An oxysterol-binding protein, called Kes1p, is involved in down-regulating Drs2p function (Kishimoto, Yamamoto, & Tanaka, 2005; Muthusamy, Raychaudhuri, et al.,

2009). Meanwhile, Drs2p is also able to downregulate Kes1p function (Muthusamy, Raychaudhuri, et al., 2009). Oxysterol-binding proteins bind and remove sterols from the membrane. A hypothesis as to the way Drs2p is able to regulate the activity of Kes1p is that Drs2p can change the membrane structure which then inhibits the ability of Kes1p from extracting sterols from the membrane (Muthusamy, Raychaudhuri, et al., 2009). Recent work (described on pages 18 and 19 of this chapter) has also indicated that Kes1p can extract PI4P from the membrane. Kes1p has been shown to stimulate a PI4P phosphatase (Alfaro et al., 2011), and lowering the levels of PI4P on the membrane hinders Drs2p flippase activity as PI4P has recently been shown to be a direct regulator of Drs2p activity (Fig. 1-6 and 1-7) (Zhou, Sebastian, & Graham, 2013).

Drs2p is strongly influenced by the phosphotidylinositol 4-phosphate (PI4P) produced by Pik1p (phosphatidylinositol 4-kinase) (Sciorra et al., 2005). The C-terminal tail of Drs2p possesses a basic patch of amino acid residues, which have been mapped to preferentially bind phosphoinositides (in the case of Drs2p, PI4P) (Natarajan et al., 2009). When PI4P production is abolished, by the deletion by its respective phosphatase or inactivation of Pik1p, in isolated TGN membranes, the activity of Drs2p is considerably diminished (Natarajan et al., 2009). Additionally, the C-tail of Drs2p possesses residues (which overlap the PI4P binding region) that have a preference for binding an ArfGEF. A stimulation of Drs2p flippase activity is detectable, in isolated Golgi membranes, when incubated with an ArfGEF (Natarajan et al., 2009).

New work from the lab of Fang-Jen Lee has also implicated Arl1 as an additional regulator of Drs2p. The Lee group shows that Drs2p, ArfGEF and Arl1p come together

to form a stable ternary complex, and the formation of this complex stimulates the flippase activity of Drs2p (Tsai, Hsu, Liu, Chen, & Lee, 2013). Their findings, and its relationship to the regulation of flippases are discussed in greater detail on pages 59 and 60 of this thesis (Chapter II).

In the secretory pathway, as Figure 1-7 indicates, Kes1p, Pik1p and Sac1p primarily function to regulate the activity of Drs2p at the TGN. Arf-GEF exerts its influence at both the TGN and early endosomes

As previously mentioned, the family of P-type ATPases have four structural domains in common – the actuator, phosphorylation, nucleotide-binding, and transmembrane domains. Additionally, some P-type ATPases possess regulatory domains (R domains) contained within the N-terminal or C-terminal sequence of the protein (Au, 1987; Hwang et al., 2000; P. James et al., 1988; Palmgren et al., 1990; Palmgren et al., 1991; Portillo et al., 1989; Rasi-Caldogno et al., 1992, 1993, 1995). The C-terminal tail of Drs2p has been implicated as an R domain and, as described above, regions have been mapped where effectors, such as PI4P and ArfGEF are able to interact. The role that the C-terminal tail of Drs2p plays, in regulating flippase activity, will be explored further in Chapter 2 of this thesis.

CHAPTER II

AUTO-INHIBITION OF DRS2P, A YEAST PHOSPHOLIPID FLIPPASE, BY ITS CARBOXYL-TERMINAL TAIL*

*This chapter was previously published as: Zhou, X., Sebastian, T. T., & Graham, T. R. (2013). Auto-inhibition of Drs2p, a yeast phospholipid flippase, by its carboxyl-terminal tail. *J Biol Chem, 288*

Abstract

Drs2p, a yeast type IV P-type ATPase (P4-ATPase), or flippase, couples ATP hydrolysis to phosphatidylserine (PS) translocation and the establishment of membrane asymmetry. A previous study has shown that affinity-purified Drs2p, possessing an N-terminal tandem affinity purification tag (TAP_N-Drs2), retains ATPase and translocase activity, but Drs2p purified using a C-terminal tag (Drs2-TAP_C) was inactive (Zhou & Graham, 2009). In this study, we show that the ATPase activity of N-terminally purified Drs2p associates primarily with a proteolyzed form of Drs2p lacking the C-terminal cytosolic tail. Truncation of most of the Drs2p C-terminal tail sequence activates its ATPase activity by approximately 4-fold. These observations are consistent with the hypothesis that the C-terminal tail of Drs2p is auto-inhibitory to Drs2p activity. Phosphatidylinositol-4-phosphate (PI(4)P) has been shown to positively regulate Drs2p activity in isolated Golgi membranes through interaction with the C-terminal tail (Natarajan et al., 2009). In proteoliposomes reconstituted with purified, N-terminally TAP-tagged Drs2p, both ATPase activity and flippase activity were significantly higher

in the presence of PI(4)P. In contrast, PI(4)P had no significant effect on the activity of a truncated form of Drs2p, which lacked the C-terminal tail. This work provides the first direct evidence, in a purified system, that a phospholipid flippase is subject to auto-inhibition by its C-terminal tail, which can be relieved by a phosphoinositide to stimulate flippase activity.

Introduction

P-type ATPases are a large family of membrane pumps that transport various substrates, such as ions, against their chemical gradients across membranes. They are divided into 5 subfamilies (P1- to P5-ATPases) and further into smaller subgroups based on sequence homology and substrate specificity (Axelsen & Palmgren, 1998; Kuhlbrandt, 2004). The P4-ATPases translocate specific phospholipid molecules from the extracellular leaflet of the plasma membrane, or lumenal leaflet of internal organelles, to the cytosolic leaflet. This activity is crucial for both the establishment of plasma membrane asymmetry, and vesicle-mediated protein transport in the secretory and endocytic pathways (Sebastian, Baldridge, Xu, & Graham, 2012). The overall architecture of P-type ATPases is exemplified by the crystal structures of several P-type ATPases. They possess three cytosolic domains (A: actuator; N: nucleotide binding; P: phosphorylation) and a multi-span transmembrane domain (Toyoshima, 2009; Toyoshima et al., 2000). In addition to these common structural features, some P-type ATPases have an additional regulatory cytosolic domain, called an R domain, within the N- or C-terminal cytosolic tail of the protein (Au, 1987; Hwang et al., 2000; P. James et al., 1988; Palmgren et al., 1990; Palmgren et al., 1991; Portillo et al., 1989; Rasi-Caldogno et al., 1992, 1993, 1995). Some

members of the P-type ATPase family also have additional beta subunits associated with them. There is evidence that these subunits, in varying degrees, aid in regulation, folding and/or proper localization of the P-type ATPase (Geering, 2001; Kuhlbrandt, 2004; Sebastian et al., 2012).

The R domain serves as an auto-inhibitory element that limits the activity of the P-type ATPase. Removal of the R domain, by limited proteolysis or genetic engineering, activates the protein. Various regulatory activities can relieve the auto-inhibition caused by this R domain. For example, the $P2_B$-ATPase subgroup, comprising the plasma membrane Ca^{2+} pumps, contains an R domain in the C-terminal tail (in animals) (Au, 1987; Carafoli, 1994; P. James et al., 1988), or in the N-terminal tail (in plants) (Hwang et al., 2000; Rasi-Caldogno et al., 1992, 1993, 1995; Sze, Liang, Hwang, Curran, & Harper, 2000). When calmodulin interacts with this R domain, it displaces the auto-inhibitory tail and activates the protein for Ca^{2+} transport. Phosphorylation of serine or threonine residues within the R domain of $P2_B$-ATPases has also been found to regulate ATPase activity by disrupting calmodulin binding and resulting in protein activation (in animals), or inactivation (in plants) (Carafoli, 1994; Caroni & Carafoli, 1981; P. H. James, Pruschy, Vorherr, Penniston, & Carafoli, 1989; Sze et al., 2000). The $P3_A$-ATPase family, which is comprised of plasma membrane proton pumps from plants and fungi, also possesses a C-terminal R domain and utilizes a similar activation mechanism, which includes phosphorylation and binding of regulatory proteins to the R domain (Fuglsang et al., 1999; Maudoux et al., 2000; Olsson, Svennelid, Ek, Sommarin, & Larsson, 1998; Palmgren, 2001; Palmgren et al., 1990; Palmgren et al., 1991; Piotrowski, Morsomme, Boutry, & Oecking, 1998; Portillo, 2000; Portillo et al., 1989). Evidence for the role of the

N-terminus in regulating P-type ATPase function has also been shown (Cornelius, Mahmmoud, Meischke, & Cramb, 2005; Ekberg, Palmgren, Veierskov, & Buch-Pedersen, 2010).

Drs2p is a P4-ATPase from the budding yeast *Saccharomyces cerevisiae*. At steady state, Drs2p is localized primarily to the *trans*-Golgi network (TGN), and is involved in multiple protein trafficking pathways between the TGN, plasma membrane and endosomes (Sebastian et al., 2012). Drs2p is structurally similar to the other P-type ATPases with A, N, and P cytosolic domains and 10 transmembrane segments (Sebastian et al., 2012). Drs2p associates with a beta subunit, Cdc50p, which is its co-chaperone and a member of the Cdc50p family of proteins. Cdc50p is essential for proper localization of Drs2p within the cell (S. Chen et al., 2006; Furuta et al., 2007; Saito et al., 2004). Drs2p catalyzes a phosphatidylserine (PS) flippase activity detected in isolated TGN membranes (Natarajan et al., 2004) and post-Golgi secretory vesicles (Alder-Baerens et al., 2006), as well as in proteoliposomes reconstituted with purified Drs2p (Zhou & Graham, 2009). Interestingly, like $P2_B$- and $P3_A$-ATPases, Drs2p appears also to have an R domain within its C-terminal tail. Features identified in the Drs2p R domain include a motif that binds Gea2p (an Arf guanine nucleotide exchange factor) (Chantalat et al., 2004) and a region that binds phosphatidylinositol-4-phosphate (PI(4)P) (Natarajan et al., 2009). Drs2p flippase activity was virtually abolished in TGN membranes isolated from yeast cells deficient in Gea2p and PI(4)P production, and addition of Gea2p and PI(4)P to these TGN membranes restored flippase activity (Natarajan et al., 2009). Additional evidence from the Lenoir lab sheds light on the role that PI(4)P plays in Drs2p regulation. It was found that, in crude membranes, PS

inhibited the dephosphorylation of the Drs2p/Cdc50p complex. It was only in the presence of PI(4)P, that PS was able to accelerate the dephosphorylation step associated with substrate transport (Jacquot et al., 2012). These results suggested that Drs2p is auto-inhibited by its C-terminal tail in the absence of Gea2p and PI(4)P, both of which are positive regulators that stimulate Drs2p activity by binding to its C-terminal R domain. In this study, we present evidence that directly supports this hypothesis.

Experimental Procedures

Reagents. IgG Sepharose 6 Fast Flow, calmodulin Sepharose 4B, and ATP (>99% purity) were from GE Healthcare. ATPγS was from Sigma and Ni-NTA agarose was from Qiagen. AcTEV protease and SimplyBlue SafeStain (Coomassie G-250) were from Invitrogen. Bio-Beads SM-2 was from Bio-Rad, and Triton X-100, polyoxyethylene (9) dodecyl ether ($C_{12}E_9$), and polyoxyethylene (8) dodecyl ether ($C_{12}E_8$) were from Anatrace. Phospholipids and fluorescent derivatives were from Avanti Polar Lipids and were: DOPC (1,2-dioleoyl-*sn*-glycero-3-phosphocholine), DOPS (1,2-dioleoyl-*sn*-glycero-3-phospho-L-serine), PI(4)P (L-α-phosphatidylinositol-4-phosphate from porcine brain), NBD-PC (1-palmitoyl-2-[6-(NBD-amino)hexanoyl]-*sn*-glycero-3-phosphocholine), C6 NBD-PS (1-palmitoyl-2-[6-(NBD-amino)hexanoyl]-*sn*-glycero-3-phosphoserine), and C12 NBD-PS (1-palmitoyl-2-[12-(NBD-amino)dodecanoyl]-*sn*-glycero-3-phosphoserine). Lipids were dissolved in chloroform except PI(4)P, which was dissolved in chloroform/methanol/water (20:9:1, vol:vol:vol), and stored at -20°C. Antibodies used in this study were rabbit primary antibodies against Drs2p, and an Alexa Fluor 680-labeled goat secondary antibody against rabbit IgG (Invitrogen).

Media and strains. Yeast cells were grown in standard rich medium (1% yeast extract/2% peptone/2% dextrose) or synthetic minimal media containing required supplements (Sherman, 1991), and nutrients were doubled in cell cultures for protein purification purposes.

The yeast strains used were XZY63b (*MATα his3 leu2 ura3 lys2 atp2*Δ*::URA3* P_{GPD}*::CDC50 pRS425-*P_{GPD}*::*TAP_N*::DRS2*), XZY51 (*MATα his3 leu2 ura3 lys2 atp2*Δ*::URA3* P_{GPD}*::CDC50 pRS425-*P_{GPD}*::DRS2:*TAP_C), XZY85 (*MATα his3 leu2 ura3 lys2 atp2*Δ*::URA3* P_{GPD}*::CDC50 pRS425-*P_{GPD}*::*TAP_N*::DRS2::*TAP_C), XZY94 (*MATα his3 leu2 ura3 lys2* P_{GPD}*::CDC50 pRS425-*P_{GPD}*::DRS2::*$_{(TEV)}$*::*TAP_{C2}), XZY95 (*MATα his3 leu2 ura3 lys2* P_{GPD}*::CDC50 pRS425-*P_{GPD}*::DRS2*$_{(TEV)}$*CT121::*$_{(TEV)}$*::*TAP_{C2}), XZY96 (*MATα his3 leu2 ura3 lys2* P_{GPD}*::CDC50 pRS425-*P_{GPD}*::DRS2*$_{(TEV)}$*CT121::*TAP_{C2}), and XZY60m (*MATα his3 leu2 ura3 lys2 atp2*Δ*::URA3* P_{GPD}*::*TAP_N*::DRS2* P_{GPD}*::CDC50*), where TAP_N encodes the protein A-TEV protease cleavage site-His_{10} tag, TAP_C encodes the calmodulin binding peptide (CBP)-TEV protease cleavage site-protein A tag, $_{(TEV)}$ encodes the TEV protease cleavage site, TAP_{C2} encodes the protein A-His_{10} tag, and *DRS2*$_{(TEV)}$*CT121* encodes a modified Drs2 protein that has the TEV protease cleavage site inserted in its C-terminal tail at the position that is 121-residue away from the C-terminal end of wild-type Drs2p.

Protein purification. TAP-tagged Drs2p was affinity purified using a TAP procedure described previously with some modifications (Zhou & Graham, 2009). Briefly, yeast cells were cultured to 3-6 OD_{600}/ml in minimal media or 5-10 OD_{600}/ml in rich media at 30°C, harvested and lysed using an EmulsiFlex-C3 High Pressure Homogenizer

(Avestin). The cell lysate was centrifuged at 15,000 x g for 12 min, and 20% of Triton X-100, $C_{12}E_9$, or $C_{12}E_8$ was added to the supernatant to a final concentration of 1% to solubilize Drs2p. TAP-tagged Drs2p was then purified using an IgG column plus either a Ni^{2+} column (for TAP_N and TAP_{C2}) or a calmodulin column (for TAP_C). In experiments where Drs2p was first purified using the TAP_N tag and then different Drs2p populations were separated using the TAP_C tag, the procedure was a combination of the TAP_N purification plus the second affinity step (the calmodulin column) of the TAP_C purification. Experiments where proteins were purified for the purposes of performing flippase assays were performed using $C_{12}E_8$ exclusively.

Purified Drs2p samples (except samples to be used in flippase assays) were centrifuged in Microcon YM-100 filter (Millipore) at 13,000 x g for 15 min at 4°C to near dryness, and resuspended in desired amount of storage buffer (40mM Tris-HCl, pH 7.5, 150mM NaCl, 40% glycerol, 0.1% Triton X-100) to store at -20°C. Recovery of Drs2p was determined using Odyssey Infrared Imaging System (LI-COR) to quantify SimplyBlue-stained bands relative to a BSA standard curve. Recombinant Sec7 domain of Gea2p was purified as previously described (Natarajan et al., 2009).

Proteoliposome formation. Purified Drs2p was reconstituted into proteoliposomes as previously described with some modifications (Zhou & Graham, 2009). Briefly, 0.5mL of single-step affinity purified Drs2p using Ni-NTA column was mixed with 2mg of lipid mixture solubilized in 0.5mL of 1% $C_{12}E_9$ for 30 min at 4°C. After addition of 200mg of extensively washed SM-2 beads, and 12-15 h of incubation on an end-over-end rotator at 4°C, the supernatant containing proteoliposomes was carefully removed, stored at 4°C.

We found that proteoliposomes formed with Drs2p purified in $C_{12}E_9$ were often too "leaky" to use in flippase assays. Membrane seal was significantly improved when reconstitutions were performed using $C_{12}E_8$ solubilized protein. Therefore, the following changes were made during proteoliposome formation. 2mg of lipids were solubilized in a 0.5mL volume that contains 1.5% $C_{12}E_8$ and incubated for 30 min at 4°C. 150mg of extensively washed SM2 Bio-beads were then added to this solution and it was incubated for 6 h on an end-over-end rotator at 4°C. After this, another 300mg of SM-2 beads were added and the sample was incubated for a further 12-15 h with end-over-end rotation. The supernatant containing proteoliposomes was carefully removed and stored at 4°C.

Flotation of proteoliposomes. 200µl of the proteoliposome sample was first incubated with 10mM dithionite, for 5 min at 4°C, to pre-quench the fluorescence in the outer leaflet of the proteoliposomes. The sample was, then, mixed with 200µl of 80% glycerol and placed at the bottom of a bipartite glycerol step gradient. 600µl of 10% glycerol was laid on the top. The samples were centrifuged in a TLS-55 rotor (Beckman Coulter) at 50,000rpm for 6 h at 4°C, and 200µl, each, of the top two fractions were collected by pipetting. These fractions contain pure Drs2p proteoliposomes.

ATPase Assay. Purified Drs2p was assayed for ATPase activity in ATPase buffer (50mM Tris-HCl, pH 7.5, 100 mM NaCl, 50 mM KCl, 1 mM NaN_3, 0.1% Triton X-100, 4 mM Na^+-ATP, pH 7.5, 10 mM $MgCl_2$) at 37°C for 1 h. For ATPase assays using proteoliposomes, detergent was omitted from ATPase buffer. Released phosphate was measured colorimetrically using modified protocols previously described (Carter & Karl, 1982;

Paterson et al., 2006; Zimmerman & Daleke, 1993). Briefly, the volume of the sample was brought to 275µl with deionized water, and the ATPase reaction was stopped by addition of 150µl of molybdate solution (2 M HCl/50 mM Na_2MoO_4) and 75µl of malachite green solution (0.042% malachite green in 1% polyvinyl alcohol solution). The sample was mixed for 2 min before addition of 500µl of citric acid (7%), and the optical density at 660 nm was read at 30 min after addition of the citric acid solution. The amount of released phosphate was determined by a phosphate standard curve constructed in the same ATPase buffer.

Flippase Assay. Floated proteoliposomes were assayed for flippase activity using previously published methods (McIntyre & Sleight, 1991; Zhou & Graham, 2009). Briefly, 40µL of floated, Drs2p-containing, proteoliposomes were incubated, at 37°C, with 5mM $MgCl_2$ and either 5mM ATP or 5mM ATPγS in a flippase buffer (40 mM Tris-HCl, pH 7.5, 200mM NaCl). At time 0 min and 40 min, 20µL samples were removed and mixed with 1mL of flippase buffer in a cuvette. Baseline fluorescence readings, were taken for 30 s, on an AB2 fluorometer (SLM Instruments, Inc.) at λ_{ex} = 460nm, and λ_{em} = 534nm. 10µL of 1M dithionite (dissolved in 1M Tris, pH 9.4) was then added to the sample and fluorescence was recorded for 120 s. Finally, the fluorescence was completely quenched by addition of 50µL of 10% Triton X-100 and background fluorescence was recorded for 30 s. The percentage of NBD-phospholipid in the outer bilayer of each of the proteoliposome samples (both ATP and the ATPγS control, at time t = 0 min and 40 min) was calculated using previously described formulae (Zhou & Graham, 2009). To calculate the percentage of NBD-phospholipid flipped, the values for an ATPγS control were subtracted from the respective ATP activated sample.

Western blotting. Western blotting was performed as previously described (C. Y. Chen et al., 1999). The primary antibody used was rabbit anti-Drs2p (1:2000). The secondary, Alexa Fluor 680-labeled goat anti-rabbit IgG antibody (Invitrogen) was used at 1:2000. Western blots were imaged with Odyssey Infrared Imaging System (LI-COR).

Results

Drs2p retains ATPase activity after purification by the N-terminal TAP_N tag, but not the C-terminal TAP_C tag. In a previous study, both TAP_N-Drs2p and Drs2p-TAP_C were expressed from chromosome-integrated expression cassettes and affinity purified to comparable yields and purities (Zhou & Graham, 2009). Although both TAP-tagged Drs2p forms appeared to be functional *in vivo*, only TAP_N-Drs2p retained ATPase activity after purification, whereas purified Drs2p-TAP_C was inactive. Interestingly, purified Drs2p-TAP_C did not seem to be aggregated or denatured, suggesting that the differing activities between the two Drs2p proteins may have a biologically relevant cause (Zhou & Graham, 2009).

To further address this issue and to more easily manipulate Drs2p, the expression cassettes for Drs2p were transferred to a multicopy plasmid (pRS425) to produce constructs (I) and (II), while the β-subunit Cdc50p was overexpressed using the strong GPD promoter integrated into the endogenous chromosomal locus (Fig. 2-1A, B). Both TAP_N-Drs2p and Drs2p-TAP_C were successfully expressed and purified using this plasmid system (Fig. 2-1B, C), and they still showed differential levels of ATPase activity, as previously observed (Fig. 2-1D). Cdc50p was recovered at low, substoichiometric

levels in these preparations and was not visible in the coomassie stained gel. The band migrating just above the 28kDa marker is the TEV protease used to elute the tagged proteins from an IgG column.

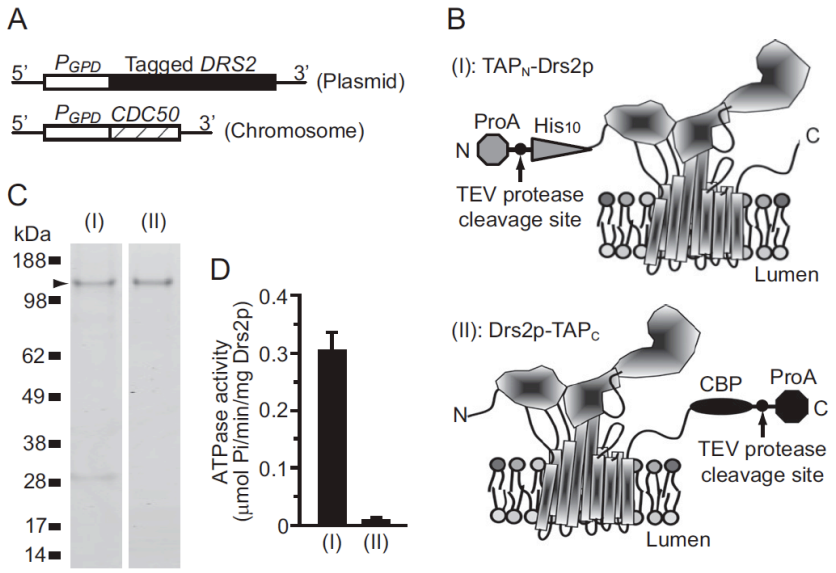

Figure 2-1. TAP_N-Drs2p has ATPase activity. (A) Tagged *DRS2* was expressed from a 2*ƒ* plasmid, and *CDC50* was from the chromosome. (B) Schematic of TAP_N-Drs2p (I) and Drs2p-TAP_C (II) was modeled on the crystal structure of SERCA1 in the nucleotide-free $E1•2Ca^{+2}$ conformation (7). The cytosolic domains are facing upward. (C) purified TAP_N-Drs2p (I) and Drs2p-TAP_C (II) were subjected to SDS-PAGE, and the gel was stained with SimplyBlue. (D) ATPase activity of purified TAP_N-Drs2p and Drs2p-TAP_C preparations. Samples were assayed with or without orthovanadate, and the orthovanadate controls were subtracted from the experimental value to obtain the nmol of orthovanadate released. ProA: protein A.

ATPase activity is associated with a faster-mobility form of Drs2p in purified samples. The major molecular difference between purified TAP_N-Drs2p and Drs2p-TAP_C is different tag appendages (His_{10} vs. calmodulin binding peptide (CBP)) to different positions of Drs2p (N- vs. C-terminus) (Fig. 2-1B).

To test if different tags at the termini caused varying levels of ATPase activity of purified Drs2p, a dual TAP-tagged construct of Drs2p (TAP_N-Drs2p-TAP_C (III)) was

expressed (Fig. 2-2A). Cdc50p was, again, overexpressed using a strong GPD promoter. Purification of TAP_N-Drs2p-TAP_C, using either the TAP_N tag or the TAP_C tag, yielded purified protein levels that were comparable to the previous experiments (Fig. 2-2B). Theoretically, both preparations should contain Drs2p of the same molecular composition (His_{10}-Drs2p-CBP), which indeed appeared as a single major band on Coomassie-stained gels for both preparations (Fig. 2-2B). Surprisingly, however, ATPase activity was only detected in samples of TAP_N-Drs2p-TAP_C purified using the TAP_N tag, but not the TAP_C tag (Fig. 2-2C), indicating some difference between these two preparations. Western blots revealed a minor Drs2p band with faster mobility in TAP_N-Drs2p-TAP_C samples purified with TAP_N tag, but not with TAP_C (Fig. 2-2D), suggesting a possible link between this faster-mobility band and ATPase activity.

It was possible that the faster-mobility band of Drs2p was a C-terminally cleaved form of Drs2p, which had lost some C-terminal sequences along with the TAP_C tag during purification. This form would not be recovered during purifications using the TAP_C-tag because the tag was lost. To explore this idea, and better determine the relationship between ATPase activity and the faster migrating (or cleaved) Drs2p, TAP_N-Drs2p-TAP_C purified by TAP_N ((III)N) was further applied to a calmodulin column. Consistently, the unbound fraction was enriched with the faster-mobility form of Drs2p (Fig. 2-3A, "U"), whereas the bound fraction was almost devoid of this minor band (Fig. 2-3A, "B"). Furthermore, ATPase activity was significantly higher in the unbound fraction (U) and much lower in the bound fraction (B) (Fig. 2-3B). The simplest explanation for these data is that a C-terminally cleaved, faster migrating Drs2p is primarily responsible for the ATPase activity observed in N-terminally purified Drs2p samples.

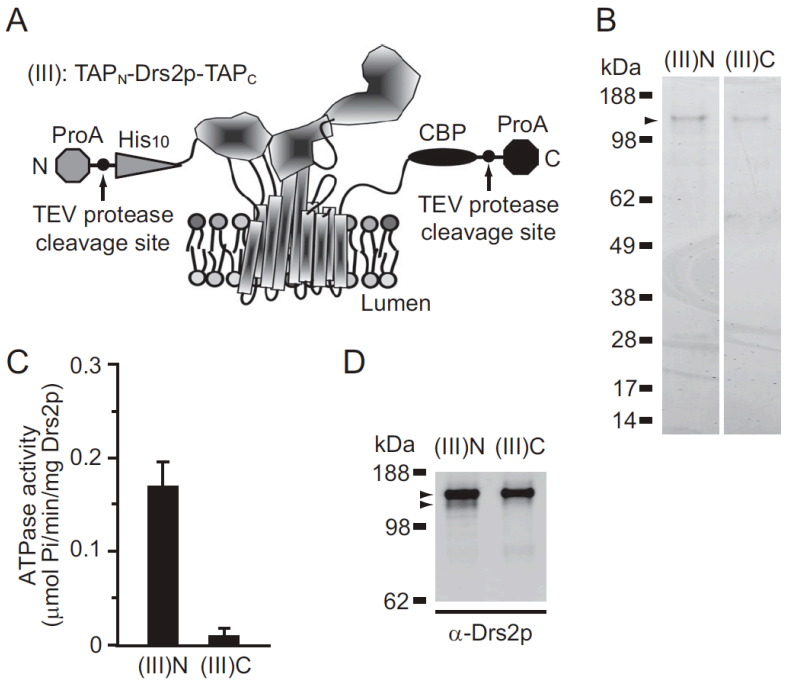

Figure 2-2. Differential activity of TAP$_N$-Drs2-TAP$_C$ purified with either the N-terminal or C-terminal tag. (A) Schematic of TAP$_N$-Drs2p-TAP$_C$ modeled on the SERCA1 crystal structure. (B) Purified TAP$_N$-Drs2p-TAP$_C$ samples from strain XZY85 (*atp2Δ*) using the TAP$_N$ tag (lane 1, (III)N) or TAP$_C$ tag (lane 2, (III)C) were subject to SDS-PAGE and the gel was stained with SimplyBlue. (C) ATPase activity of purified TAP$_N$-Drs2p-TAP$_C$ preparations. (D) Samples from (B) were electrotransferred to polyvinylidene difluoride (PVDF) membrane for western blotting using Drs2 antibodies. The *upper arrowhead* indicates the intact TAP$_N$-Drs2p-TAP$_C$ form and the *lower arrowhead* indicates a minor band with faster mobility. Another faint band migrated below the two arrowheads, but was unlikely to contribute significantly to the ATPase activity. ProA: protein A.

Removal of Drs2p C-terminal tail stimulates Drs2p ATPase activity. To directly test if proteolytic cleavage within the C-terminal tail could stimulate Drs2p activity, the expression cassette was modified so that the C-terminal tail of Drs2p was either retained or removed during purification (Fig. 2-4A, B). To do so, Drs2p was first tagged at C-terminus by the TAP$_{C2}$ tag, which lacks the TEV protease cleavage site. Then, the TEV site was inserted immediately after the C-terminus of Drs2p (Drs2p$_{(TEV)}$-TAP$_{C2}$, (IV)), or

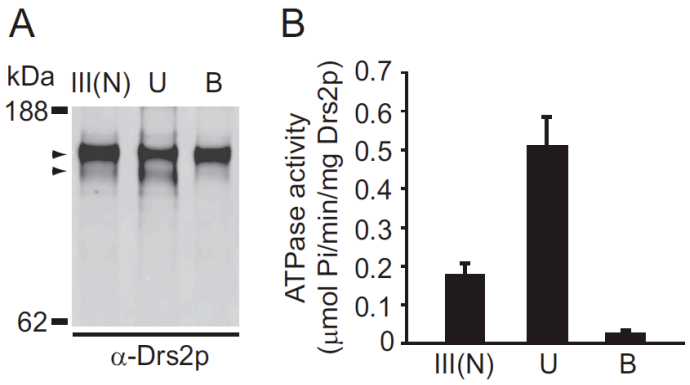

Figure 2-3. Drs2p ATPase activity associates with the faster mobility form. (A) Purified TAP_N-Drs2p-TAP_C before separation (*lane III (N)*), the unbound fraction from the calmodulin column (*lane U*), and the bound and eluted fraction (*lane B*) were subjected to SDS-PAGE and western blotting with anti-Drs2p. The *upper arrowhead* indicates the intact TAP_N-Drs2p-TAP_C form and the *lower arrowhead* indicates the faster mobility form. (B) ATPase activity was assayed with purified TAP_N-Drs2p-TAP_C before separation and the two fractions after separation.

within the C-terminus of Drs2p ($Drs2p_{(TEV)}CT121$-TAP_{C2}, (VI)), close to the C-terminal end of transmembrane segment 10. Cleavage, at the latter TEV site, removes 121 residues from the predicted 137 amino acid long C-terminal tail of Drs2p. An intermediate construct that contains both TEV sites was also constructed for analysis ($Drs2p_{(TEV)}CT121_{(TEV)}$-$TAP_{C2}$, (V)). After purification using TAP_{C2} and final release by TEV cleavage, Drs2p was found to migrate at expected sizes with either full-length or almost no C-terminal tail (Fig. 2-4B). TEV cleavage within the tail was inefficient, as indicated by the doublet in the samples for (V) and the low recovery of the faster migrating form of Drs2p in both the (V) and (VI) preparations.

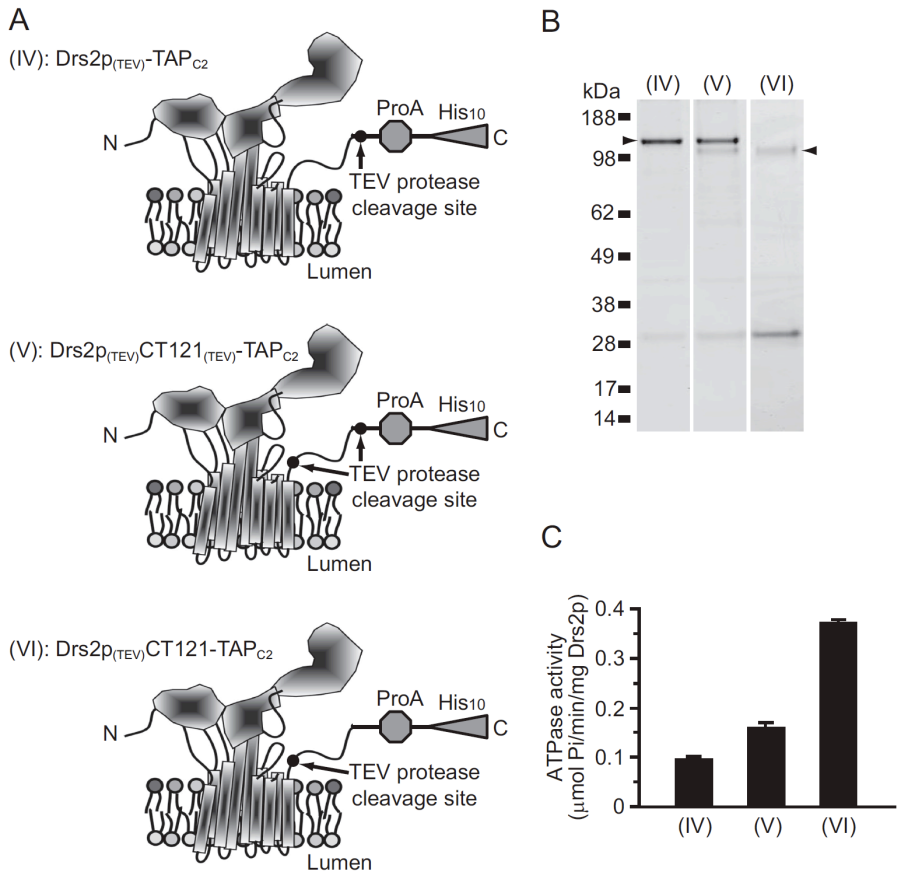

Figure 2-4. Proteolytic removal of the C-terminal tail stimulates Drs2p activity. (A) Schematic of three forms of Drs2p with TEV cleavage sites at different locations in the C-terminal tail. (IV) has a TEV cleavage site between the tail and the TAP_C tag, (V) has two TEV cleavage sites – the first is between transmembrane segment 10 and the C-terminal tail, and the second is between the C-terminal tail and the TAP_C tag, and (VI) has a TEV cleavage site between transmembrane segment 10 and the C-terminal tail. (B) These three variants were purified and the samples were applied to an SDS-PAGE gel and stained with SimplyBlue. Because of the poor recovery of (VI), the TEV protease near the 28kDa marker is overrepresented in this sample. (C) ATPase activity of (IV), (V) and (VI).

Unlike Drs2p-TAP_C (Fig. 2-1D, (II)), purified $Drs2p_{(TEV)}$-TAP_{C2} (IV) displayed low, basal ATPase activity (Fig. 2-4C, (IV)), indicating that the CBP moiety of TAP_C inhibited Drs2p. More importantly, $Drs2p_{(TEV)}$CT121-TAP_{C2} (VI), which has lost the majority of its C-terminal tail, exhibited an approximately 3.5-fold higher specific activity than that of Drs2p with an intact C-terminal tail (Fig. 2-4C, (IV) vs. (VI)). Consistently, the

Drs2p$_{(TEV)}$CT121$_{(TEV)}$-TAP$_{C2}$ (V) preparation, containing a mixture of intact and CT121-cleaved forms, showed an intermediate ATPase specific activity (Fig. 2-4C, (V)). We conclude that the C-terminal tail of Drs2p contains an auto-inhibitory domain, and removal of the C-terminal tail activates Drs2p.

To investigate whether the faster migrating (clipped) form of Drs2p was detectable *in vivo*, whole cell extracts were prepared and a Western blot was performed (Fig. 2-5). A wild-type strain was grown under a variety of conditions (low or high temperature, rich or minimal media) to determine if cleavage events would occur physiologically. Drs2p mobility was also examined in a strain lacking three other P4-ATPases (*dnf1,2,3*Δ), which along with *DRS2* constitutes an essential group of genes with overlapping function. We thought that deleting three of the four members of this group might cause the cells to express a more active form of Drs2p (possibly a cleaved form). However, in all conditions tested, Drs2p migrated slightly slower than the 160kDa marker. We could not detect a form that migrated slightly faster than the 160kDa marker at the same position of purified tail-less Drs2p, even after overexposing the blot (Fig. 2-5). A minor band was detected that migrated at ~130kDa (asterisk in Fig. 2-5), which could represent a proteolyzed form although the functional significance of this form is uncertain. While we cannot rule out the possibility that Drs2p activity can be activated physiologically by proteolytic cleavage, we suspect this cleavage event only occurs after the cells are lysed.

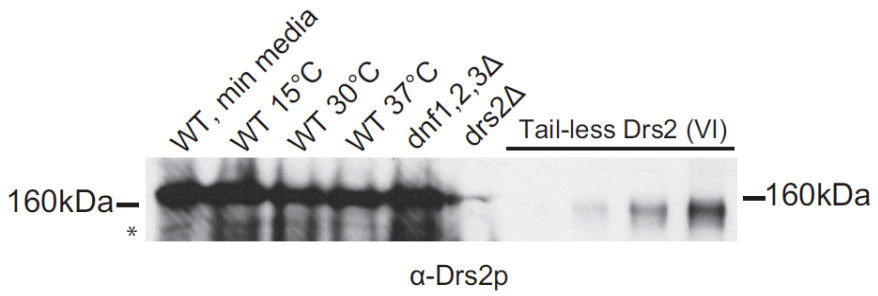

Figure 2-5. The proteolyzed form of Drs2p is not readily detected in cells. A Western blot was performed with whole cell extracts (1 A_{600} of cells) from wild-type strain (BY4742) grown in minimal media at 30°C, rich media at 15°C, rich media at 30°C, and rich media at 37°C. *dnf1,2,3*Δ and *drs2*Δ whole cell extracts were also blotted, as well as aliquots (in increasing concentrations) of purified tail-less Drs2p (Fig. 4, (VI)). A band that migrates faster than the tail-less form of Drs2p is marked with an *asterisk*. The membrane was blotted with α-Drs2p. WT: wild-type.

PS stimulates and PI(4)P activates Drs2p activity. Following observations made previously, we decided to determine the effect that increasing levels of PS had on the ATPase activity of Drs2p. Phosphatidylserine is the preferred substrate of ATPase II/ATP8a1, which has 67% amino acid sequence similarity to Drs2p (Tang et al., 1996). PS strongly stimulates the ATPase activity of Atp8a1 and Atp8a2 in detergent micelles or when reconstituted into phospholipid bilayers (Coleman et al., 2009; Ding et al., 2000; Paterson et al., 2006). In contrast, when assayed in detergent micelles, the ATPase activity of Drs2p is weakly stimulated by PS (by ~20%) (Zhou & Graham, 2009). However, TAP_N-Drs2 displayed approximately 3-fold higher specific activity when reconstituted into PC liposomes containing 20% PS compared to PC liposomes (Fig. 2-6A). Both basal and substrate stimulated activities were inhibited by vanadate as expected. Thus, substrate seems to stimulate Drs2p ATPase activity more effectively when presented in a phospholipid bilayer.

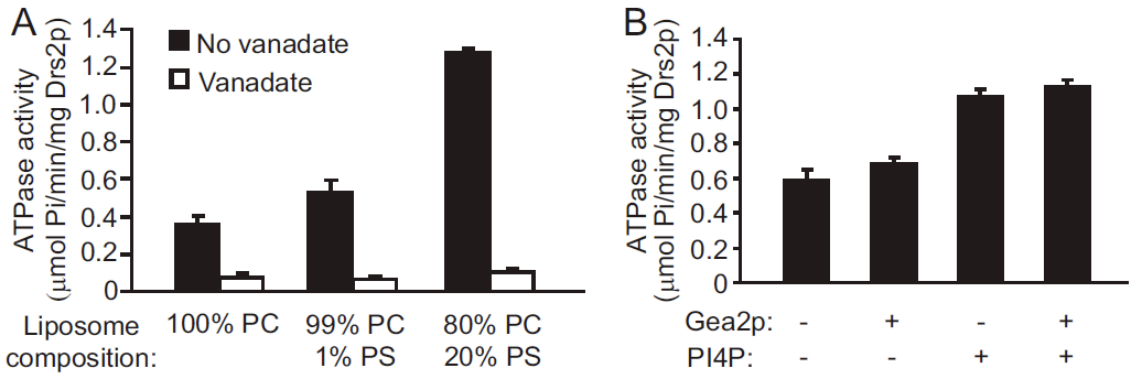

Figure 2-6. Phosphatidylserine and Phosphatidylinositol-4-phosphate stimulates ATPase activity of Drs2p. (A) Purified TAP_N-Drs2p was reconstituted into proteoliposomes containing either 100 mol% DOPC, 99 mol% DOPC with 1 mol% DOPS, or 80 mol% DOPC with 20 mol% DOPS. These proteoliposomes were assayed for ATPase activity either in the presence or absence of 100µM orthovanadate. (B) TAP_N-Drs2p was reconstituted into proteoliposomes comprised of a DOPC backbone with 1 mol% DOPS in the presence or absence of 1 mol% PI(4)P. For each of these proteoliposome samples, ATPase activity was measured in the presence or absence of Gea2p (Sec7 domain) at a ratio of ~1:20 mol:mol Drs2p:Gea2p. The proteoliposomes were incubated with Gea2p for 15 min on ice before assaying for activity. DOPC, 1,2-dioleoyl-*sn*-glycero-3-phosphocholine; DOPS, 1,2-dioleoyl-*sn*-glycero-3-phospho-L-serine.

Natarajan and colleagues have demonstrated that, in isolated Golgi membranes, Drs2p flippase activity is positively regulated by PI(4)P and Gea2p (Sec7 domain), both of which were shown to bind the C-terminal tail of Drs2p (Natarajan et al., 2009). These observations suggest that PI(4)P and Gea2p regulate Drs2p activity by directly binding its C-terminal tail. Alternatively, they may act indirectly through other factors that were present in the membrane samples. To distinguish these two possibilities, we tested whether PI(4)P and/or Gea2p could stimulate the ATPase activity of purified Drs2p reconstituted in proteoliposomes (also containing 2.5% C6 NBD-PS). PI(4)P was added at 1 mol% during proteoliposome formation and Gea2p (recombinant Sec7 domain at a Drs2p:Gea2p ratio of ~ 1:20, mol:mol) was added directly to proteoliposomes containing TAP_N-Drs2p. However, while addition of PI(4)P enhanced the ATPase activity of Drs2p, Gea2p had no effect on overall ATPase activity (Fig. 2-6B). Furthermore, the presence of

both PI(4)P and Gea2p, did not improve the ATPase activity over the levels observed by PI(4)P alone. These data suggest that PI(4)P is directly influencing Drs2p activity, while the Gea2p Sec7 domain alone is insufficient for Drs2 activation (see Discussion).

To further examine the influence of PI(4)P on Drs2p activity, TAP_N-Drs2p was reconstituted into POPC proteoliposomes containing NBD-PS and 0%, 1%, 2.5% or 5% PI(4)P. Stimulation of ATPase activity was observed at all concentrations of PI(4)P with a peak at 2.5% (Fig. 2-7A). Phospholipid translocase activity was also measured in proteoliposomes containing TAP_N-Drs2p using a dithionite quenching assay to monitor ATP-dependent translocation of NBD-PS from the inner leaflet to the outer leaflet. In this case, the amount of NBD-PS flipped by TAP_N-Drs2p also increased with increasing concentrations of PI(4)P (Fig. 2-7B). Proteoliposomes containing 5% PI(4)P did not form a tight seal to dithionite and were, therefore, not assayed. While PI(4)P appeared to stimulate TAP_N-Drs2p flippase activity, there was substantial variability between replicates leading to a large standard deviation for each data set.

We hypothesized that the variability in translocase activity with TAP_N-Drs2p likely arose from differing extents of C-terminal tail proteolysis in each preparation of enzyme. For instance, the proteoliposomes may have either the full-length form of TAP_N-Drs2p, the clipped form or a mixture of the two forms, which could lead to variability in the activity observed. One of the Drs2p preparations used in the assays shown in Figure 2-7A and 2-7B clearly displayed the full-length and clipped forms (Fig 2-7A, inset).

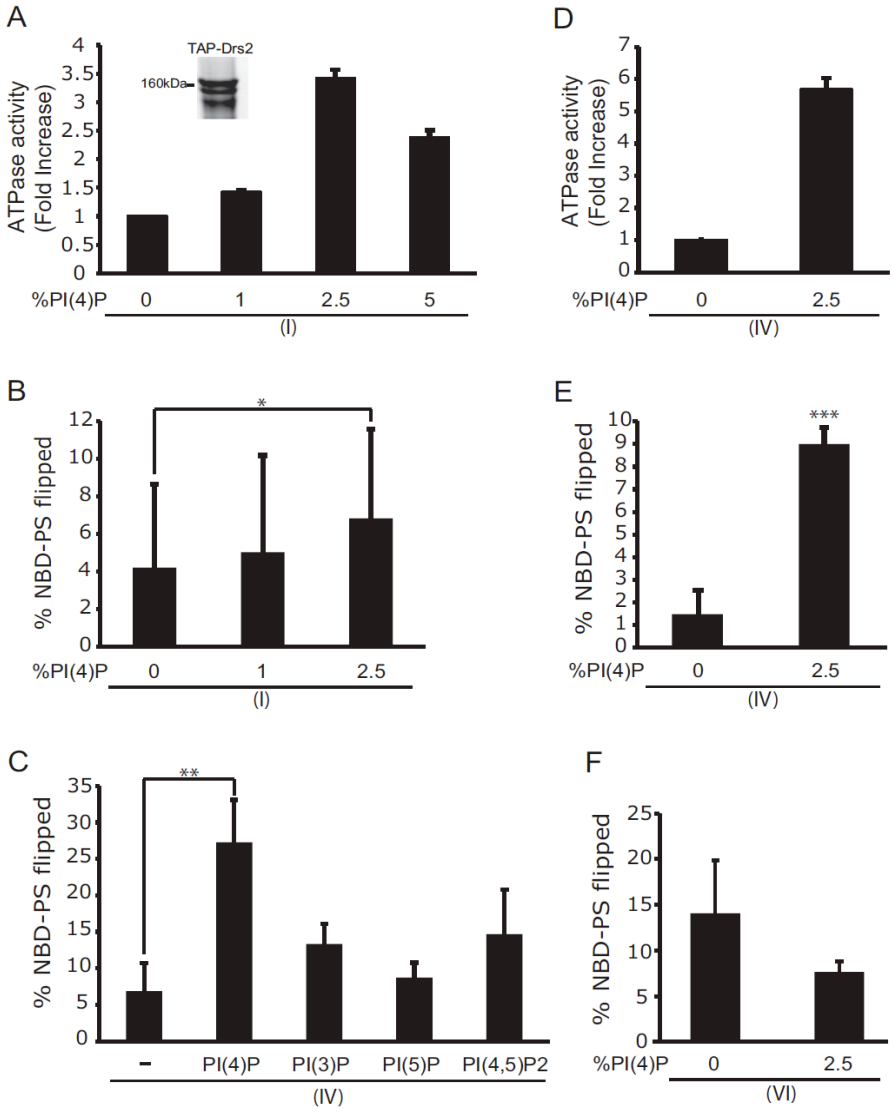

Figure 2-7. PI(4)P directly stimulates Drs2p ATPase and NBD-PS flippase activity. TAP_N-Drs2p (I) was reconstituted into proteoliposomes comprised of a DOPC backbone with 2.5mol% C12 NBD-PS and the indicated amount of PI(4)P. (A) ATPase activity of TAP_N-Drs2p (I) after subtracting the orthovanadate controls. A coomassie stained sample of purified TAP_N-Drs2p shows a faster migrating band, which is possibly the proteolyzed form of Drs2p (inset). (B) Drs2p proteoliposomes were assayed for NBD-PS flippase activity. The data are averages from 14 experiments +/- s.d. (C) $Drs2p_{(TEV)}$-TAP_{C2} (Fig. 4 (IV)) was purified and reconstituted into proteoliposomes containing DOPC, 2.5mol% C12 NBD-PS and 2.5mol% PI(4)P, PI(3)P, PI(5)P or $PI(4,5)P_2$. The sample marked "-" contains no phosphoinositide. (D) $Drs2p_{(TEV)}$-TAP_{C2} (IV) was purified, reconstituted and assayed for ATPase activity and (E) NBD-PS flippase activity (n=3 independent experiments). (F) $Drs2p_{(TEV)}$CT121-TAP_{C2} (Fig. 4, (VI)) was purified, reconstituted and assayed for NBD-PS flippase activity (n=3 independent experiments). * $p<0.05$, ** $p<0.01$, *** $p<0.0001$.

To overcome this limitation, Drs2p$_{(TEV)}$-TAP$_{C2}$ (Fig. 2-4, (IV)), which yields a full-length form of Drs2p with an intact C-terminal tail, was purified and reconstituted into proteoliposomes in the presence or absence of 2.5mol% PI(4)P. The ATPase activity of the full-length Drs2p was stimulated almost 6-fold in the presence of PI(4)P (Fig. 2-7D). The NBD-PS flippase activity was similarly enhanced by PI(4)P (Fig. 2-7E). Accordingly, the variation in flippase activity that was observed with TAP$_N$-Drs2p was no longer observed with the full-length form of Drs2p. Furthermore, Drs2p$_{(TEV)}$CT121-TAP$_{C2}$ (Fig. 2-4, (VI)) was purified and reconstituted into proteoliposomes. These samples, when assayed for flippase activity, were found to be slightly more active in the absence of PI(4)P, as they were in proteoliposomes that contained 2.5% PI(4)P (Fig. 2-7F). Thus, tail-less Drs2 is no longer responsive to PI(4)P and these data are consistent with the proposed model that PI(4)P activates Drs2p through direct interaction with the Drs2p C-terminal tail.

To determine if the C-terminal tail of Drs2p has a preference for a specific phosphoinositide, we purified the full-length Drs2p (Fig. 2-4, (IV)) and reconstituted it into PC/PS proteoliposomes containing different phosphoinositides. The proteoliposomes contained either no phosphoinositides, or 2.5mol% of PI(4)P, PI(3)P, PI(5)P or PI(4,5)P_2. PI(4)P significantly stimulated the flippase activity of Drs2p compared to the other phosphoinositides (Fig. 2-7C). Thus, PI(4)P preferentially interacts with the C-terminal tail of Drs2p to stimulate Drs2p activity.

Discussion

A model for Drs2p C-terminal tail auto-inhibition and regulation. When this study and published data are taken together, a model for the regulation of Drs2p can be proposed. Drs2p has a C-terminal cytosolic tail predicted to be 137 amino acids long. The tail likely contains an auto-inhibitory domain (an R domain) that keeps Drs2p activity at a low, basal level within membranes that lack PI(4)P (e.g. the ER and early Golgi). Upon arrival in the TGN, Drs2p would be activated by the high levels of PI(4)P in this compartment. We show that the TAP_N-Drs2p samples, purified with the N-terminal tag, and which contain a faster-migrating, clipped form of Drs2p, has a higher level of ATPase activity when compared to preparations of Drs2p-TAP_C, which lacks the cleaved form of Drs2p. Thus, it appears that a cleavage event within the C-terminal tail of Drs2p enhances activity of TAP_N-Drs2p. A Western blot of whole cell extracts of wild-type strains (grown under various conditions) and mutant strains did not show substantial cleavage of Drs2p. The cleavage event observed in the purified protein samples most likely occurs after cell lysis and there is no indication that proteolysis is a physiologically relevant mechanism for activating Drs2p.

Furthermore, when Drs2p is purified with the full-length tail intact, the ATPase activity levels of Drs2p are quite low – but still detectable (Fig. 2-4C, (IV)). Reconstituted full-length Drs2p also has low levels of flippase activity (Fig. 2-7D, 0% PI(4)P). However, once the tail is cleaved off during purification using an engineered TEV site, we observe a significant increase in Drs2p specific activity (Fig. 2-4C, (VI)). Therefore, removal of the C-terminal tail stimulates activity. As in the case of the other P-type ATPases, the R

domain (as described in the introduction) had the ability to self-regulate the activity of the P-type ATPase. Relieving the interaction between the R domain and the P-type ATPase stimulated the activity of the protein (Carafoli, 1994; Palmgren, 2001; Portillo, 2000; Sze et al., 2000). This study, similarly, provides direct evidence for a role of the C-terminal tail (and an R domain) in regulating the activity of Drs2p.

The role of effectors in regulating the activity of Drs2p. In purified TGN membranes, it has been shown that the addition of Gea2p (Sec7 domain) stimulates the phospholipid translocase activity of Drs2p (Natarajan et al., 2009). Furthermore, the addition of both PI(4)P and Gea2p to the samples, stimulated the flippase activity of Drs2p to greater levels than either of them did individually. In this study, we attempted to recapitulate these observations in the reconstituted system. And, while addition of PI(4)P to Drs2p-proteoliposomes activated the P4-ATPase (Fig. 2-6B, Fig. 2-7), the Gea2p Sec7 domain had little effect on the specific activity of Drs2p, even when added in concert with PI(4)P (Fig. 2-6B).

During the course of our studies, work published recently from the lab of Fang-Jen Lee provides a likely explanation for these observations (Tsai, Hsu, Liu, Chen, & Lee, 2013). Arl1p (Arf-like protein 1) is a member of the small GTP-binding protein family that cycles, like Arf, between active GTP-bound and inactive GDP-bound forms. Like Drs2p, Arl1p also localizes to the TGN in yeast (Peyroche, Courbeyrette, Rambourg, & Jackson, 2001; Peyroche, Paris, & Jackson, 1996). The Lee group was able to show that all three proteins – Drs2p, Gea2p, and Arl1p – form a stable ternary complex through direct interactions with each other. This complex is important for stimulating the flippase

activity of Drs2p at the Golgi. Furthermore, Arl1p function at the Golgi also requires this complex. To our reconstituted system, we added the recombinantly purified Sec7 domain of Gea2p. However, it is the N-terminal portion of Gea2p (upstream of the Sec7 domain) that is responsible for interacting with Arl1p (Tsai et al.). Additionally, Arl1p was absent from our reconstituted reactions. However, in purified Golgi membranes, it is likely that Arl1p-GTP co-purifies with the membrane (Natarajan et al., 2009). As a result, in the presence of Gea2p, the activity of Drs2p was stimulated. Our data imply that the interaction of Gea2p Sec7 domain is insufficient to activate Drs2p when Arl1p-GTP is absent. More work will be needed to determine the temporal and spatial organization of these various effectors and regulators during the formation of transport vesicles at the Golgi.

While a previous study was able to show that PI(4)P stimulates the flippase activity of Drs2p in purified Golgi membranes (Natarajan et al., 2009), this study provides the first evidence, in a reconstituted system, that PI(4)P directly regulates the activity of Drs2p. When the full-length form of Drs2p (Fig. 2-4, (IV)), is reconstituted, PI(4)P is able to stimulate a 6-fold increase in the ATPase and flippase activities (Fig. 2-7D, 2-7E). In contrast, tail-less Drs2p (Fig. 2-4, (VI)) does not display a difference in lipid translocase activity when reconstituted in the presence or absence of PI(4)P (Fig. 2-7F).

The step at which PI(4)P exerts its influence seems to be the dephosphorylation step of the Drs2p catalytic cycle (Jacquot et al., 2012). P4-ATPases do not require the presence of substrate for phosphorylation (E1 to E2-P), although for the mammalian orthologs of Drs2p, ATP8A1 and ATP8A2, the PS substrate potently stimulates dephosphorylation

(E2-P to E1) (Coleman, Vestergaard, Molday, Vilsen, & Andersen, 2012; Ding et al., 2000). In contrast, PS slows down the ability of Drs2p to undergo dephosphorylation, whereas addition of PI(4)P to the reaction strongly accelerates this step. Addition of PI(4)P in the absence of PS, meanwhile, only had a small effect on dephosphorylation (Jacquot et al., 2012). So, the major role that PI(4)P plays is at the dephosphorylation step – the point at which the phospholipid substrate has been loaded into the flippase, presumably at a site we described as the exit gate formed from residues in the first four transmembrane segments (Baldridge & Graham, 2012; Baldridge & Graham, 2013; Baldridge, Xu, & Graham, 2013). Displacement of the C-terminal R domain by interaction with PI(4)P would then allow dephosphorylation and ejection of substrate into the cytosolic leaflet.

CHAPTER III

INFLUENCE OF Drs2p FLIPPASE ACTIVITY ON MEMBRANE MORPHOLOGY

Introduction

As described in Chapter I, we hypothesized that the flippase activity of Drs2p plays a part in bending the membrane during transport vesicle formation. The reason is that the flipping of phospholipids across membrane leaflets causes an increase in the number of phospholipids on one leaflet compared to the other. This increase in phospholipid number results in the expansion of the surface area of the leaflet. In response to this expansion, the other leaflet contracts because both leaflets are coupled. In this chapter, I outline experiments and assays designed to determine what role is played by Drs2p in the creation of membrane curvature.

The initial strategy was to purify TGN membranes containing either a wild-type copy of Drs2p or a temperature sensitive form of Drs2p, and determine if activating Drs2p flippase activity with the addition of ATP induces any morphological change in the isolated membranes. The second approach was to purify Drs2p, reconstitute this protein in giant unilamellar vesicles (GUVs) and test whether activation of Drs2p would induce shape changes in the membrane.

Influence of Drs2p Activity on the Morphology of Purified Golgi Membranes

Our lab has been able to show that, in the absence of Drs2p, there is no AP-1/CCV function even though the coat is recruited to the TGN. We believe that Drs2p contributes to membrane curvature based on the bilayer-couple hypothesis proposed by Sheetz and Singer (Sheetz & Singer, 1974). Drs2p, we hypothesize, catalyzes flipping of phospholipids from one leaflet to the other, expands the outer leaflet causing membrane bending since the two leaflets are coupled. This curvature is captured by curvature-sensing proteins that are able to recruit AP-1 and clathrin onto the membrane (Graham & Kozlov, 2010). In this section, I put forth experiments to test the role of Drs2p on membrane curvature and its influence in vesicle budding using purified Golgi membranes.

Results and Discussion

A former graduate student, Zhaolin Hua, created yeast strains that are deficient in four of the five yeast P4–ATPases (Natarajan et al., 2004). These four flippases, Drs2p, Dnf1p, Dnf2p and Dnf3p, form a group of essential genes since deletion of this group of genes is fatal to the cell (Hua et al., 2002). The strains created were kept alive with either a wild–type or temperature–sensitive copy of *DRS2* on a plasmid (*DRS2* or *drs2-ts*). These strains are designated ZHY409 (*drs2Δ dnf1Δ dnf2Δ dnf3Δ pRS313 DRS2*) and ZHY410–3A (*drs2Δ dnf1Δ dnf2Δ dnf3Δ pRS313 drs2–31*). The advantage of using these strains, for my experiments, is that *drs2-ts* can be inactivated by temperature shift of purified Golgi

membranes (Natarajan et al., 2004). Thus, we can determine if any ATP-induced changes in membrane morphology is due to Drs2p activity.

To purify *trans*-Golgi membranes, fractions were prepared by differential centrifugation and sucrose gradient fractionation as described in Natarajan and Graham (Natarajan & Graham, 2006). The sucrose gradient fractionation step allows for the separation of early Golgi membranes (*cis*–Golgi) from the late Golgi membranes (*trans*–Golgi network). The various fractions containing these membranes are distinguished by the amount of Kex2p activity present. Kex2p is normally found on the late Golgi membranes and Drs2p co–fractionates with this protein. High values for Kex2p activity in the colorimetric Kex2 assay allows the determination of fractions concentrated in TGN membranes (Natarajan & Graham, 2006). The Bicinchoninic Acid Assay Kit (BCA Kit: a colorimetric assay) was used to determine the concentration of protein present in the TGN membrane preparations.

The strains ZHY409 (*DRS2*) and ZHY410–3A (*drs2-ts*) were grown in 2L of YPD at 27°C (permissive temperature) to an OD_{600} value of approximately 0.4–0.45 OD_{600}/mL. Half of each of the cultures (1L) were then shifted for one hour to 37°C which is a non–permissive temperature for the *drs2-ts* strain. This shift should abrogate Drs2p protein function in the *drs2-ts* cells. The other half of the culture was maintained at 27°C for an hour. The cells were then harvested and the Golgi membranes were isolated as described. Late Golgi membrane fractions were identified using the Kex2 Assay and these membranes were used for further study.

The morphology of purified late Golgi membranes was first studied by using negative stain EM (Fig. 3-1 A and B). The population of membranes were very heterogenous in size and the average diameter of the membranes ranged from 65 – 100nm, with membranes as large as 500nm, and as small as 30nm. This observation held true for Golgi membranes from both *DRS2* and *drs2-ts*, harvested from cells grown at 27°C (Fig. 3-1A), as well as from cells shifted to 37°C (Fig. 3-1B). Most of these are assumed to be Golgi membranes although some may be small transport vesicles or early endosomal membranes. The average diameters of the membranes is presented in Fig. 3-1C. The protein composition of the Golgi membrane preps was compared to whole cell lysates of each of the strains by running them on SDS–PAGE and immunoblotting (Fig. 3-1D). Analysis of the membranes by Western blot showed that they were enriched for Drs2p compared to the whole cell extract samples. There was no obvious difference in the amounts of Drs2p detected in Golgi membranes from either of the two strains tested and at either of the temperatures tested. Arf and Clathrin, meanwhile, were depleted in the late Golgi membranes compared to the whole cell extracts. Work done by other members of the lab have suggested that these membranes also lack detectable AP–1.

The goal for these experiments was to observe whether late Golgi membranes would vesiculate or tubulate, in the presence of ATP, due to the flippase activity of Drs2p. The large variation in the membrane size would hinder analysis of this reaction. Furthermore, *DRS2* and *drs2-ts* are very slow-growing strains and have other defects due to the loss of three of the four flippases in the essential gene family (Fig. 3-3A). To determine if the heterogeneity in membrane size was due to defects in the strains, I purified late Golgi

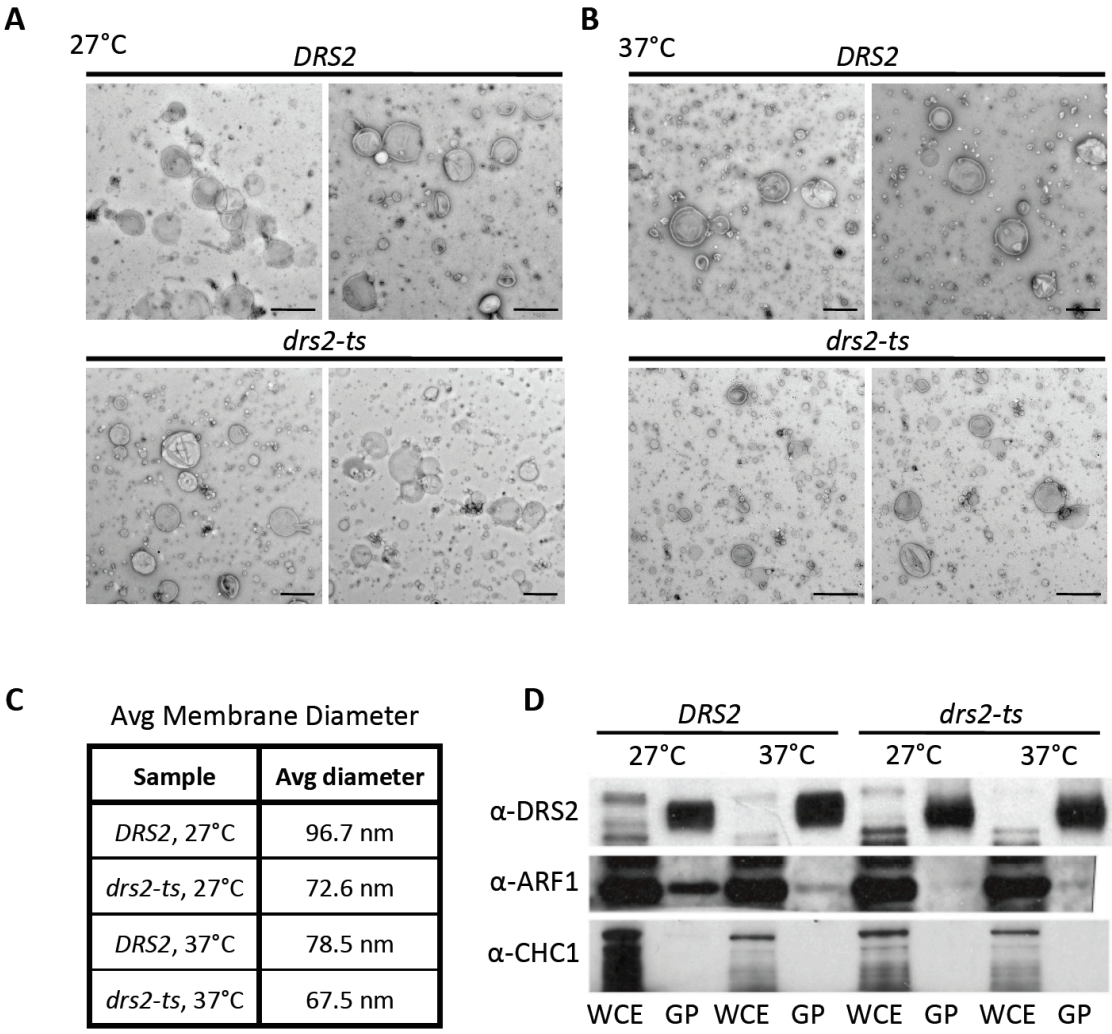

Sample	Avg diameter
DRS2, 27°C	96.7 nm
drs2-ts, 27°C	72.6 nm
DRS2, 37°C	78.5 nm
drs2-ts, 37°C	67.5 nm

Figure 3-1. Morphology and protein composition of TGN membranes purified from *DRS2* and *drs2-ts*. (A) Negative EM images of TGN membranes from *DRS2* and *drs2-ts*, grown at 27°C. (B) Negative EM images of TGN membranes from *DRS2* and *drs2-ts*, grown at 27°C then shifted to 37°C for 1 hour prior to harvesting. Scale bar: 100nm. (C) Average diameter of the membranes imaged in (A) and (B). n > 200 membranes. (D) Western blots for *DRS2* and *drs2-ts* TGN membranes (grown either at 27°C, or 27°C + 37°C for 1 hour) blotted for the presence of Drs2p, Arf1p, and clathrin heavy chain (CHC1). WCE: whole cell extract. GP: TGN membrane prep.

membranes from a wild-type strain (BY4742) and a *kes1*Δ strain. Kes1 is an oxysterol binding protein homolog in yeast and is a negative regulator of vesicle budding at the Golgi. The advantage of using a *kes1*Δ strain is that Drs2p-dependent phosphatidylserine flippase activity is hyperactive in *kes1*Δ TGN membranes (Muthusamy, Raychaudhuri, et al., 2009).

When the late Golgi membranes from the WT and *kes1*Δ strains were imaged by negative stain EM, I observed more larger membranes (80-200nm) and considerably fewer small membranes (<50nm) in the preps (Fig. 3-2A). Consequently, there was an increase in the average diameter of the membrane (around 150nm) (Fig. 3-2B). The presence of more, larger membranes will make it easier to distinguish tubulation and vesiculation of the membranes in the future experiments. Analysis of the membranes by Western blots showed that Drs2p, in the Golgi preps, was enriched compared to the whole cell extracts, while the (mostly) cytosolic proteins, Arf, Clathrin and Swa2p (or auxilin), were depleted in these samples (Fig. 3-2C).

One interesting observation was that, on the Western blots, the Drs2p band migrated about 10kDa faster in the Golgi membrane preps than in the whole cell extract samples (Fig. 3-3B). Two possible reasons for this migration pattern are that: (a) Drs2p is getting cleaved during the membrane purification process, or (b) native Drs2p, at the late Golgi membrane, could be present in a cleaved form. Although the following information was not known at the time these experiments were performed, as discussed in Chapter 2 of this thesis, cleaving the C-terminal tail of Drs2p, removes self-regulation and increases

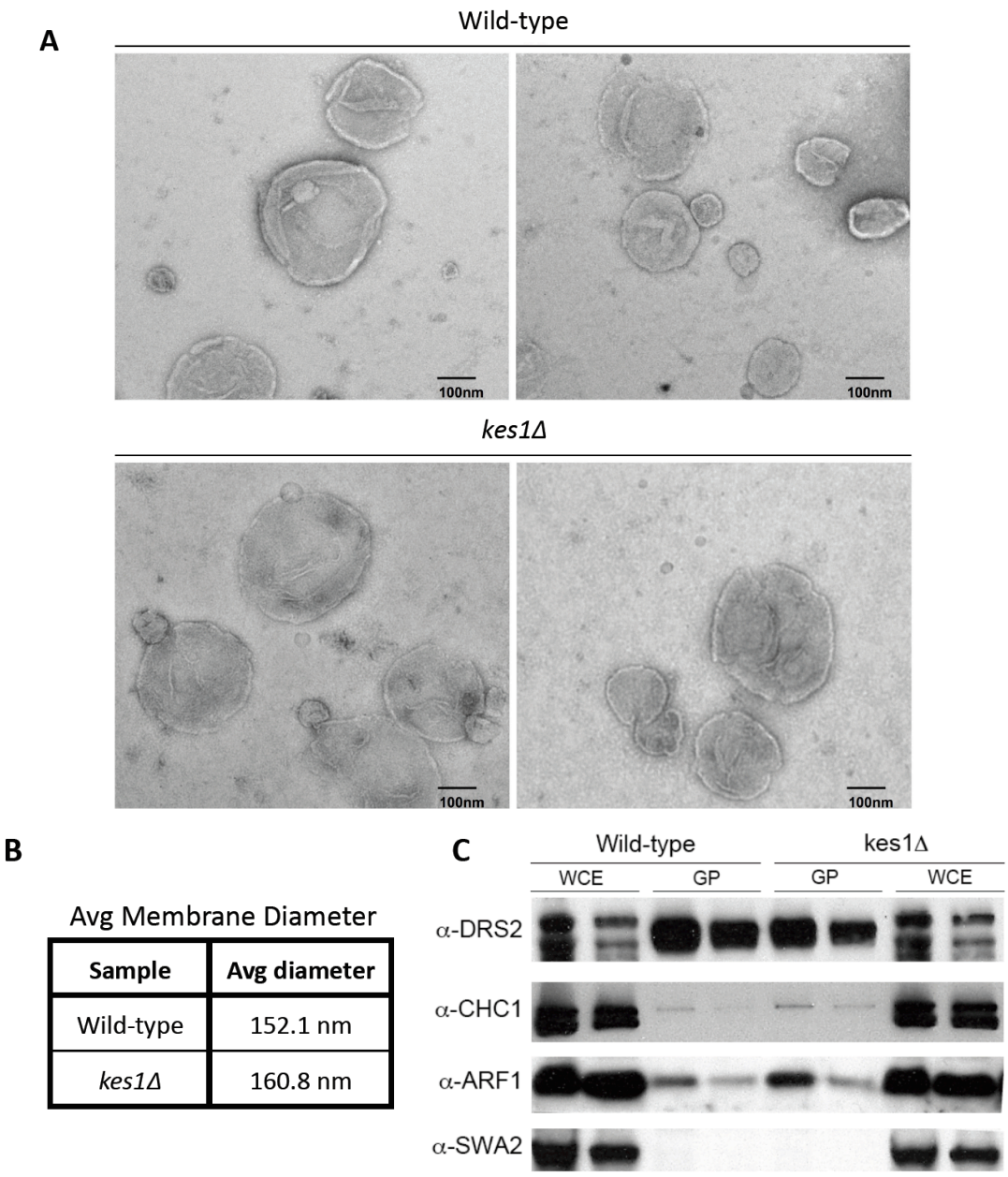

Figure 3-2. Morphology and protein composition of TGN membranes purified from wild-type (WT) and *kes1*Δ. (A) Negative EM images of TGN membranes from wild-type and *kes1*Δ, grown at 27°C. Scale bar: 100nm. (B) Average diameter of the membranes imaged in (A). n > 200 membranes. (C) Western blots for wild-type and *kes1*Δ TGN membranes (grown at 27°C) blotted for the presence of Drs2p, Arf1p, clathrin heavy chain (CHC1), and Swa2p (auxilin). For each sample, the well on the right represents half the amount of sample loaded in the left well. WCE: whole cell extract. GP: TGN membrane prep.

its activity (Zhou et al., 2013). It is possible that Drs2p might be present in a more active form at the late Golgi; hence its presence, in purified late Golgi membranes, in the clipped form. Another possibility is that Drs2p is partially proteolyzed during the purification of the TGN membranes. The initial sample (WCE) had very little, if any, of the faster-mobility form of Drs2p, which appeared after the purification of the TGN membranes. Thus, proteolysis appears to occur during purification. In Fig. 3-3A, the relative growth rates of the strains used for these experiments is examined. Serial dilutions were done of wild-type (WT), *DRS2* (ZHY409), *drs2-ts* (ZHY410-3A), *kes1*Δ, and *drs2*Δ (which was used as a control). *DRS2* and *drs2-ts* are slow growing strains at all the temperatures tested, and *drs2-ts* is unable to grow at 37°C (which is non-permissive for the temperature sensitive strain, *drs2-ts*). *DRS2* is also extremely slow-growing at 37°C.

To test the influence that addition of ATP would have on the morphology of these Golgi membranes, each of the four strains were incubated with an ATP regeneration system at 37°C. Samples were taken at 0 min and 15 min respectively and imaged by negative stain EM. The wild-type membranes, when imaged, exhibited both elongation and tubulation (Fig. 3-4A). When membranes were counted (n ~ 500), 8 times as many membranes exhibited tubulation, while 2 times as many membranes showed elongation, after 15min ATP incubation (compared with the 0min, +ATP control). In total, approximately 7% of WT membranes exhibited tubulation or elongation 15min after incubation with ATP, compared to 2.2% of the 0min (+ATP) control and 1.7% of the –ATP (15 min) control (For table, see Fig. 3-4B).

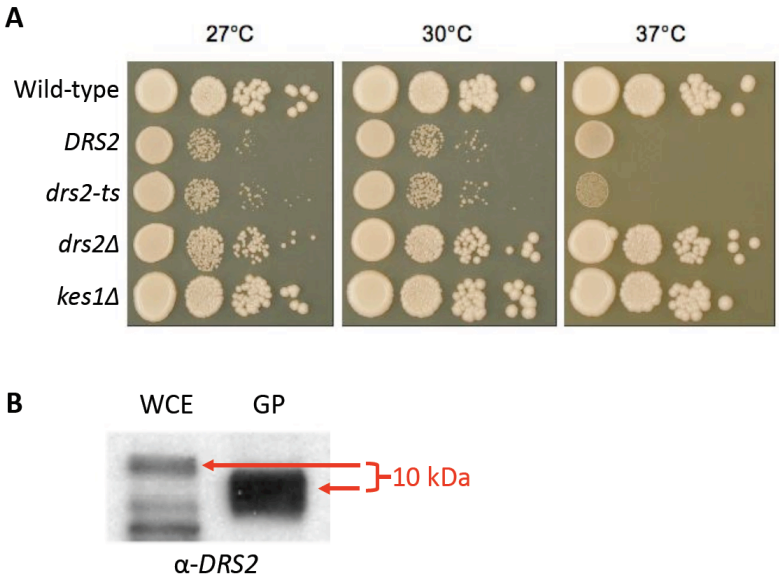

Figure 3-3. Growth rate of strains and cleavage of Drs2p in TGN preps. (A) Serial dilutions to determine the relative growth rate of the various strains used for TGN membrane preps at 27°C, 30°C, and 37°C. The plates were grown for 3 days. (B) Western blot showing the difference in migration between Drs2p in whole cell extracts versus Golgi preps. WCE: whole cell extract. GP: TGN membrane prep.

To examine whether ATP would have a similar effect on *kes1*Δ membranes or the quadruple mutant (*DRS2* or *drs2-ts*; both grown at 27°C) membranes, the above experiment was repeated with samples of each of the respective membranes (Fig. 3-4 C-E). When these membranes were imaged, tubulation or elongation of the membranes was not as easily detectable as with the WT membranes. However, another phenotype is evident between the +ATP, 15min sample and the –ATP, 15min control samples. In *kes1*Δ and *DRS2*, the number of small membranes present in the +ATP sample (Fig. 3-4C and D, left panels) was significantly decreased compared to the control samples (Fig. 3-4C and D, right panels). In the *drs2-ts* samples, however, the difference is not quite so stark. These membranes were grown at 27°C and should have active Drs2p. It would be

expected that when *drs2-ts* is incubated with ATP at 37°C, Drs2p should be inactivated and there should be no significant difference between +ATP (15min) and the control samples. When the experimental and control images are compared, this seems to be the case (Fig. 3-4E). However, ATP incubation is done at 37°C and it is possible that the short amount of time between ATP addition and the temperature of the sample reaching 37°C might have caused a small amount of fusion of the membranes to occur. This is a possible explanation why there is a slight decrease in the number of small membranes in the +ATP *drs2-ts* samples compared to the control. However, the change is not quite as drastic when it is compared to the +ATP samples of *kes1*Δ and *DRS2*.

Another observation is that the number of large membranes in the population (in *kes1*Δ and *DRS2*, +ATP samples) increases after ATP incubation. From the images obtained, it appears that incubation of the membranes with ATP is causing membrane fusion. Re-examining the WT membranes shows this to be true in that case as well – you can clearly see that there are more small membranes in the –ATP, 15min (Fig. 3-4A, lower panels) when compared to the +ATP sample. Thus, it seems that ATP incubation is causing membrane fusion and the elongation and/or tubulation that was being detected in the WT membranes may be the fusion of smaller membranes to form larger membranes.

Another goal of this project was to define the influence that Drs2p activity had on clathrin-coated vesicle budding. Previous work from our lab has shown that AP-1/Clathrin function is lost in *drs2*Δ cells, even though the coat is recruited to the TGN (Liu et al., 2008). One of the hypotheses presented in this chapter proposes that the

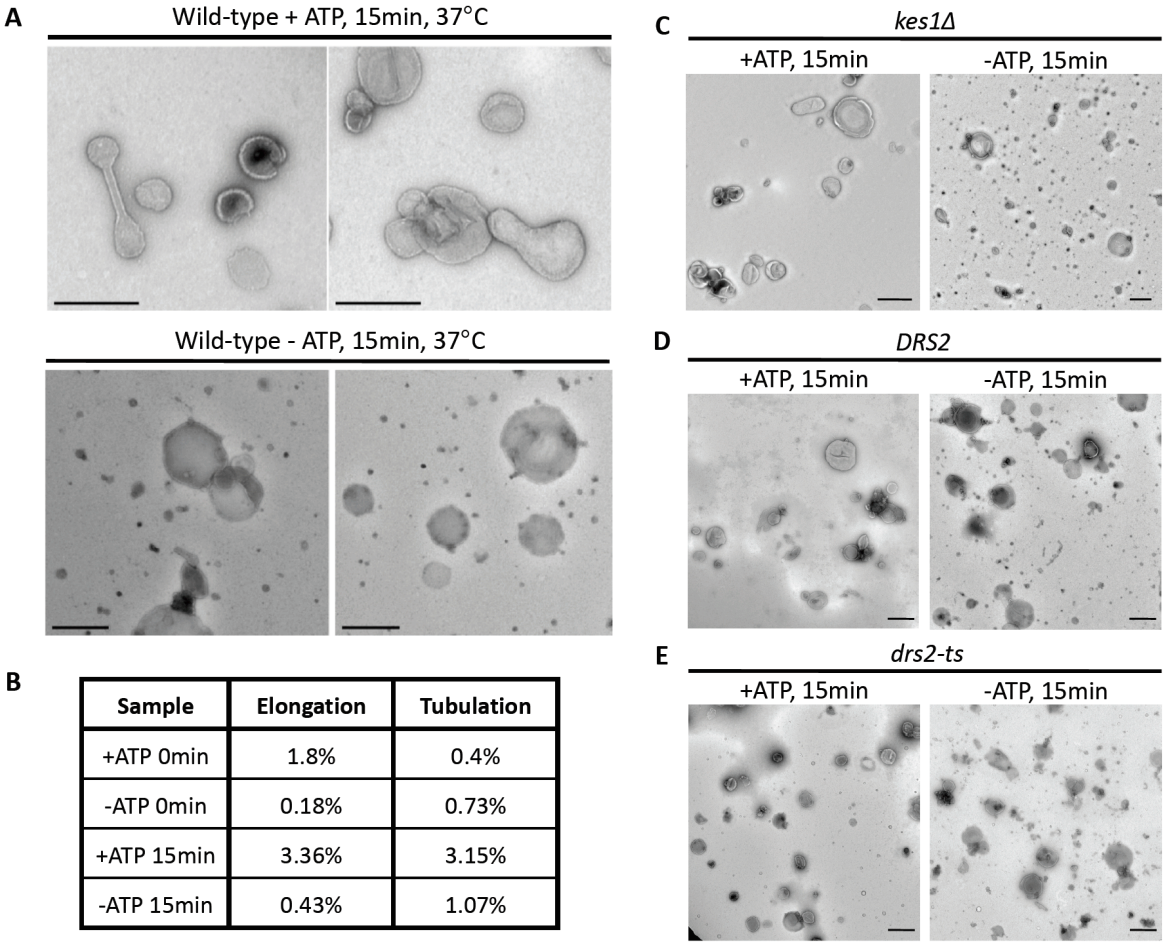

B

Sample	Elongation	Tubulation
+ATP 0min	1.8%	0.4%
-ATP 0min	0.18%	0.73%
+ATP 15min	3.36%	3.15%
-ATP 15min	0.43%	1.07%

Figure 3-4. Influence of ATP addition on late Golgi membranes. (A) Wild-type membranes were incubated in the presence or absence of an ATP regeneration system for 15min, at 37°C, and imaged by negative stain EM. (B) Table showing the amount of elongation or tubulation observed in the wild-type samples at 0min and 15min, +/- ATP regeneration system. (C) Negative EM of *kes1*Δ TGN membranes after incubation +/- ATP at 15min. (D) Negative EM of *DRS2* TGN membranes after incubation +/- ATP at 15min. (E) Negative EM of *drs2-ts* TGN membranes after incubation +/- ATP at 15min. Membranes in (C) – (E) were harvested from strains grown at 27°C. Scale bar: 500nm.

flippase activity of Drs2p generates membrane curvature and allows for the formation of clathrin-coated vesicles at the TGN (Liu et al., 2008). To this end, the goal was to establish a system where the Golgi membranes would provide Drs2p, while the cytosol

fraction would provide the factors (such as Arf, AP-1 and clathrin) needed for creating clathrin-coated vesicles.

As observed in the Western blots, Golgi membrane preps lack many of the cytosolic proteins, such as AP-1 and clathrin, that are needed to make clathrin-coated vesicles (Fig. 3-1D, Fig. 3-2C). Cytosol was purified from wild-type cells using a differential centrifugation approach (Vida, Graham, & Emr, 1990). Basically, cells were lysed and subjected to centrifugation at extremely high speeds to pellet most of the membranes and vesicles. The concentration of protein in the remaining supernatant, considered the cytosol, was determined by BCA Assay. When this cytosolic prep was imaged (Fig 3-5A, 3mg/mL protein concentration), a lot of small structures, that resembled small "membranes" or "vesicles" similar to ones observed in late Golgi membrane preps, were observed. A Western blot of the cytosol preps showed that Drs2p was detectable in the prep (Fig. 3-5B); this suggested that vesicles were present in these preps, and these small vesicles did not pellet with the larger membranes during preparation of the cytosol. The presence of Drs2p in the cytosol proved problematic since I wanted the activity that was detected to come from, and be due to, the Drs2p present in the late Golgi membranes (especially when considering that the Drs2p present in *drs2-ts* was a mutant temperature sensitive form, and *drs2-ts* is an important strain in these experiments). Furthermore, it is unclear how much AP-1 and clathrin is associated with these vesicles which would hinder the development of the *in-vitro* assay for the reconstitution of clathrin-coated vesicle budding.

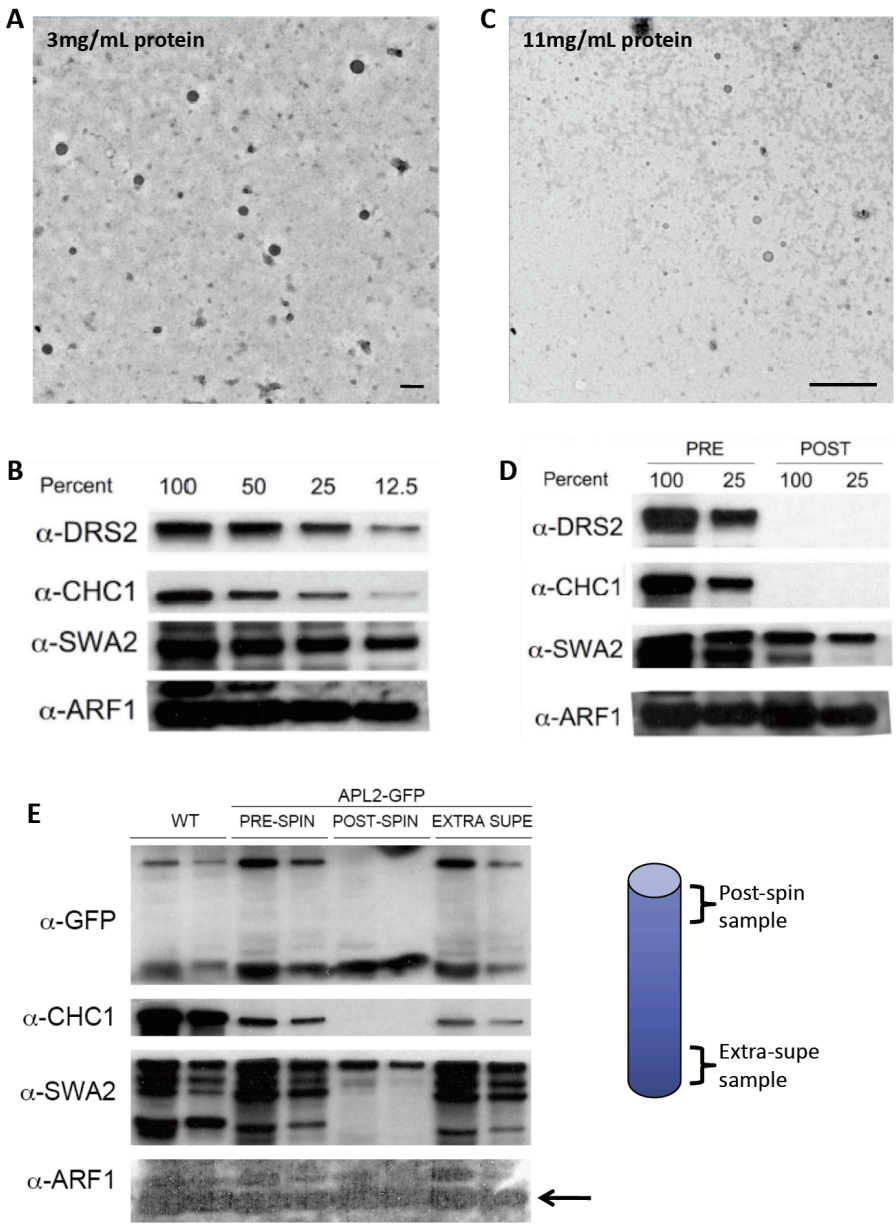

Figure 3-5. Purification and composition of cytosol. (A) Negative stain EM of cytosol purified from wild-type cells. 3mg/mL protein as determined by Bicinchoninic Acid (BCA) assay. (B) Western blot showing the relative amounts of Drs2p, clathrin heavy chain (CHC1), Swa2p (auxilin), and Arf1p in the cytosol prep. The 100% sample contains 30μg of overall protein. (C) Negative stain EM of cytosol after centrifugation at 300k x g for 1 hour. 11mg/mL of protein as determined by BCA assay. (D) Western blot showing the relative amounts of Drs2p, clathrin heavy chain (CHC1), Swa2p, and Arf1p in the cytosol prep imaged in (C). The 100% sample contains 55μg of overall protein. (E) Western blot showing the relative amounts of GFP, Chc1p, Swa2p and Arf1p in the APL2-GFP cytosol prep, both before and after high speed centrifugation (left panel). Image of a tube showing the where the "Post-spin" and "Extra-supe" samples were derived. Scale bar: 100nm.

To remove the vesicles containing Drs2p, the cytosol was centrifuged at 300,000 x g for 1 hour. The resulting sample was imaged at a concentration of 11mg/mL protein (Fig. 3-5C), and there is a considerable decrease in the number of "vesicles" present in this supernatant sample. The Western blot (Fig. 3-5D), showed that Drs2p and clathrin heavy chain were undetectable in the 300,000 x g supernatant sample (Fig. 3-5D, Post), compared to the pre-spin sample (Fig. 3-5D, Pre). Meanwhile, Swa2 (auxilin) and Arf1, which are both cytosolic proteins, were present in similar amounts in both the pre-spin and 300,000 x g supernatant samples.

It is possible that the vesicles containing Drs2p might near the bottom of the centrifuge tube rather than solely in the pellet. The post-spin samples were being loaded onto the carbon grids (for negative EM) and into the gels (for Western blotting) had been taken from the top of the centrifuged sample. I was also attempting to make cytosol from *APL2-GFP* strain, and was facing the same issue, i.e. seeing Drs2p present in the prep. Both the post-spin sample (taken from the top of centrifuge tube), as well as an additional sample, called "extra-supe sample" (drawn from the bottom of the centrifuge tube above the pellet) were run on an SDS-PAGE gel and probed with antibodies for the presence of various proteins. When these samples were compared side-by-side, it is evident that the "extra-supe" sample is comparable to the pre-spin sample (Fig. 3-5E, left panel). It appears that, during centrifugation, there is a gradient being formed in the tube (Fig. 3-5E, right panel), and that the heavier vesicles (which were expected to pellet) is actually settling into a layer at the bottom of the tube while the lighter, cytosolic proteins are remaining near the top. To confirm whether this is true of the cytosol

prepared from the wild-type strain, a Western blot was done with the "extra-supe" sample (bottom of the tube), and the same results were obtained (as was observed in Fig. 3-5E) – the formation of the gradient in the centrifuge tube, and the presence of Drs2p in the "extra-supe" sample (data not shown; this data can be accessed from my electronic files: Data Images -> Western blots -> new western). Since Drs2p, and by extension vesicles, are present in the cytosol preps, and centrifugation at higher speeds removed the clathrin in the sample, these cytosol preps were not useful for vesicle budding assays.

Weaknesses and Future Directions

Attempts to calculate tubulation or elongation in the *kes1*Δ and *DRS2* strains were fruitless. It is possible that most of the membranes counted in the WT strain (Fig. 3-4A and B) were in the process of undergoing fusion when they were imaged which is why I was able to count membranes that were tubulating or elongating. Another disadvantage here is that it is not clear if the flipping activity of Drs2p is mediating this fusion. It is also likely that other proteins present on or in the Golgi membranes, or present in the samples is contributing to or causing this activity. Finally, it is unclear how many of the membranes contain or possess active Drs2p which is another limitation to these experiments.

One way to address this problem is to use a tagged version of Drs2p to purify the Golgi membranes. Drs2p membranes can be separated from membranes that do not contain Drs2p by the use of beads which could recognize a tagged version of Drs2p. Another

possibility is to use immuno-gold techniques to determine which (and what percent of) membranes contain Drs2p. Negative EM staining of the cytosol (Fig. 3-5) shows that there is a lot of background in the cytosolic preparations which might affect my ability to identify changes due to Drs2p activity. One way to overcome this is to dilute the cytosol before addition and to supplement it with purified proteins that we know are essential for vesicle budding to occur. For instance, clathrin can be stripped off of vesicles or clathrin baskets and purified. Another option is to prepare the cytosol at a pH of 8.0 which would ensure that the clathrin in the prep is cytosolic and not associated with any membrane.

The substantial number of small membranes within the *DRS2* and *drs2-ts* preps could make the detection of changes, especially if the changes are slight, in membrane morphology difficult. The pellet that is obtained during the TGN membrane preps is relatively compact and difficult to resuspend. As a result, much force is used to resuspend the pellet. For instance, a combination of dounce homogenizing and high speed vortexing is used to loosen the pellet before it is added to the sucrose gradient for fractionation. Such forces might be fragmenting the Golgi, resulting in the large number of small membranes in the preps.

A different approach, to resolve this issue, would be to pellet membranes onto a "sucrose cushion", essentially two layers of sucrose at differing concentrations between which the membranes would settle during centrifugation. This would eliminate the need for large amounts of force to be used for membrane resuspension and might better

maintain the integrity of the late Golgi membranes. The larger membranes can also be purified from the TGN membrane preps by size exclusion chromatography in a Sephacryl S–1000 column. One of the caveats of this process will be to determine whether Drs2p activity is maintained after this long process.

Ultimately, the problem faced with the Golgi preps is their complexity. It is difficult to control the composition of the preps and any changes observed could be driven by the action of proteins or substrates that are not directly being assessed, but which are, nevertheless, present in these preps. The reconstituted system provides a purer, more direct approach to testing the same questions.

The Purification and Reconstitution of Drs2p

Previous work done by Paramasivam Natarajan, in our lab, has demonstrated that Drs2p is necessary for flippase activity in late Golgi membranes (Natarajan et al., 2009; Natarajan et al., 2004). A senior graduate student, Xiaoming Zhou, has been successful at purifying and reconstituting Drs2p into proteoliposomes (Zhou & Graham, 2009). His work demonstrated that Drs2p is sufficient to catalyze flippase activity *in vitro*. However, the proteoliposomes used were too small (~40nm in diameter) to score morphological changes in liposome shape. The goal of this project was to recapitulate the experiments done by Xiaoming (i.e. the purification and reconstitution), and to move this work forward by developing assays to introduce Drs2p into giant unilamellar vesicles (GUVs) so that we can determine whether flippase activity, at the membrane, causes changes in membrane morphology. The importance of achieving this goal is that it then provides evidence for the importance of flippases at membranes and the role they play in vesicle-mediated protein transport. This section outlines experiments and assays that were designed and optimized for the purification and reconstitution of Drs2p.

Results and Discussion

It had been determined, from quantitative western blots, that there are about 300–500 Drs2p molecules per TGN cisterna. To increase the yield of Drs2p obtained, Zhou constructed a yeast strain that has 10–20 fold overexpression of TAP–tagged Drs2p and HA–tagged Cdc50p (the Drs2p chaperone) using the strong glycerol–3–phosphate

dehydrogenase (GPD) promoter to drive their expression. The TAP_N–tag for Drs2p was placed on both the N– and C–terminal ends. It was found that the N–terminally tagged TAP_N–Drs2p, which was reconstituted into proteoliposomes, was active *in vitro* while Drs2p–TAP_C is enzymatically dead (there was no flippase activity detected using this protein). Additionally, the purified TAP_N–Drs2p was found to be sensitive to orthovanadate and has Mg^{+2}–dependent ATPase activity (Zhou & Graham, 2009). Data suggests that phosphatidylserine (PS) is also the preferred substrate for Drs2p (Natarajan et al., 2004).

To recapitulate the work done and published by Xiaoming, I first set about purifying and reconstituting Drs2p using protocols established in the lab. TAP_N-Drs2p was purified by two-step purification methods using both its N-terminal Protein-A and 10x-Histidine tags. The protein yield using two-step purification method was low - about 7ng/μL (Fig. 3-6A). Since more protein was needed for reconstitution into proteoliposomes, a single-step purification method was used utilizing the 10x-His tag on TAP_N-Drs2p. The concentration of Drs2p, in this case, was greatly improved – about 25 ng/μL. However, there were a lot of other protein bands visible in the Coomassie (Fig. 3-6B), suggesting that this sample is not as pure as the two-step purified material. This protein sample is active and has a specific activity of about 0.3 μmol Pi/min/mg Drs2p (Fig. 3-6C) – similar values to those detected by Xiaoming Zhou (Zhou & Graham, 2009).

This sample was then reconstituted, using adbsorbent Biobeads, in the presence of PC and 1mol% NBD-PS, and the seal of the resulting proteoliposomes was tested. I found

that these proteoliposomes only had 3-5% resistance to quenching by dithionite (Fig. 3-6D). This means that only 6-10% of the proteoliposomes in the population were completely sealed and were able to shield the NBD lipids in the inner membrane layer from quenching by dithionite (Fig. 3-6E). Liposomes that were reconstituted in the same manner, meanwhile, showed about 45% resistance to quenching by dithionite (Fig. 3-6D).

These proteoliposomes were floated in a bipartite glycerol gradient to: (a) separate the proteoliposomes from unincorporated proteins and lipids, and (b) determine if these floated proteoliposomes, once separated away, would have a better seal. When the five resulting fractions were run on an SDS-PAGE gel and coomassie stained, most of the protein is observed in fraction 3 (F3), and a little less in fraction 4 (F4), which is second from the top (Fig. 3-6F). The NBD-lipids are also primarily distributed between F3 and F4, when assessed by a fluorescence spectrometer trace (Fig. 3-6G). The seals of these floated proteoliposomes don't improve either. Both fractions have only 3-5% resistance to ditihionite quenching (Fig. 3-6H). Fractions F3 and F4 are slightly higher specific activities than the pure protein sample, around 0.35 – 0.4 μmol Pi/min/mg Drs2p (Fig. 3-6I).

At the time of these experiments, the issue of poorly sealed, or leaky, proteoliposomes was one that Xiaoming was facing as well. Independently, he spent several months attempting to rectify this problem before his departure from Vanderbilt. On my end, I made several changes to the reconstitution protocol to pinpoint the problem and identify potential solutions. Several options were considered to rectify this problem.

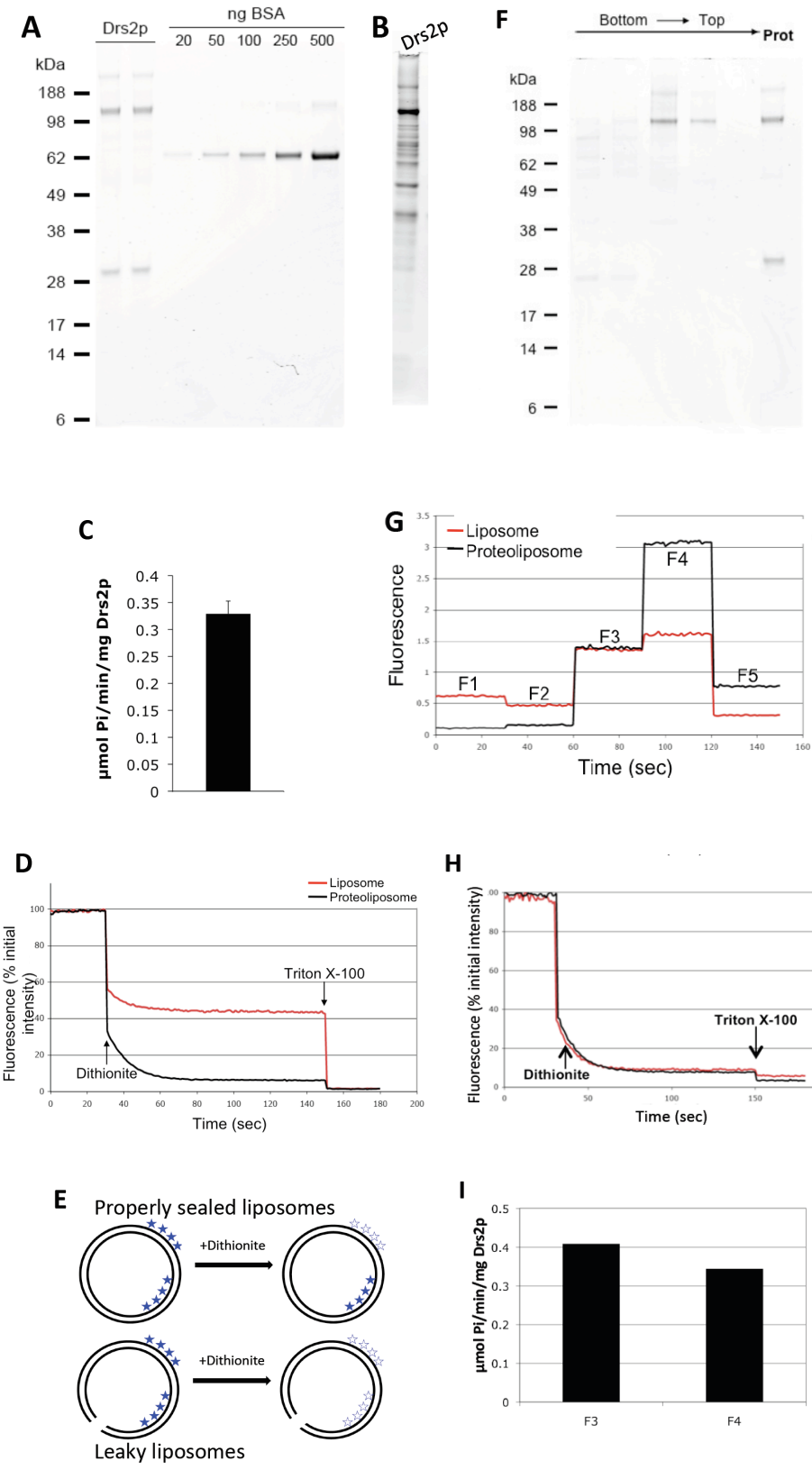
A
Drs2p
ng BSA
20 50 100 250 500
kDa
188
98
62
49
38
28
17
14
6
B
Drs2p
F
Bottom → Top
Prot
kDa
188
98
62
49
38
28
17
14
6
C
µmol Pi/min/mg Drs2p
0.4
0.35
0.3
0.25
0.2
0.15
0.1
0.05
0
G
Liposome
Proteoliposome
Fluorescence
F1
F2
F3
F4
F5
Time (sec)
D
Liposome
Proteoliposome
Fluorescence (% initial intensity)
Triton X-100
Dithionite
Time (sec)
H
Fluorescence (% initial intensity)
F3
F4
Triton X-100
Dithionite
Time (sec)
E
Properly sealed liposomes
+Dithionite
+Dithionite
Leaky liposomes
I
µmol Pi/min/mg Drs2p
0.5
0.4
0.3
0.2
0.1
0
F3
F4

Figure 3-6. Purification and Reconstitution of Drs2p using C12E9. (A) Two-step purification (coomassie stained gel) of Drs2p using ProteinA and 10x Histidine tags. Drs2p was run on the gel in duplicate. BSA standards (in ng) were run on the gel to enable quantitative calculations. (B) Coomassie stained gel of single-step purification of Drs2p using 10x Histidine tag. (C) Graph showing the specific activity of single-step purified Drs2p determined using ATPase assay. (D) Fluorescence trace assaying the resistance to dithionite quench, of protein-free and proteo-liposomes. Dithionite is added at 30sec, and 10% Triton X-100 is added at 150sec. The trace is collected for 180sec. (E) Animation showing the difference in NBD-phospholipid quench in leaky versus properly sealed liposomes. Properly sealed liposomes will only have 50% resistance to quenching of the fluorescent probe as the other half of the NBD-lipids are protected by the sealed inner membrane of the proteoliposome. (F) Coomassie stained gel showing the distribution of Drs2p in floated fractions with the fractions from the bottom loaded on the left side of the gel and the fractions from the top of the tube loaded on the right side. The well labeled "Prot" is an aliquot of the original sample, prior to flotation. (G) The distribution of NBD-lipids in the floated fractions (liposome vs. proteoliposome samples). Where F1 is the fraction from the bottom of the tube and F5 is the fraction on the top. (H) Since F3 and F4 had the most NBD-lipids, those proteoliposome fractions were assayed for resistance to quenching by dithionite. Dithionite is added at 30sec, and 10% Triton X-100 is added at 150sec. The trace is collected for 180sec. (I) Graph showing the specific activities of the F3 and F4 proteoliposome samples (see (F-H)) determined using ATPase assay.

First, it was possible that the proteoliposomes may need to be incubated for a longer period of time with the Biobeads. Normally, 100mg of methanol-activated Biobeads are added to a protein+lipid mixture and mixed by end-over-end rotation. After 6 hours, 200mg of activated Biobeads are added and the sample is mixed for another 12 hours. Thus, the sample is incubated with the Biobeads for a total of about 18 hours.

Liposomes and proteoliposomes were formed using this established reconstitution protocol and they were tested for seal at 18h 45min post incubation with Biobeads (6h 30min with 100mg, followed by 12h 15min with an additional 200mg). The liposomes were 40% resistant to quenching by dithionite, while the proteoliposomes were only 4% resistant (Fig. 3-7A). The samples were allowed to mix end-over-end for an additional 2 hours and were then tested for seal. At the 20h 45min time point, the liposomes

improved their seal to 43% while the proteoliposome seal was at approximately 5% (Fig. 3-7B). At this point, 100mg of fresh Biobeads were added to the sample and it was allowed to mix for an additional 2 hours 15 min. At the 23 hour time point, the seal was checked again. This time the liposomes had an almost 50% resistance to dithionite quench while the proteoliposomes were still around 5% resistant (Fig. 3-7C). The samples were floated to determine if the fractions would have an improved seal. As determined by coomassie (to determine which fractions contained the most protein), and fluorescence traces (to determine which of the fractions contained the most fluorescent lipids), fractions F3 and F4 were chosen, in both the liposome and proteoliposome samples, and the seal was tested (data not shown). In the liposome samples, F3 had about 42% resistance and F4 had 37% resistance to dithionite quenching (Fig. 3-7D). Both F3 and F4, of the proteoliposome sample had about 5% resistance to dithionite quenching (Fig. 3-7E). In these experiments, both F3 and F4 proteoliposomes were active (Fig. 3-7F).

Since preparation of protein takes a long time, and in order to optimize the reconstitution conditions, I switched to using liposomes. At first, decreasing amounts of detergent were used during liposome formation (Fig. 3-7G). In the figure, 100% detergent is the amount of detergent normally used to reconstitute protein into liposomes. The other values tested were 87%, 73% and 47% of detergent relative to the original amount. A decrease of 13% of detergent (87% sample), shows an increase in the liposome resistance to a value greater than 50% dithionite resistance. The problem with decreasing the amount of detergent is that a large number of multi-lamellar vesicles

form in these samples. Future experiments, using proteoliposomes and a decreased amount of detergent, did not yield proteoliposomes that floated. Rather, the lower levels of detergent kept most of the lipids in micellar form and the protein did not incorporate into liposomes (data not shown).

One observation was that the previous batch of Biobeads were considerably drier than the batch that was in use. As such, the new Biobeads were dessicated in a speed-vac for 20min prior to methanol activation. The effect that normal Biobeads and the dessicated Biobeads had on liposome formation was compared. Dessication of the Biobeads seemed to improve the seal of the liposomes by about 5% (Fig. 3-7H), so future reconstitutions (while using C12E9) were done with dessicated batches of Biobeads.

Another thought was that other protein(s) that were co-purifying with the single-step purified Drs2p was affecting the ability of the proteoliposomes to seal. To test this, Drs2p was purified away from smaller contaminating proteins using centrifugal filter systems with molecular weight cut-offs at 30 kDa. Unfortunately, I was not able to recover much of the Drs2p in the final eluate (data not shown). This may be because the protein was getting trapped in the centrifugal column membrane.

TAP_N-Drs2p has two purification tags at its N-terminus – a Protein A module and a 10x Histidine module (Zhou & Graham, 2009; Zhou et al., 2013). Drs2p was purified, out of yeast, in two batches. The first batch was purified using IgG beads against the ProteinA module, followed by elution of the protein by TEV cleavage. The second was purified

A

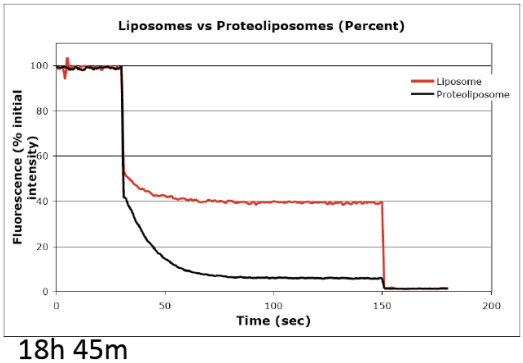

18h 45m

B

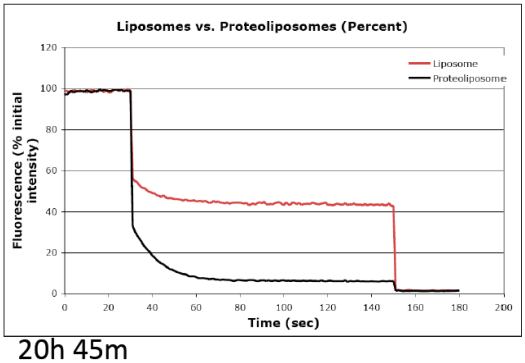

20h 45m

C

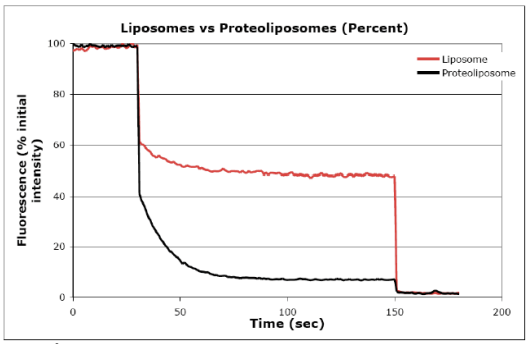

23h

D

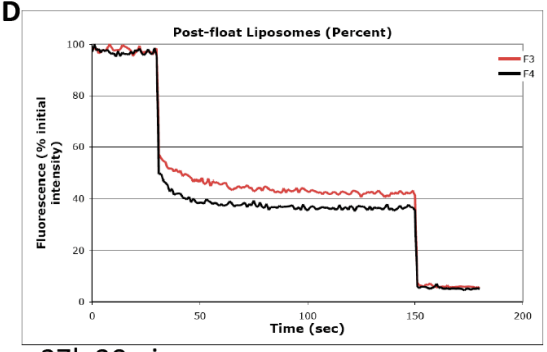

27h 30min

E

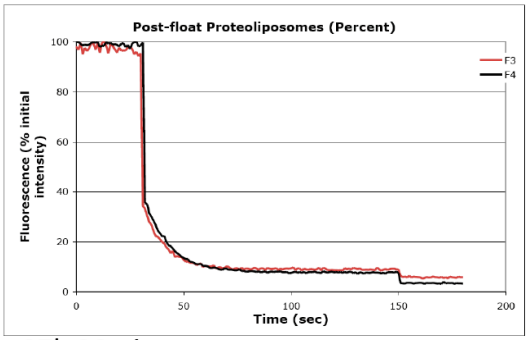

27h 30min

F

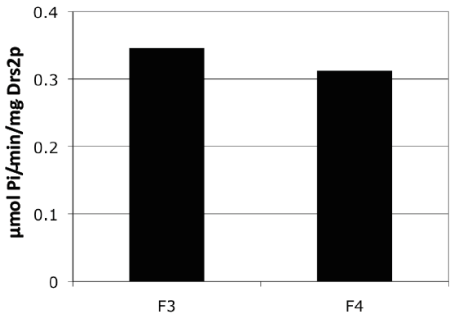

G

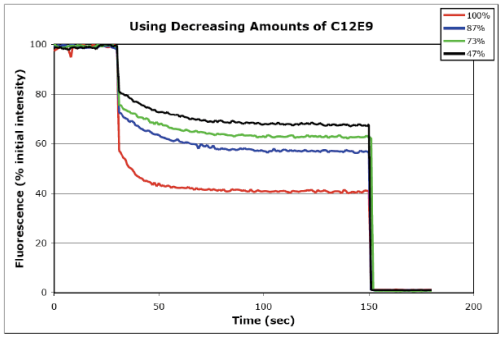

H

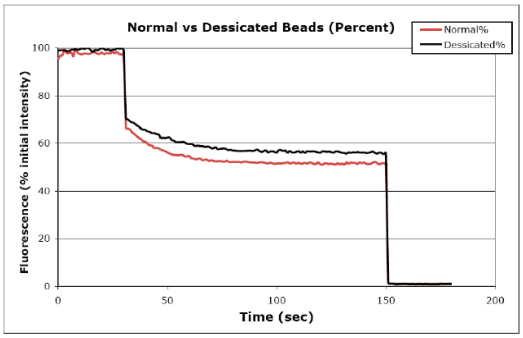

Figure 3-7. Testing conditions to solve the leaky liposome problem. (A) Protein-free and proteo-liposome seal was assessed by fluorescence quenching assays after 18h 45min of incubation using BioBeads during the reconstitution protocol. (B) The samples from (A) were incubated for an additional 2h and seal was re-assessed at time 20h 45min. (C) Fresh Biobeads were added to the samples and allowed to incubate for over 2h. At time 23h, seal was re-assessed. (D) and (E) The samples were floated and F3 and F4 fractions (middle and second from top) were assessed for resistance to dithionite quench. Where (D) are liposome samples and (E) are the proteoliposome samples. (F) Specific activities of the F3 and F4 samples assayed in (E). (G) Liposome samples were reconstituted using decreasing amounts of C12E9 and assayed for proper seal. Where 100% is the normal amount of detergent used during reconstitution, and 87%, 73% and 47% are corresponding decreases in the amount of detergent. (H) Biobeads were either dried in a Speedvac for 15min (Dessicated) or added directly from the jar (Normal) during reconstitution and the effect on liposome seal was assessed.

using the Ni-NTA beads against the 10x Histidine module and elution by high concentration of imidazole. Each of these samples were reconstituted into PC + 1% NBD-PS liposomes and the resulting sample was tested for seal. Side-by-side with the proteoliposome formation, I made liposomes using the same elution buffers that were used for the proteoliposome reconstitution. The reason for doing this, i.e. purifying using different tags, is that during the different single-step purifications (Protein A vs 10x His), some of the contaminating proteins that co-purify with Drs2p are different between the preps. The hope was that one of these preps would lack the contaminants causing the leaky liposome problem and would allow the proteoliposomes to form proper seals during reconstitution. Furthermore, I increased the number of washes, during purification, to get rid of as many contaminating proteins as possible. During this experiment, the prep that I obtained for purification by 10x His was more pure than the one obtained for purification by the ProA module (Fig. 3-8E).

Meanwhile, the resistance of 10xHis-purified Drs2p proteoliposomes improved considerably. They displayed 20% resistance to dithionite quenching which means that 40% of the proteoliposomes formed had a good seal (Fig. 3-8A, B). Comparatively, the ProA-purified Drs2p proteoliposomes were leakier. They displayed about 10% resistance to dithionite (Fig. 3-8C, D). All of the liposomes made were 50 – 60% resistance to dithionite quenching (Fig. 3-8A-D). While I tested the seal of each set of proteoliposomes at two time points (18h and 21h), to determine if the additional incubation time improved the seal, there did not appear to be a significant difference between the samples at either time point (Fig. 3-8A vs B, Fig. 3-8C vs D). Furthermore, liposome traces show that differences in elution buffer does not appear to affect the seal.

These proteoliposomes were then floated and the amount of protein in each fraction was determined by coomassie staining. In the 10x His purified Drs2p proteoliposomes, the protein is detected in the F4 and F5 fractions. However, the bands are very faint. There may be several reasons for this: (a) there may have been some protein degradation during the final incubation with Biobeads and preparation of fractions for flotation, (b) I started out with a slightly lower concentration of protein (5ng/μL concentration) than what I normally use (about 20ng/μL), and (c) the proteoliposomes has spread itself out over several fractions (Fig. 3-8F). Furthermore, the top two fractions (F4 and F5) which contains most of the proteoliposomes have 0.7 and 1.1ng/μL protein concentrations. This was disappointing because it was this sample that had the best seal. Additionally, I had pre-quenched the sample in the hopes of performing flippase assays with it. The fractions from the ProA-purified Drs2p proteoliposomes were also rather faint.

However, I did start out with more protein during reconstitution (10ng/μL concentration). Fractions 3 and 4 for this sample had the most protein and had concentrations of 2 and 3.5ng/μL respectively (Fig. 3-8G).

When the various fractions – F4 and F5 for 10x His sample, and F3 and F4 for ProA sample – were assayed for activity, it was obvious that the protein was not very active. When you look at the average ATPase assay values (Fig. 3-8H) you can tell that there is very little difference between the sample versus the boil or vanadate control values. The specific activities (Fig. 3-8I) of the samples do not accurately reflect the small variation because the differences in the amount of protein present in the fractions influence the specific activity. Ultimately, I was not able to use these samples for flippase assays. Between the extremely low concentrations of protein present in the floated proteoliposomes and the low levels of specific activity, these samples were not useable for further experiments.

To improve the purification and reconstitution protocols, I tried new protocols using different detergents. The lab of Robert Molday (Coleman et al., 2009), had developed an assay for purification and reconstitution of ATP8A2 from bovine photoreceptor outer segments. ATP8A2, along with ATP8A1, are two mammalian P4-ATPases that are the most closely related to Drs2p. They, like Drs2p, use PS as a substrate. The protocol developed by the Molday group uses CHAPS and n-octyl-β-D-glucopyranoside as detergents and they purify the protein in the presence of lipids (Coleman et al., 2009).

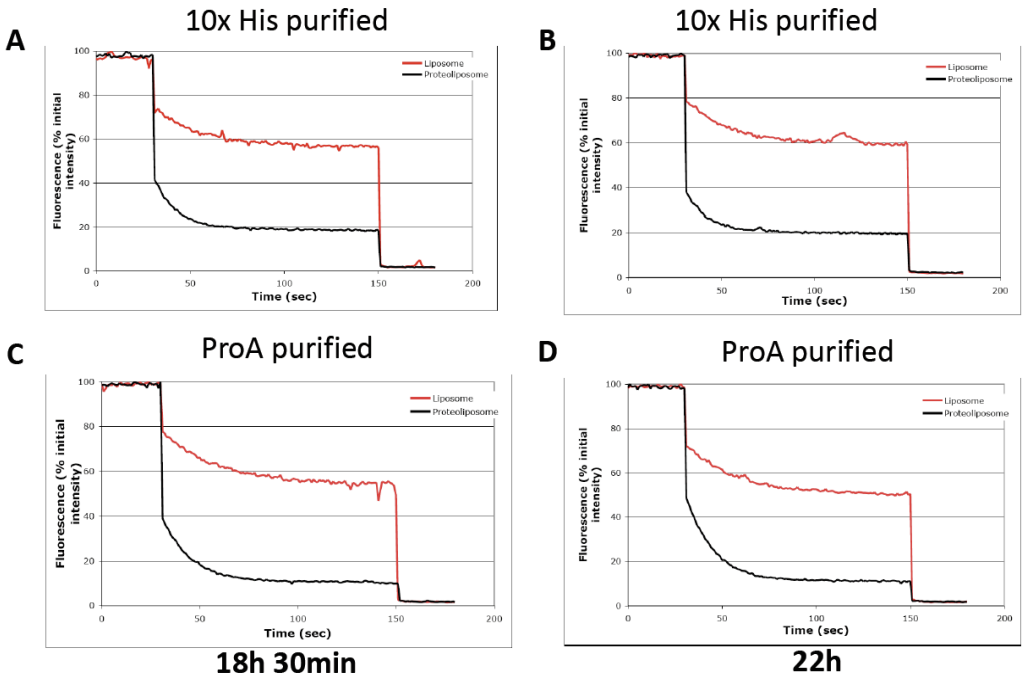
A
10x His purified
B
10x His purified
Liposome
Proteoliposome
Fluorescence (% initial intensity)
Time (sec)
C
ProA purified
18h 30min
D
ProA purified
22h

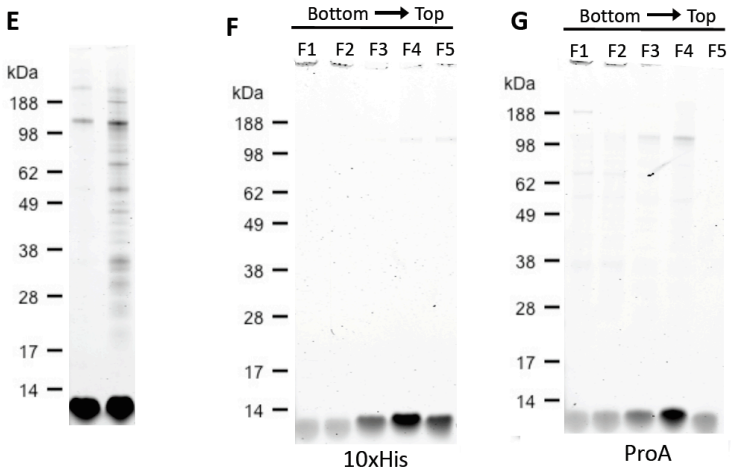
E
kDa
188
98
62
49
38
28
17
14
F
Bottom → Top
F1 F2 F3 F4 F5
10xHis
G
Bottom → Top
F1 F2 F3 F4 F5
ProA

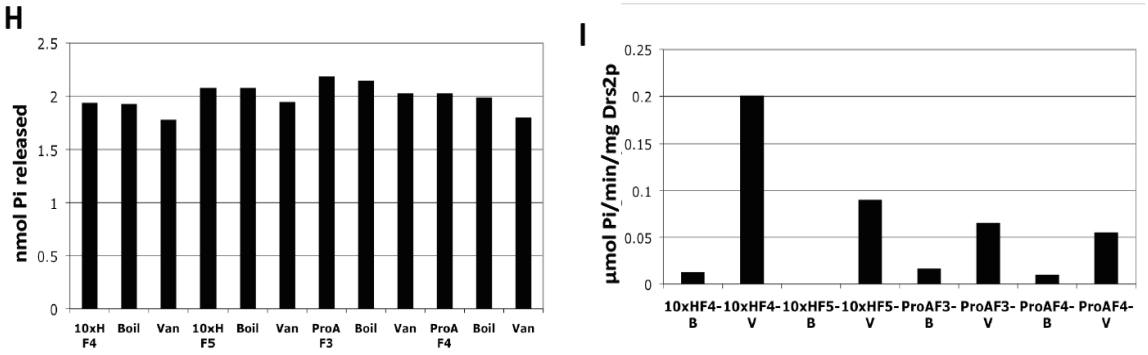
H
nmol Pi released
10xH F4
Boil
Van
10xH F5
ProA F3
ProA F4
I
µmol Pi/min/mg Drs2p
10xHF4-B
10xHF4-V
10xHF5-B
10xHF5-V
ProAF3-B
ProAF3-V
ProAF4-B
ProAF4-V

Figure 3-8. Testing different protein purification conditions and its impact on proteoliposome seal. (A) and (B) Drs2p was single-step purified using 10x Histidine tag and eluted by imidazole. (C) and (D) Drs2p was single-step purified using Protein A tag and eluted by cleavage using TEV protease. (A) and (C) Protein-free and proteo-liposome seal after 18h incubation with Biobeads during reconstitution. (B) and (D) Liposomes from (A) and (C) after 4 additional hours of incubation with Biobeads. (E) Coomassie stained gel showing the single-step purified Drs2p from 10x His samples (left well) and ProA samples (right well). (F) and (G) Gels looking at the distribution of protein from floated fractions of 10x His proteoliposomes (F) and ProA proteoliposomes (G). (H) nmol of Pi released by the fractions when assayed for ATPase activity. Each of the samples also has a Boil and vanadate ("Van") sample associated with it. These samples were run in duplicate. (I) The specific activities of the 10x His and ProA fractions, F3 and F4. The "-B" samples are sample minus its respective boiled control sample and "-V" samples are sample minus its respective vanadate control sample. These values were calculated from raw values presented in (H).

Dialysis cassettes are used, instead of Biobeads, to remove the detergent. I developed a protocol to mirror the changes of the Molday protocol and to adapt it to Drs2p (see Protein Purifications and Reconstitutions Protocols section). The purified protein was run on an SDS-PAGE gel and coomassie stained to determine yield. The protein was eluted from the column three times. In the first two eluates, there is a double band running at about 150kDa (Fig. 3-9A). The concentration of eluates are 37 and 21 ng/μL respectively. The third eluate (19 ng/μL) only possesses the faster migrating of the two bands. The protein from the first elution was reconstituted into PC + 1% NBD-PS liposomes and an aliquot was run in the fourth lane. There is only one band present for Drs2p (the faster migrating band) which suggests that the upper band might have degraded to form the lower band. The proteoliposomes have a protein concentration of 19 ng/μL (Fig. 3-9A).

The proteoliposome sample was assayed for ATPase activity and was so active that it had to be diluted 20x so that the activity would fall within the measurable range of the

assay. The protein was assayed, for activity both in the presence and absence of detergent to determine whether the presence of the membrane influenced the activity of the protein. In the presence of detergent, the protein had a specific activity of 3.5 μmol Pi/min/mg Drs2p, while in the absence of detergent the specific activity was higher, about 5.2 μmol Pi/min/mg Drs2p (Fig. 3-9B). This suggests that the presence of the membrane stabilizes the protein and enhances its function. The reconstituted protein was checked for seal and it was almost 25% resistant to dithionite quenching (Fig. 3-9C). This was promising.

The proteoliposome sample was floated and the amount of proteins in the fractions were assessed by running them on, and coomassie staining, an SDS-PAGE gel (Fig. 3-9D). Most of the protein remained in the bottom fractions with a very small percentage floating to F4, which is one of the two fractions which had most NBD-lipids (the other being F5). Calculations show that only 1 Drs2p molecule is present in every 400 liposomes. Xiaoming was able to incorporate 1 Drs2p molecule in every 2-3 liposomes using his protocol. These data suggest that the reconstitution protocol was unsuccessful.

Fractions F3 and F4 were assayed for ATPase activity and it was found that they had very high specific activities – F3 was 60 μmol Pi/min/mg Drs2p, and F4 was 115 μmol Pi/min/mg Drs2p. Both these values are significantly higher (150 – 300 fold higher) than specific activities that were previously published. The actual specific activity of F3 and F4 might be slightly different since the calculation of the amount of Drs2p in those

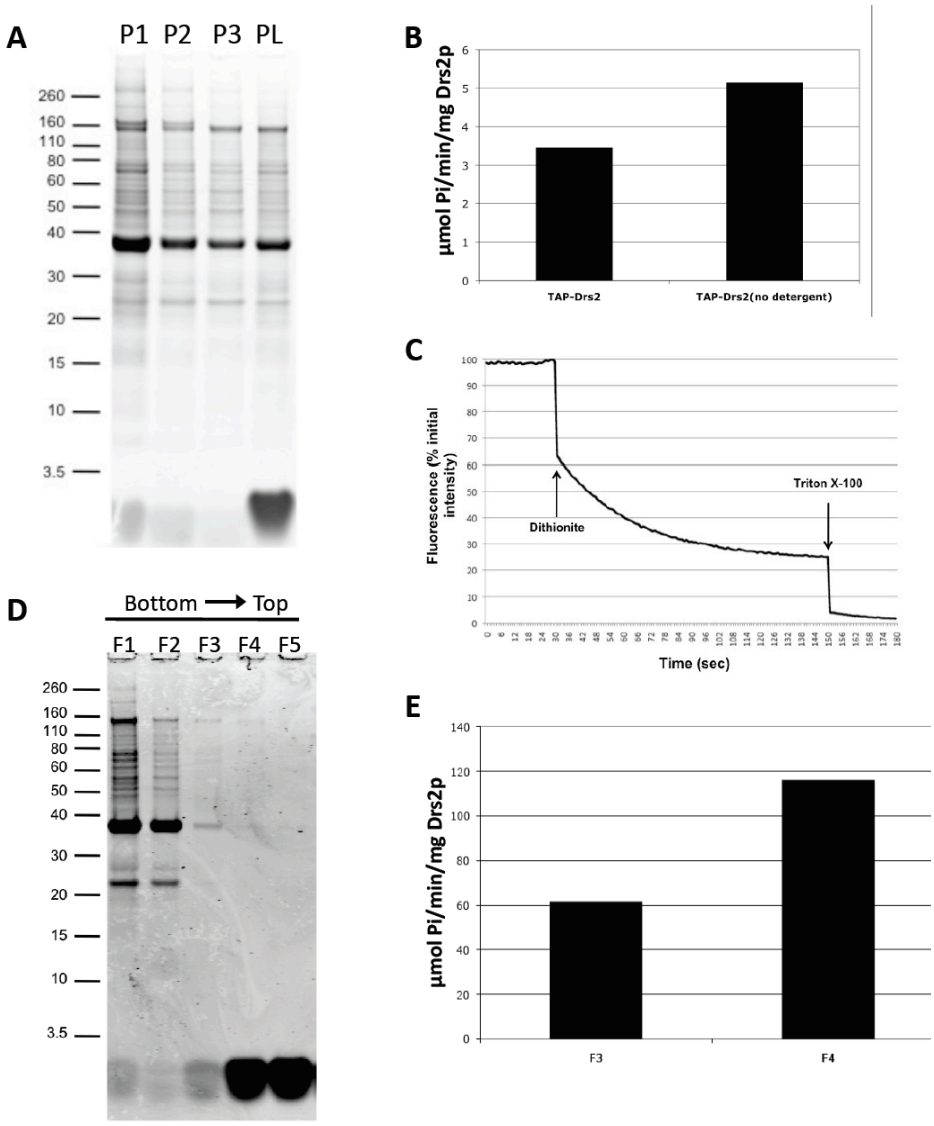

Figure 3-9. Purification of Drs2p using CHAPS and n-octyl-β-D-glucopyranoside. (A) Coomassie stained gel showing single-step purified Drs2p. P1 – P3 are three different elutions from the same column. PL is the proteoliposome sample after reconstitution. (B) The specific activity of proteoliposomes reconstituted using single-step purified Drs2p both in the presence (left bar) and absence (right bar, "no detergent") of detergent during the ATPase assay. (C) Fluorescence trace of the proteoliposome sample showing approximately 25% resistance to quenching by dithionite. Dithionite was added at 30sec and 10% Trition X-100 was added at 150sec. The trace was run for 180sec. (D) Distribution of Drs2p in fractions after flotation. Where F1 is the fraction at the bottom of the centrifuge tube and F5 is the fraction at the top. (E) Specific activity of F3 and F4 fractions as detected on the gel in (D).

samples is an estimate extrapolated from the equation for the BSA standards (from gel image, Fig. 3-9D). F3 was estimated to have 0.7 ng/μL and F4 was estimated to have 0.18 ng/μL of Drs2p. Even if these values are slightly off, it doesn't take away from the fact that these preps are extremely active, especially when compared to our former purification and reconstitution methods.

Since the reconstitution did not work with n-octyl-β-D-glucopyranoside, I substituted C12E9 into the purification and reconstitution protocols. It seemed that purifying the protein in the presence of lipids as well as the other minor modifications that were made to the protocol might enhance the yield and overall activity of the protein. To that end, Drs2p was purified using this protocol, reconstituted by dialysis, and the protein yield was assessed by Coomassie staining. A lot of background bands were observed on the gel, and the yield of protein was very low compared to the other proteins in the solution (Fig. 3-10A). When this sample was reconstituted (using C12E9 and dialysis), there was absolutely no resistance to dithionite quenching (Fig. 3-10B). I observed that the sample seemed to have detergent in it even after the dialysis step (sample was a bit sudsy).

After a literature and web search, it became clear that n-octyl-β-D-glucopyranoside has a critical micelle concentration (CMC) of 23-25mM (0.67-0.73% w/v), while C12E9 has a critical micelle concentration of 0.05mM (0.003% w/v). Since n-octyl-β-D-glucopyranoside has such a high CMC, it can be removed from a solution by dialysis or gel filtration. C12E9, on the other hand, has a very low CMC, which inhibits removal by these methods. This is why C12E9 was not removed by dialysis, and why, as a result, the

proteoliposomes did not seal (i.e. the presence of the detergent). C12E9 removal from a solution, by dialysis cassettes, can be achieved with extremely long incubation times (several days up to a week or so), but for my purposes, this would mean degradation of the protein.

The protocols modified from the Molday lab were revised again. The purification protocol was kept intact, including the detergents used, and the reconstitution protocol was modified. Instead of removing the detergent using dialysis, the final eluate was split into two. One aliquot was reconstituted using dialysis and the other aliquot was reconstituted using Biobeads. It seemed likely that the reason dialysis had not worked initially was because, when the reconstituted sample (with octylglucoside) is being dialyzed, the detergent may be being removed too quickly from the sample. This is probably leading to the formation of liposomes rather than proteoliposomes. It is also possible that such liposome formation is happening at a faster rate than the proteins are capable of incorporating into the membrane bilayer. I hoped that using Biobeads might slow down the rate of detergent removal. The dialyzed samples were to act as a control.

The purified protein was run on a gel and coomassie stained to determine yield. The first elution of protein had a concentration of 18 ng/μL (Fig. 3-10C). After the protein and lipids were mixed, an aliquot was taken which was also run on the gel (see lane "PL", Fig. 3-10C). After reconstitution, either by Biobeads or by dialysis, the resulting proteoliposomes were run on the same gel as the above samples. The proteoliposome samples from the Biobeads (see lane "Bb", Fig. 3-10C), had a very faint band for Drs2p.

In fact, it looked like most of the protein was stuck in the well of the gel. Compare that with the proteoliposome samples from the dialysis cassette (see lane "Di", Fig. 3-10C), where there is a distinct band for Drs2p (at about 150kDa) and there is no protein detectable in the well. It appears that, for some reason, incubating protein (that has been reconstituted with n-octyl-β-D-glucopyranoside in the presence of Biobeads) is causing protein aggregation.

A trace to determine the seal of the proteoliposome samples shows that in both reconstitution samples, there is 25% resistance to quenching by dithionite (Fig. 3-10E). When these samples are floated, meanwhile, very little, if any, of the protein is found in the top fractions (Fig. 3-10D). Most of the protein is found in the lower fractions and separated from most of the NBD-lipids. In this case too, the protein in the Biobeads sample is found in the wells of F1 and F2 (Fig. 3-10D). A trace for the fluorescence of the fractions also shows that most of the lipids float to the top (data not shown), indicating that liposomes formed, but the protein is not incorporating into them.

The activity of these proteoliposome samples were tested. From the average ATPase activity, measured in nmol Pi released, the dialyzed samples have higher activities than the Biobeads samples (Fig. 3-10F). However, depending on how you calculate the specific activity – whether you use the value for the amount of Drs2p from the band on the gel only (Fig. 3-10G), or you include the protein in both the band and the well (Fig. 3-10H) – you get two different values. When I calculated the specific activity using the

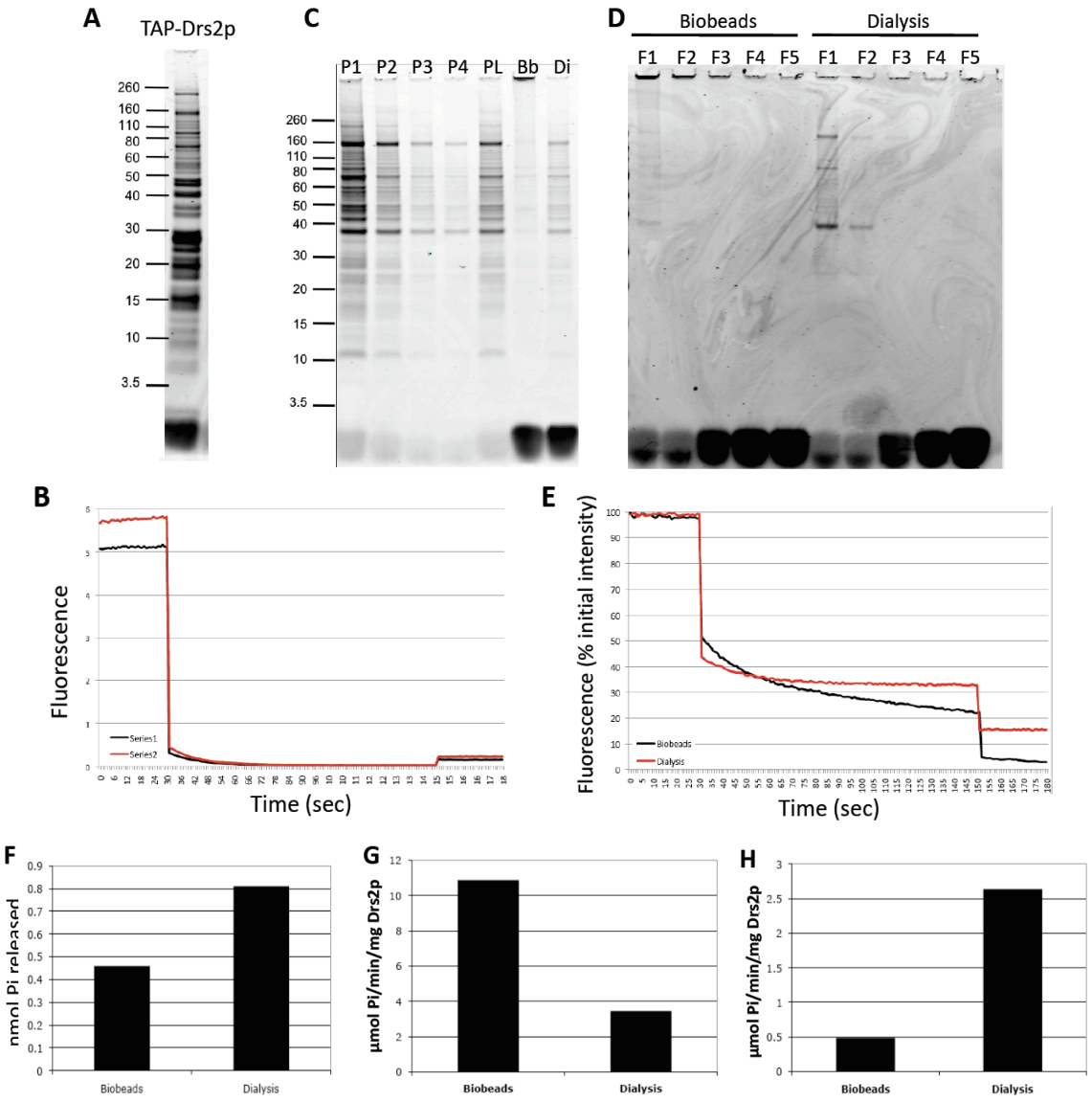

Figure 3-10. Substitution of C12E9 instead of CHAPS and octylglucoside. (A) Single-step purified TAP-Drs2p purified using C12E9 as substituted into the protocol instead of CHAPS and octylglucoside. (B) The proteoliposome samples had absolutely no resistance to quenching by dithionite. The black and red lines represent two different lipid compositions used during reconstitution. (C) Drs2p was re-purified using the C12E9 substitution protocol (P1 – P4 are different eluates off the same column) and mixed with lipids for reconstitution ("PL" sample). This sample was split into two and reconstituted using either Biobeads (Bb) or Dialysis (Di). (D) The resulting proteoliposomes were floated and the fractions run on an SDS-PAGE gel. Where F1 is the bottom fraction and F5 is the top. (E) Seal of proteoliposomes reconstituted using either Biobeads or Dialysis. (F) nmol of Pi released for Biobeads and Dialysis proteoliposomes. The specific activity of these samples was calculated using either the band detectable for Drs2p only (G) or the amount of protein in both the band and stuck in the well (H).

amount of protein found at the 150kDa band *and* the well (which I believe is a more accurate representation of the amount of Drs2p present in the tube), the graph shows that the dialyzed sample is more active than the sample incubated with Biobeads (Fig. 3-10H). Thus, it seems that n-octyl-β-D-glucopyranoside and dialysis is the best method to give me the most active protein; however, it has still not solved the leaky liposome problem.

Please note that, for the ATPase assays, the samples were diluted 25-fold in order to have the activity fall within the measurable range of the assay.

Looking through general protein purification papers from other labs, and a seminar talk at Vanderbilt by Tina Iverson (Dept. of Pharmacology, Dept. of Biochemistry) about different purification methods, led me to look closely at other detergents that are commonly used for protein purification. C12E8 is a popular choice and closer inspection of C12E8 shows that, structurally, it is similar to C12E9 (Fig. 3-11A). Additionally, both detergents have similar CMC's – 0.05mM (0.003%) for C12E9 and 0.09mM (0.0048%) for C12E8. The slightly higher CMC for C12E8 makes it likely to allow more lipids to remain free in the solution allowing for better incorporation of the protein into liposomes during reconstitution. Furthermore, this detergent would fit in very well with the existing protocols in the lab.

Both TAP_N-Drs2p (using the 10x His tag) and Drs2p-TAP_C (using the calmodulin binding peptide (CBP) tag) were single-step purified using C12E8. Minor modifications

were made to the C12E9 purification protocol to adapt it for use with C12E8, as well as to incorporate those techniques that would improve aspects of the purification and reconstitution (see Purification protocols section). When the gel was run for these two samples, TAP_N-Drs2p ran as a slightly faster migrating band compared to Drs2p-TAP_C (Fig. 3-11B). From other on-going work in the lab (see Chapter 2 of this thesis), I learned that this was likely due to clipping of the protein during purification. Furthermore, purification using C12E8 yielded larger concentrations of protein. TAP_N-Drs2p, in the figure, has a concentration of 40 ng/μL and Drs2p-TAP_C has a concentration of 65 ng/μL (Fig. 3-11B) – much higher that what was previously purified. TAP_N-Drs2p was also active, with a specific activity of 0.23 μmol Pi/min/mg Drs2p, while Drs2p-TAP_C had very little activity (Fig. 3-11E). This result agreed with previously published data.

When the two sets of protein were reconstituted into proteoliposomes (PC + 1% NBD-PS), they were both about 15% resistant to quenching by dithionite (Fig. 3-11D). Further work improved this seal to be between 20-25% resistance (data not shown). Figure 3-11C shows a coomassie image of the proteoliposome samples. These proteoliposomes were also very active. TAP_N-Drs2p had a specific activity of 0.85 μmol Pi/min/mg Drs2p while Drs2p-TAP_C continued to have negligible activity (Fig. 3-11F). This improvement in the activity could be due to the presence of a membrane that is stabilizing the protein. Best of all, a portion of the proteoliposomes floated (Fig. 3-11G).

Concluding Remarks

It was the development of the protocols utilizing C12E8 that allowed me to perform the experiments that led to the publication of the work regarding auto-inhibition of Drs2p by its C-terminal tail (See Chapter 2 in this thesis). Furthermore, it enabled me to use the reconstituted samples for flippase assays (also found in Chapter 2 in this thesis) (Zhou, et al., 2013).

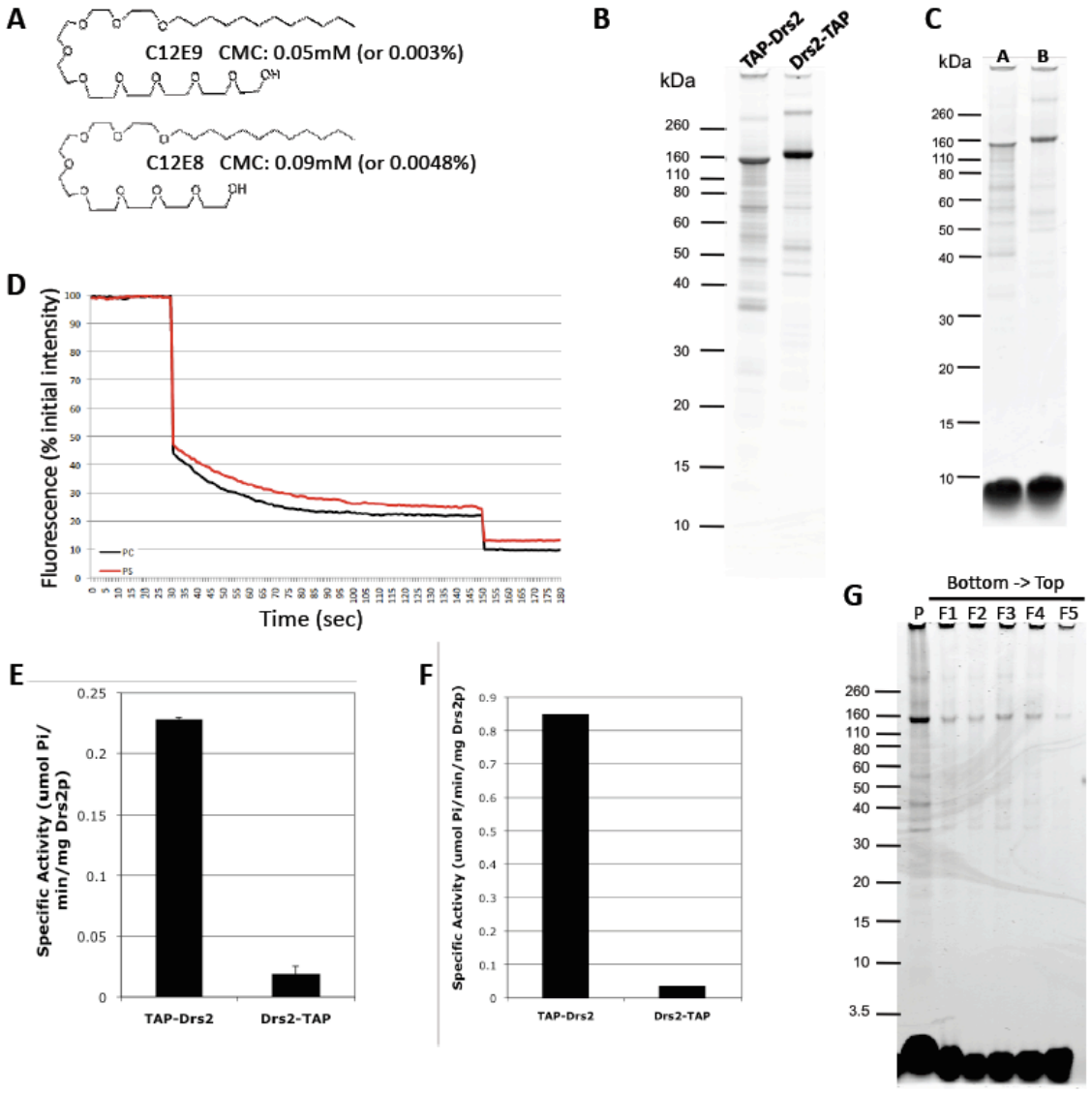

Figure 3-11. Purification of Drs2p using C12E8. (A) The chemical structure and critical micelle concentrations of C12E9 and C12E8. (B) Coomassie stained gel of single-step purification of TAP-Drs2p and Drs2-TAP. (C) Proteoliposome samples (DOPC + 1% NBD-PS) of TAP-Drs2p (lane A) or Drs2p-TAP (lane B). (D) Resistance to dithionite quenching of the samples shown in (C), where the black line is TAP-Drs2p and the red line is Drs2p-TAP. (E) Specific activity of the protein samples from gel in (B), and (F) specific activity graph of proteoliposomes of gel in (C). (G) Flotation of fractions of TAP-Drs2p. Where P is a sample of the protein, and F1-F5 are fractions (bottom -> top).

Electroformation of Giant Unilamellar Vesicles (GUVs)

The process of vesicle budding, within a cell, is tightly regulated and occurs at a very rapid pace (Kinuta et al., 2002). Cargo proteins are selected and recruited to sites of vesicle formation, membranes deform and this deformation is captured by proteins, which shape the budding membrane into transport vesicles (Graham & Kozlov, 2010; Kirchhausen, 2000b). It is important in the trafficking field to determine the major players in this reaction and the role that they play. It is especially important to note which proteins are responsible for creating this membrane curvature – the point at which a vesicle can begin to take shape. Much work has been done purifying cytosolic proteins (such as Arf) and adding them to artificial membranes to show that they are able to cause membrane deformation (Beck et al., 2011; Matsuoka et al., 1998; Spang, Matsuoka, Hamamoto, Schekman, & Orci, 1998; Takei et al., 1998). However, this deformation seems to be a product of protein crowding (Stachowiak et al., 2012). The question then is – what protein(s) are able to create membrane curvature within the tightly regulated and spatially controlled environment of the cell? Our lab has hypothesized that Drs2p is a major player in this process.

Proteoliposomes containing purified Drs2p are excellent for *in vitro* experiments testing ATPase and flippase activities of the protein. However, these structures are very small, about 40nm in diameter, and much smaller than most transport vesicles (which are 50-100nm in diameter) (Kirchhausen, 2000b; Zhou & Graham, 2009). One way to address the role of Drs2p on membrane morphology is to incorporate Drs2p proteoliposomes

into giant unilamellar vesicles (GUVs). GUVs are 5-100μm in diameter, so they are easily imaged by optical microscopy and experiments can be done in real time.

There are several techniques for GUV formation. Uncontrolled swelling involves drying lipids onto a film and then rehydrating them to form GUVs (Criado & Keller, 1987; Manley & Gordon, 2008). Another technique is called electroformation and is the major technique that will be addressed in this section. In electroswelling, lipids are dried down onto a conductive slide and then rehydrated in the presence of an A/C electric field (Farge & Devaux, 1992; Girard et al., 2004; Mathivet, Cribier, & Devaux, 1996; Papadopulos et al., 2007). The advantage of the latter technique is that the GUVs are unilamellar and homogeneous in size.

In this chapter, I introduce work that was developed to electroform lipids into GUVs and to grow Drs2p proteoliposomes into GUVs. Different electroformation techniques are also discussed, and technical aspects (questions, trouble-shooting, etc.) that were faced during the course of the experiments.

As this project was initiated, the goal was to provide a direct test of the role that Drs2p flippase activity plays in membrane deformation and budding.

Results and Discussion

Xiaoming Zhou developed protocols for electroformation of giant unilamellar vesicles (GUVs) both in the absence and presence of Drs2p. He was able to successfully form protein-free GUVs (as published in his thesis). Using these same protocols as a starting point, Charles Day and I began work to grow Drs2p proteoliposomes into GUVs. I provided Charlie with Drs2p proteoliposomes and, using a combination of GUV protocols #1 and #2 (see "Protocols" section above), he electroformed them into GUVs at both room temperature and 4°C. The changes made included spreading, and drying, a film of lipids (DOPC and Rho-PE) onto the ITO slides. After this, the proteoliposome sample was spread on top and gently dehydrated the solution. Then, the sample was electroformed in the presence of the appropriate buffers.

The GUV sample was analyzed by running it, as well as a sample of the proteoliposome, on SDS-PAGE gels and staining with coomassie as well as immunoblotting. The GUV sample, since it was diluted during formation by the electroformation buffer, was loaded in at 5-fold the amount of the proteoliposome sample. In both the proteoliposome and GUV lanes (in the coomassie and Western blot), bands are visible for Drs2p (Fig. 3-12A and B). In Fig. 3-12C, we see that the GUV sample also had measurable specific activity (when compared to the DOPC+1% NBD-PS+ 5% PI4P proteoliposome sample). The seal of the GUV sample was tested by the dithionite quenching assay and it was found that there was almost 50% resistance to quenching by dithionite (Fig. 3-12D). These data indicate that the process of electroformation did not adversely affect the structure and activity of Drs2p. The question then becomes – is

Drs2p present in the GUV structures? And can we detect changes in membrane morphology?

Charlie worked on optimizing our electroformation and imaging conditions. He determined that working with 1V and 10Hz was ideal for producing the best quality GUV structures (Table 3-1). As shown in Fig. 3-12E, when a GUV is 20μm or larger (as in the lower panel), it makes the imaging easier – the larger size allows for better detection of these structures and these larger GUVs tend to move less making the images clearer. When the proteo-GUV structures were imaged, we found that the Rho-PE (Fig. 3-12F, left panel) – present in the lipid film – co-localized with the NBD-PS (Fig. 3-12F, center and right panels) – present in the proteoliposome samples. This co-localization (Fig. 3-12F, right panel), suggests that the proteoliposomes are merging with the lipid film to create these GUVs.

However, it was still unclear whether Drs2p was present in these structures. This method of GUV formation gives a very heterogeneous population of membranes (Fig. 3-12G). There is a mix of large and very small vesicles, as well as many membrane tubules. Only a few GUVs are formed that are suitable for imaging and reproducibility of the data is difficult since there's a great variation between the different GUV preparations. Also, addition of ATP to the few GUVs that could be imaged did not yield any positive results (data not shown). While this suggests that the GUVs with NBD-PS may not contain Drs2p, it doesn't exclude that possibility. There are a few explanations that could fit. It is likely that the NBD-PS, which has an NBD moiety on a C6 chain, is dissociating from the proteoliposomes during electroformation and, thus, the GUVs we

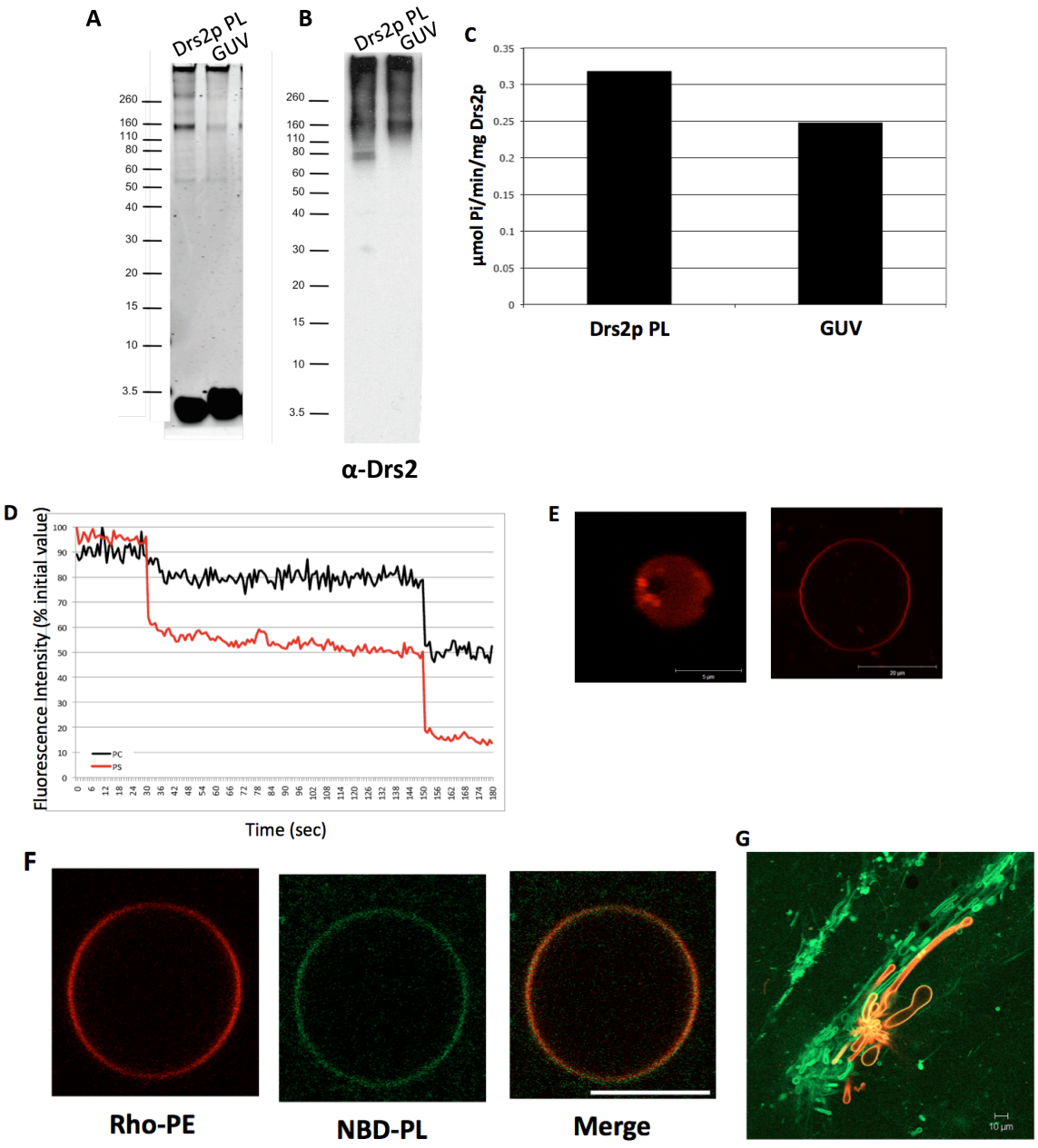

Figure 3-12. Basic electroformation techniques and assays for activity. Coomassie stained gel (A) and Western blot (B) of Drs2p proteoliposomes and electroformed GUV sample. Five-fold amount of the GUV sample was loaded compared to the proteoliposome sample. (C) Specific activity of proteoliposomes versus GUVs. The GUV sample had 5-fold greater amount of sample added than the proteoliposome sample. (D) Checking the seal of the GUV samples using fluorescence traces. The red versus black lines indicate different lipid compositions for the GUVs. (E) Larger GUVs are easier to image. Scale bars: 5µm (left) and 20µm (right). (F) Rho-PE from the lipid film and NBD-PL from the proteoliposomes are both found in the GUVs. Scale bar: 10µm. (G) Other structures visible after electroformation. Scale bar: 10µm.

observe in the green channel results from the transfer of NBD-PS from the proteoliposomes to the GUVs, rather than a merging of the entire membrane. Another possibility is that since we have such a small number of GUVs to image, there are no active Drs2p molecules present in those structures. Ultimately, we need to improve the yield of GUVs and the ability to detect Drs2p in proteo-GUVs.

Table 1: The effects of varying the voltage during GUV electroformation

V	Hz	Result
0.5	10	many MLV's and tubules; all ULV's under 3 mm diameter
1	10	~2 dozen GUV's in the 20-30 mm in diameter
2	10	nothing over 5 mm in diameter; most ULV's under 1 mm diameter
3	10	mostly very small vesicles

Table 2: The effects of varying the frequency during GUV electroformation

V	Hz	Result
1	10	~2 dozen GUV's in the 20-30 mm in diameter
1	20	mostly very small vesicles

Charlie visited the lab of Sarah Veatch at the University of Michigan and learned their technique for forming GUVs. Sarah is well known for her work with artificial membranes and Charlie was able to pick up several technical tips and tricks to enable us to form better GUVs. The protocol, provided by the Veatch lab, has been copied into the "Protocols" section of this Appendix chapter. The main changes include the techniques

used to spread the lipids on the ITO slides and the voltage and frequency at which the structures are electroformed. Using this technique, Charlie was able to form protein-free GUVs using DOPC+ DilC12 (Fig. 3-13A) as well as DOPC and Rhodamine-PE (Fig. 3-13B). These GUVs were large compared to the size of the GUVs that we previously made, and were on the order of 20 – 150 μm in diameter. When the same protocol was used to make proteoliposomes (including spreading the proteoliposomes on top of the dried lipid film), we found the proteo-GUVs that were forming were similar to the ones previously formed. The proteo-GUVs were small, with the largest ones having sizes of about 10μm (Fig. 3-13C and D). Furthermore, both Rho-PE (red, present in the lipid film), as well as NBD-lipids (green, present in the proteoliposome samples) were detected in the proteo-GUVs. Again, this suggests that the proteoliposomes and the lipid film are swelling into the GUV structures and it is possible that Drs2p can be found in them. However, experiments where ATP was added to these structures were fruitless, since the membranes exhibited no changes to membrane morphology (data not shown). So, the same questions remain as did with the previous protocol and preps – is Drs2p present in these proteo-GUVs? Are the NBD-lipids that we are observing from the merging of proteoliposomes into these structures or are they from micelles present in the samples?

I had the opportunity to visit Denmark and learn GUV electroformation techniques from them. The lab of Thomas Günther-Pomorski (at LIFE) was working a project where they were trying to reconstitute purified proton pump, from *A. thaliana*, into proteoliposomes and then incorporate this protein into GUVs. The goals of my visit included learning techniques from them (especially a different technique for electroformation), as well as

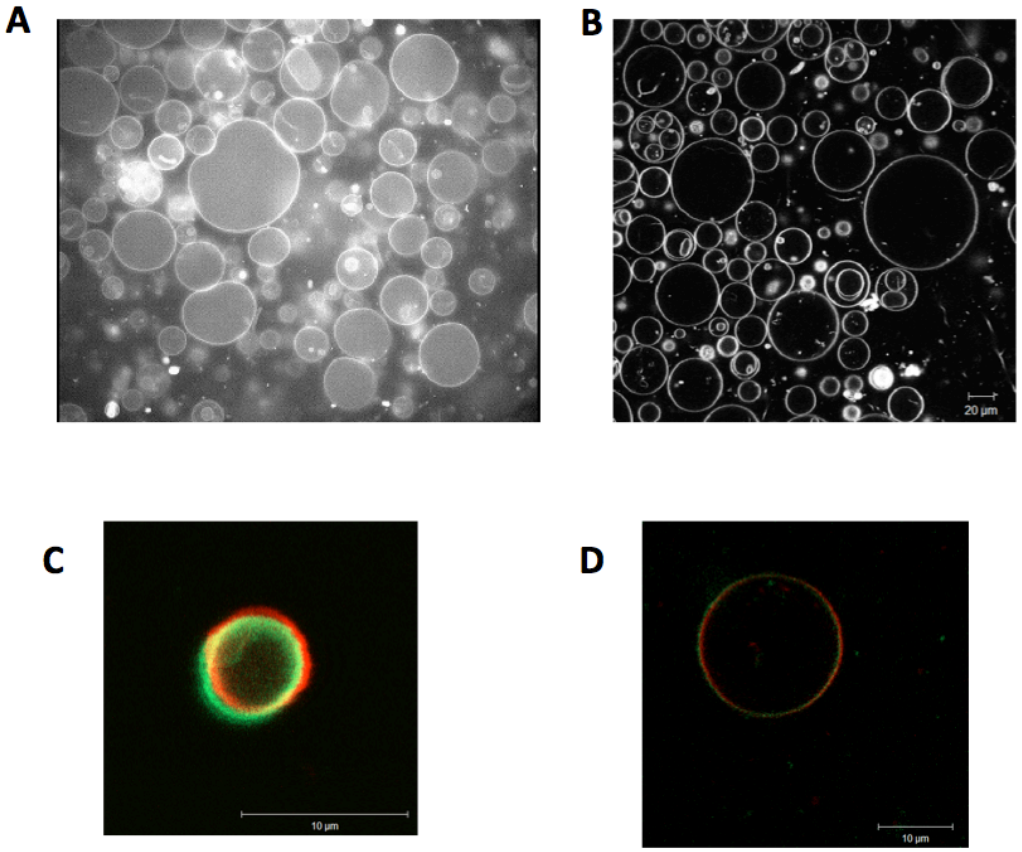

Figure 3-13. Electroformation of GUVs learned from the lab of Sarah Veatch. (A) GUVs formed in the lab of Sarah Veatch using DOPC + DilC12. (B) GUVs electroformed at Vanderbilt using the same techniques used in (A). Lipids are DOPC + Rho-PE. Scale bar for (A), (B): 20µm. (C) and (D) Electroformation of proteo-GUVs. Rho-PE from lipid film and NBD-PS form proteoliposomes. Merged images are shown. Scale bar for (C), (D): 10µm.

setting up a collaboration to combine our efforts and data into a larger paper. Prior to my visit, I purified large amounts of Drs2p and shipped it to their lab. These stocks of Drs2p had been assayed for yield (and concentration) and ATPase activity. I've included their reconstitution, ATPase assays, and GUV formation protocols in the Appendix chapter of this thesis.

The Drs2p was reconstituted and re-assayed for ATPase activity in Copenhagen. The Drs2p proteoliposomes had ATPase specific activity and Drs2p was detectable by coomassie staining. These proteoliposomes were electroformed into GUVs by spotting the samples onto ITO slides, partially dehydrating the samples, and electroforming for over 6 hours in the presence of a sucrose solution. All of the imaging in Copenhagen was done with a DIC microscope.

In Fig. 3-14, frames from movies for 2 of the GUVs, which tubulated after the addition of ATP, are presented (Fig. 3-14A and B). The GUVs shown are composed of DOPC and 20% DOPS. There are distinct tubes growing out of the larger GUV structure. Upon viewing the movie (which can be found with my electronic data), you can see these tubes begin to form within moments of ATP addition. As the tubes elongate, the main body of the GUV (which begins as a semi flaccid structure), becomes taut due to the increased loss of phospholipids from the inner leaflet. Within 30-40 seconds, the reaction is complete - the GUV tightens as the tubes grow and eventually bursts, probably because it can no longer sustain the pressure associated with the redistribution of the lipids and the need to maintain membrane bilayer coupling.

Drs2p was reconstituted into several lipid compositions (see below), which were then tested for changes in GUV membrane morphology. In all, of about 50 experiments done, only 3 of the experiments yielded GUVs where we were able to see such directed growth of the membrane tubules. One issue that was constantly faced was difficulty in finding GUVs to image, especially considering that we were using DIC imaging. In Fig. 3-14, you can see how difficult it is to distinguish GUVs from the background of the slide.

Furthermore, these GUVs are constantly flowing so finding a GUV and capturing it is quite difficult. Lisa Theorin, our Danish collaborator, helped with the imaging. When ATP was added to the sample, it exacerbated GUV movement. In addition to flowing, the GUVs often tended to float. This was an additional layer of difficulty because the GUV would move out of the field of focus. As a result, I was constantly trying to re-focus to find it. This was often unsuccessful. Moreover, because the GUVs were bursting within seconds, there was only one shot at collecting data on each slide.

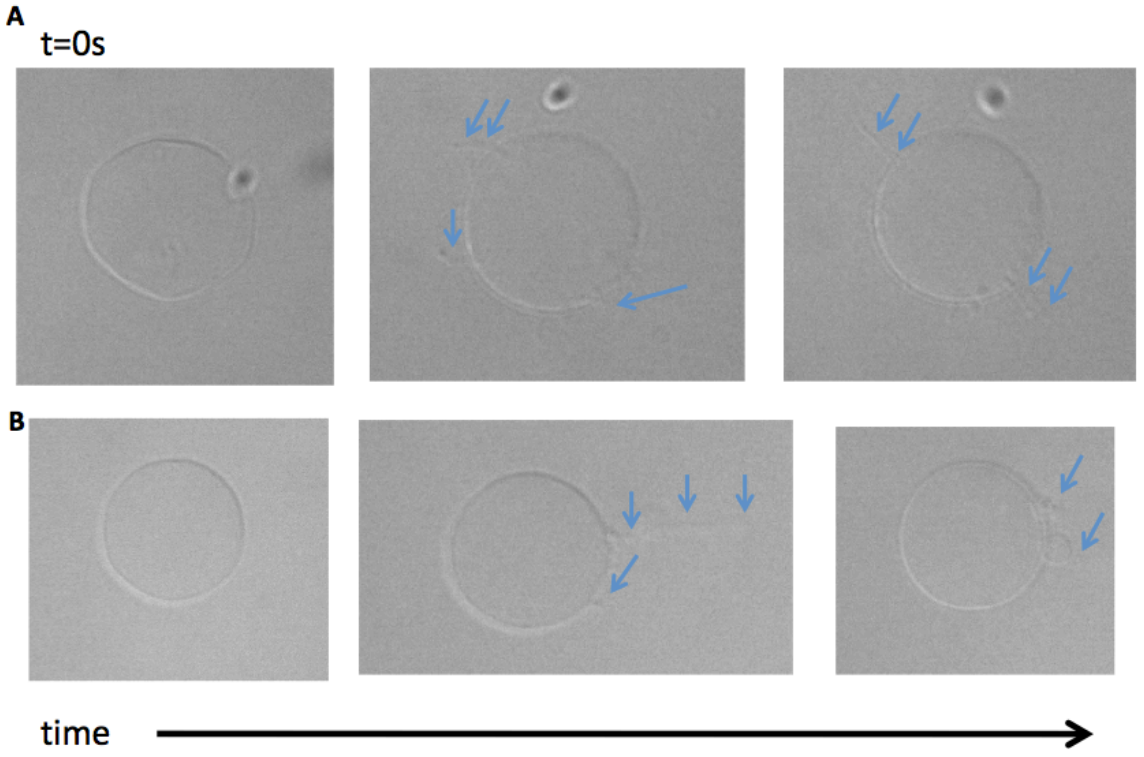

Figure 3-14. Assaying GUVs for changes in membrane morphology after ATP addition. (A) and (B) Upon addition of ATP at time = 0sec, the GUVs immediately began tubulating and producing thin and long projections from different parts of the GUV. As these tubes grow, the main body of the GUV became more rigid. When the GUV was no longer able to withstand the pressure resulting from the growth of these tubes, it finally burst. The light blue arrows point to the tubes that are forming. The entire reaction lasts about 40 seconds. Imaging was done using microscopes with DIC capabilities. For these experiments, Drs2p was reconstituted into proteoliposomes consisting of DOPC and 20% DOPS.

Lipid conditions tested for GUV electroformation:

DOPC

DOPC + 20% DOPS

DOPC + 20% DOPS + 1% PI4P

DOPC + 0.1% Rhod-PE

DOPC + 20% DOPS + 0.1% Rhod-PE

DOPC + 10% DOPS

DOPC + 10% DOPS + 1% PI4P

* These samples were assayed with and without ATP, and with ATPγS

In the US, I worked to recapitulate the experiments done in Denmark. I brought back ITO slides and silicon spacers from their lab. The reason being that they did not have catalog information or technical specifications for any of these items. As a result, neither they, nor I, were able to order more quantities of these items. The electroformation generator that was being used, was also quite different from the one at LIFE. So, I wasn't able to recapitulate the settings on the machine. I tried to find (and purchase) a generator that was similar but was unable to do so. Again, they were unable to provide any purchase information for their equipment. I tried to make the GUVs with as close settings as possible on our machine, but I wasn't able to obtain any GUVs. When I tried to adapt the Veatch protocols (since we had previous success using their settings on our generator), it scorched the ITO slides from Denmark. This tells me that their ITO slides have a different (probably lower) level of conductivity than the ones we're using. Unfortunately, there is no way to know what those levels are.

Moreover, since I wasn't able to find a lab or inverted microscope that had DIC settings, I resolved to use fluorescence instead. This was also helpful because it meant that I would be able to find the GUVs much more easily in the field of view, even if there was a low yield of GUV structures in my sample.

Since it was difficult to recapitulate the Danish group's protocol, I used techniques from both the Danish group and the Veatch lab (as well as trial-and-error) to develop a protocol that gave me consistent preps of GUVs. These GUVs were large and could be easily found using a fluorescent microscope (Fig. 3-15A and B). Furthermore, a lipid film was no longer deposited onto the ITO slides, so all the lipids in the GUVs came from proteoliposomes. Most of the proteoliposomes had 1% NBD-lipids or 0.1% Rho-PE which made GUV detection by fluorescence microscopy easier. This protocol is the last protocol provided in the "GUV Protocols" section in the Appendix chapter.

When imaging these GUVs, some of the same issues arose that were faced with the GUVs in Denmark. These GUVs tended to flow within the plane of imaging and sometimes floated to the surface of the sample (out of the field of view). This was a problem especially during ATP addition. Furthermore, small changes in the osmolarity of the solution caused big changes in the GUV structure (Fig. 3-15C). They tended to become flaccid and often elongated into tubular structures or had large tubules extend from their main body. Occasionally, they re-formed into circular GUVs. Some GUVs, meanwhile, were extremely taut and burst when ATP was added to the solution. It was also essential to image these GUVs quickly because evaporation on the slides caused rapid changes in osmolarity and, as a consequence, in the flaccidity or tautness of the

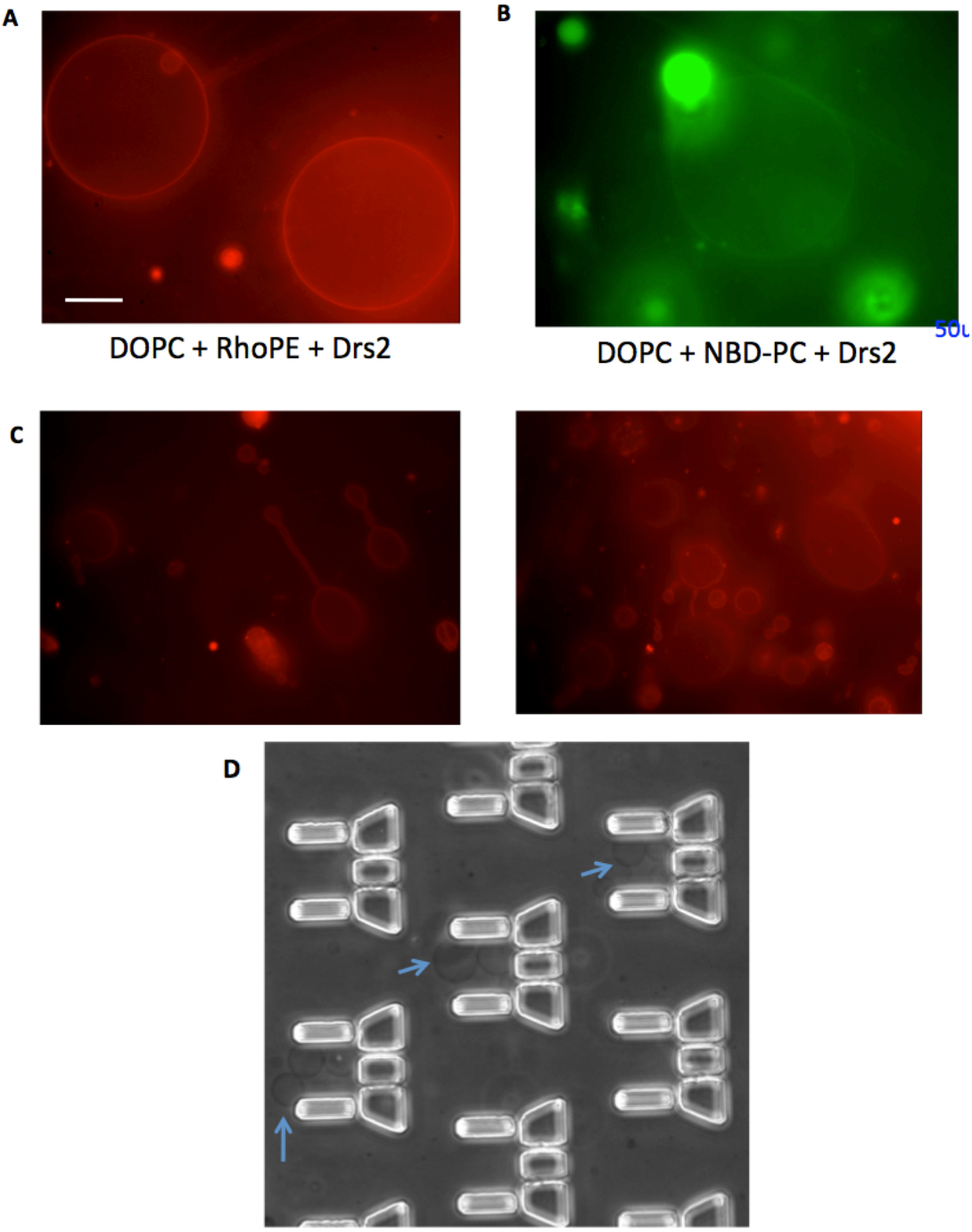

Figure 3-15. New electroformation techniques using fluorescence analogs. GUVs were electroformed using DOPC + Rho-PE (trace) + Drs2p (A), or DOPC + NBD-PC (1%) + Drs2p (B) to test a new electroformation technique using a fusion of the Veatch and Danish protocols. Scale bar: 50μm. (C) Large bulbs and tubes extend out of the GUVs due to uncontrollable shifts in the osmolarity of the solution. (D) GUVs trapped in a microfluidic chamber (see light blue arrows). Images obtained using DIC.

GUV membrane. Thus, imaging these samples, especially during ATP addition, was difficult.

I was able to detect tubulation similar to those observed in Denmark in these samples. The proteo-GUVs used to form the same types of tubes observed previously and then burst, when the pressure of tubule formation was too great for the GUV structure. None of these tubulation events were captured by video because the GUVs used to float away faster than I could turn on the camera while tracking their movements.

Several different techniques were attempted in order to improve imaging GUVs both before, during, and after ATP addition. First, the GUVs were sunk to separate the larger GUVs from smaller GUVs. Since GUVs are electroformed in the presence of sucrose and imaged in the presence of the same concentration of glucose, the GUVs tended to sink. This is because sucrose is denser than glucose even though they were present in the imaging sample in equimolar concentrations. To sink GUVs, you must gently pipet the GUVs (after electroformation) into a glucose solution of equimolar concentration to the sucrose concentration used during electroformation. Allow the GUVs to settle for several minutes and then remove small aliquots from the bottom of the tube. When this process is done using protein-free GUVs, one tends to get a large GUVs concentrating at the bottom of the tube (also see Fig. 3-13A and B for an example). However, when this process was done using proteo-GUVs, the large GUVs in the population were not separable from smaller membrane structures – in fact, no GUVs could be isolated.

An alternate approach was, during ATP addition, to decrease the disturbance to the solution on the slide by adding in the ATP using a syringe or gel-loading tip. The idea was that adding ATP, in this manner, would be much gentler than pipetting a drop onto the surface of the solution. While this did decrease the movement a little, it was not enough to help with the imaging issues. I worked with Yuantai Wu (lab of Chris Janetopoulous) to add ATP using a micro-injector. This device is commonly used in the Janetopoulous lab to gently add reagents at a specific location on the slide for chemotaxis experiments. The micro-injector is hooked up to a microscope which enables imaging during addition of the desired reagents. This technique, again, did not work. There were several reasons for this – (a) we could not control or determine the amount of ATP that was being released by the micro-injector, (b) while the Janetopoulous lab uses cells (which adhere to the surface of the glass slide and moves less than GUVs), the GUVs are free floating and addition of ATP caused them to float out of the field of view, and (c) many of the GUVs burst during addition of ATP and/or had large tubules form due to sudden changes in the osmolarity of the solution (as described previously). The videos showing this phenomenon can be found with GUV imaging data in my data folders.

I worked with Neil Dani (Kendal Broadie lab) and Greg Pask (Larry Zweibel lab) to try to hold GUVs in place during ATP addition using a suction pipet and applying a gentle vacuum. We attempted the application of this vacuum both by manual and computerized methods. No matter how low the vacuum pressure applied, the GUVs, because they did not have a cytoskeleton or other mechanism that gave them structure, were getting sucked into the micro-pipet tip. In collaboration with the lab of John

Wickswo, I worked with Tommy Byrd and Kailey MacNamara to trap the GUVs in microfluidic devices. The goal was to flow the GUVs into these structures and then flow ATP into the system. When ATP makes contact with the GUVs, we can observe tubulation through a microscope and camera system that is hooked up to these devices. While GUVs were easily trapped in the microfluidic devices (Fig. 3-15D), and ATP was flowed in, we were not able to observe tubulation because the objectives on their microscope were not powerful enough to detect the small changes in the GUVs. Also, the objectives in their microscope could not be changed because of the way the system was set up. Most of the imaging was done in DIC. We tried to move into fluorescence microscopy but because the objectives did not provide sufficient magnification, nothing could be detected. Thus, there are several issues that remain with imaging the GUVs and getting good quality videos for publication. On a basic level, the tubulation of the GUVs (during ATP addition) could be observed and captured, but the question still remains – where is Drs2p during this event? On the tube? On the GUV? At the intersection between the two?

To better answer this question, a protein labeling kit for Alexa 488 (which dyes proteins for fluorescence in the green channel) was used to label purified Drs2p. After trying several methods, the following method worked best for labeling Drs2p. After incubation of Drs2p with the dye, the protein-dye mixture was applied to a Ni column and the excess dye was allowed to flow through. The column (with labeled Drs2p) was washed to remove traces of the dye and the labeled protein was eluted using imidazole. A separate sample of Drs2p was treated as a mock labeled control – it was not labeled (but was incubated with the same buffers) and was passed through the Ni column just

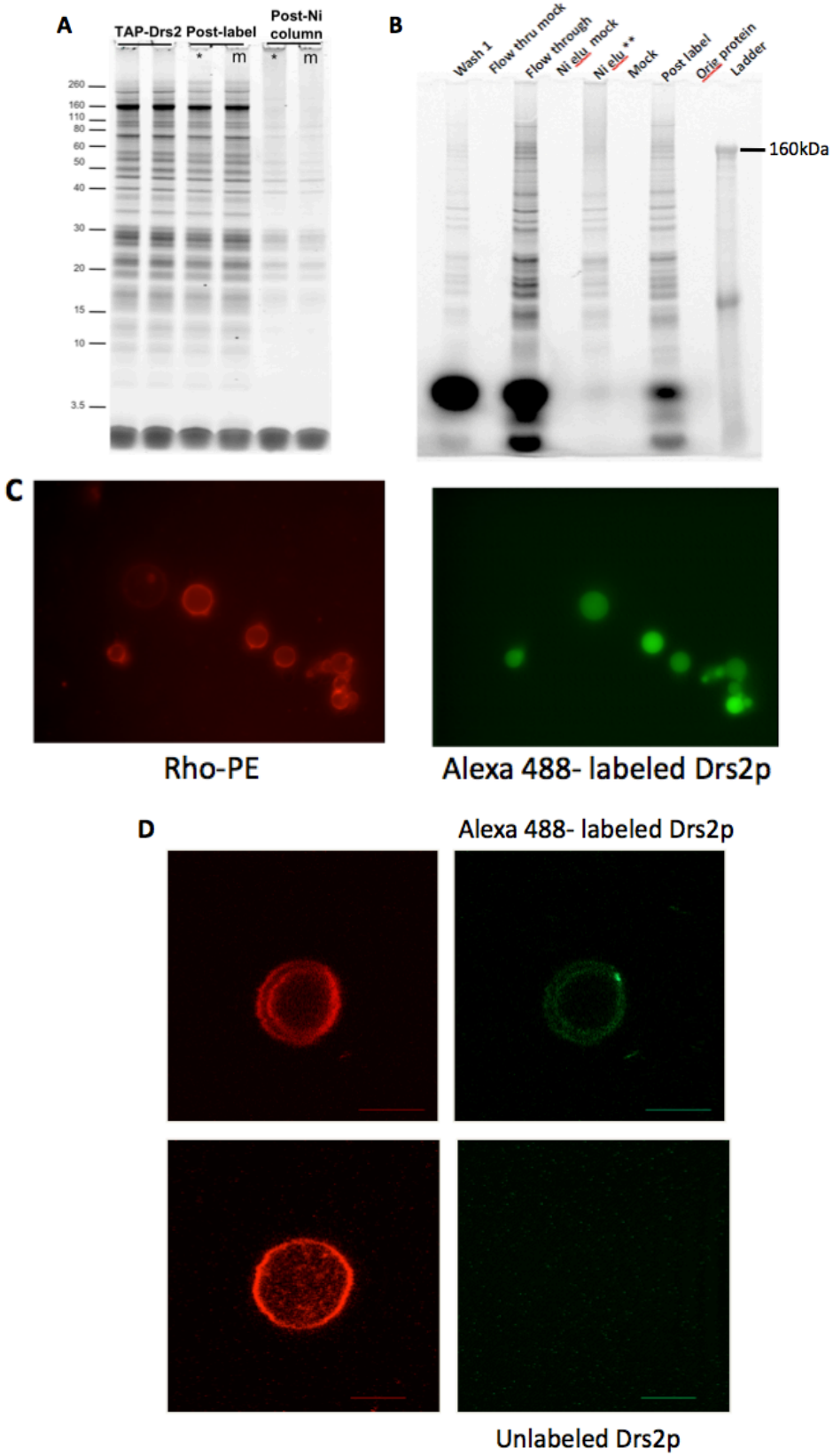
A
TAP-Drs2
Post-label
Post-Ni column
*
m
*
m
260
160
110
80
60
50
40
30
20
15
10
3.5
B
Wash 1
Flow thru mock
Flow through
Ni elu mock
Ni elu **
Mock
Post label
Orip protein
Ladder
160kDa
C
Rho-PE
Alexa 488- labeled Drs2p
D
Alexa 488- labeled Drs2p
Unlabeled Drs2p

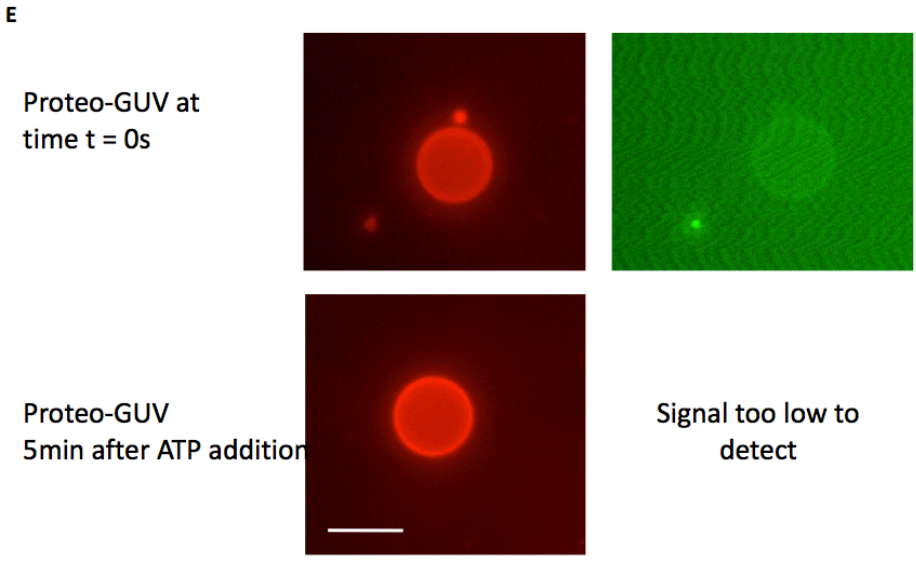

Figure 3-16. Chemical labeling of Drs2p. (A) Single-step purified Drsp2 was labeled using an Alexa-488 chemical dye. Coomassie showing pure protein (TAP-Drs2), protein post-labeling (Post-label, where "*" is labeled protein and "m" is mock control), and labeled protein after application to a Ni^{+2} column (where "*" is labeled protein and "m" is mock control). (B) The gel in (A) was analyzed using a Typhoon scanner to determine if Drs2p fluorescence could be detected on the gel. Where "Ni elu**" is labeled protein, and a few of the flow-through and wash samples are also run on the gel. (C) GUVs were electroformed using the labeled Drs2p and imaged. Rho-PE was present in the lipid mixture added during reconstitution. (D) GUVs (with Rho-PE in red) electroformed and imaged using either labeled Drs2p (top panels) or unlabeled Drs2p (bottom panels). Scale bar: 10μm. (E) Proteo-GUVs with labeled Drs2p (same samples as used in (D)) both before and 5 min after addition of ATP.

like the labeled sample. Aliquots of these samples were run on an SDS-PAGE gel. The gel was imaged using a Typhoon system to try and pick up the fluorescence of the labeled sample (Fig. 3-16A), and the gel was then stained with Coomassie to determine amount of protein (Fig. 3-16B). From these images, you can see that after elution of the protein from the Ni column, it was difficult to detect any protein on the Coomassie (for the labeled and mock samples). Also, I hoped to detect a clear fluorescent band on the Typhoon exposed gel image, but was unable to do so. This suggests that the protein is not getting labeled. Furthermore, the Drs2p is unable to interact with the Ni beads (since

it's flowing through and there's no band detectable for Drs2p on the Coomassie). Another attempt at labeling showed that most of the Drs2p is not present in the flow-through (data not shown). ATPase assays on the remaining protein shows that there's barely any ATPase activity (data not shown). This could be either because there's so little protein present or because the label is interfering with the protein activity.

Since there were a few (faint) bands detectable for labeled Drs2p in the Typhoon images, I reconstituted the labeled Drs2p (into PC + 0.1% Rho-PE) and electroformed the proteoliposomes into GUVs. When imaged, several GUV structures that fluoresced green were detected (Fig. 3-16C). These labeled structures, though, looked like they were filled with dye instead of having a circular fluorescence (suggesting labeling of the membrane) like the Rho-PE. Although several attempts were made, none of these structures tubulated during ATP addition.

Lisa Theorin (from Denmark) visited our lab to learn these techniques, and during her time here, worked on labeling Drs2p and imaging proteo-GUVs. She successfully purified, labeled and reconstituted Drs2p into PC + 0.1% Rho-PE proteoliposomes, and electroformed them into GUVs. When these samples were imaged, Alexa dye was detected in the membrane of the GUV (Fig. 3-16D, top panels). Such fluorescence was not detected in the mock-labeled samples (Fig. 3-16D, bottom panels).

Lisa's samples were used to test for tubulation of the GUVs during ATP addition. If Drs2p had indeed been labeled, most of the GUVs that fluoresce in the green channel should tubulate during ATP addition. However, when ATP was added, no changes in

GUV morphology were detected. Moreover, at least 50 GUVs that fluoresced in the green channel were tested and none of them had any tubulation or elongation phenotypes. In Fig. 3-16F, an experiment is shown where a labeled proteo-GUV is imaged, both before, and 5 minutes after, ATP addition. There are no changes to the GUV membranes in any of the frames. So, either the Alexa-488 labeled Drs2p is inactive, or it is possible that the flippase activity of Drs2p is not capable of deforming membranes as we hypothesized.

Weaknesses and Future Directions

Ultimately, Drs2p was electroformed into proteo-GUVs that could be imaged with fluorescence microscopy. Tubulation of these membranes was also observed and, at a preliminary level, captured by video. The dependence on ATP addition, of this particular type of membrane tubulation, suggests that this reaction is Drs2p-dependent. Unfortunately, there are several technical issues that plague this project – GUVs that flow and float, proper labeling of Drs2p, and appropriate imaging techniques.

Improving imaging techniques will enable the rapid collection of better quality images and videos. In addition to the approaches attempted (as described in this section), I tried to gently tether the GUVs to the surface of a steptavidin coated slide, by incorporating small amounts of biotinylated phospholipids in the GUVs, but not much work was done with this protocol. Optimizing conditions for gently tethering GUVs might enable the reduction of GUV flow and flotation during data collection. Gerdi

Kemmer (from the Pomorski lab), provided a basic protocol which she developed and this is included in the "Electroformation Protocols" section of the Appendix chapter.

Answering the question of where Drs2p is, relative to the tubulation event, will be a major step towards completing this project. At the 2012 ASCB conference, I had the opportunity to speak to several scientists who were experts or were actively working in the area of GUV formation. While most of them work primarily with cytosolic proteins, they were kind enough to give me some feedback about this project. One of their suggestions was to avoid using fluorescence labeling kits to label Drs2p. In their experience, they observed much secondary labeling of the membrane by these dyes (which may explain the results that were observed). Their advice was to clone GFP onto Drs2p or clone in SNAP tags into the protein, so that these tags could be chemically labeled. It is unclear what effect, if any, these cloning steps might have on the purification, yield, and activity of Drs2p.

Based on these suggestions, the best way to proceed to complete this project is to clone GFP onto the N-terminus of Drs2p, between the TAP tag and the protein. This protein will, most likely, be active because GFP-Drs2p is a construct that is commonly used in the lab for *in vivo* experiments. However, the stability of the protein structure and activity of Drs2p, after protein purification, will have to be determined experimentally.

Other questions that need to be addressed include the following:

- Was the tubulation observed in Denmark (and in the recapitulated experiments) due to the flippase activity of Drs2p? (labeling the protein will help answer this).

  The protein used for these experiments was single-step purified and there are many proteins that co-purify with Drs2p. Are any of these proteins causing or contributing to the tubulation that was observed?
- Can active preps of GFP-Drs2p be obtained?
- Is Drs2p truly incorporated into the proteo-GUVs we're imaging?
- If Drs2p is chemically labeled, is it still active?

  An email from Lisa indicated that when they chemically labeled their purified proton pump, it was no longer active. This could be why addition of ATP to our labeled Drs2p-GUVs failed.

Other aspects to look into include different methods for making GUVs, such as using fusion of proteoliposomes to create GUVs by using fusogenic peptides, lipids, or proteins (such as SNAREs). Although this makes the system more complex, it might resolve many of the issues that are present in the current system and results in the formation of larger sized proteo-GUVs with several molecules of protein present.

CHAPTER IV

SUMMARY AND FUTURE DIRECTIONS

The movement of proteins from the Golgi complex to various parts of the cell is mediated by small transport vesicles. These vesicles bud off from the Golgi and carry with them macromolecules and proteins that are targeted to the various organelles or regions of the cell (Bonifacino & Glick, 2004). This trafficking is essential for the normal function and growth of a cell. In *Saccharomyces cerevisiae*, Drs2p, the founding member of the type IV P–type ATPase (P4–ATPase) family, is known to be responsible for aiding in the formation of these transport vesicles from the *trans*–Golgi network (TGN) and early endosomes (C. Y. Chen et al., 1999; Graham, 2004; Hua et al., 2002). This is achieved by the flipping of specific phospholipids from the exoplasmic to the cytoplasmic leaflet of the membrane. Such translocation results in membrane asymmetry, and also allows for the formation of transport vesicles in association with specific adaptors, coat proteins (such as clathrin), and cargo.

The plasma membrane of most eukaryotes is asymmetric in both protein and lipid composition. The lipids that are typically found in the extracellular leaflet of the membrane bilayer are phosphatidylcholine (PC) and sphingomyelin, while phosphatidylserine (PS), phosphatidylethanolamine (PE) and phosphatidylinositol (PI) are found in the cytosolic leaflet (Devaux, 1992; Zachowski, 1993). This difference in

membrane lipid composition is critical to the normal functioning of the cell. For instance, loss of membrane asymmetry that leads to the exposure of PS on the extracellular face of the cell can trigger various signals including platelet activation, clearance of senescent red blood cells and phagocytosis of apoptotic cells (Williamson & Schlegel, 2002; Zwaal, Comfurius, & van Deenen, 1977; Zwaal & Schroit, 1997).

Phospholipids are amphiphilic molecules that consist of hydrophilic heads and hydrophobic tails. Several phospholipids can come together to form energetically favorable structures, such as micelles and bilayers, which allow them to expose their hydrophilic head groups to the aqueous exterior and bury their hydrophobic tails (Alberts, Johnson, et al, 2008). Phospholipids are able to diffuse very rapidly through the plane of the leaflet. However, they are unable to translocate from one leaflet of the membrane bilayer to the other without overcoming a substantial energy barrier (Daleke, 2003; Dolis, Moreau, Zachowski, & Devaux, 1997; Pomorski, Holthuis, Herrmann, & van Meer, 2004). The half–time for spontaneous phospholipid flip–flop in liposomes is on the order of several hours to days depending on the lipid and the membrane.

Several types of protein transporters exist which are able to cause rapid phospholipid flip–flop across the membrane. These transporters are classified according to substrate specificity, requirement for energy and direction of transport. The major focus of our lab is on phospholipid translocases, or ATP–dependent flippases. Flippases use energy from ATP hydrolysis to translocate specific phospholipids such as PS and PE from the lumenal leaflet to the cytosolic leaflet of a membrane. This activity is uni–directional and

ATP–dependent (Daleke, 2003; Dolis et al., 1997; Graham, 2004; Menon, 1995; Pomorski et al., 2004). P4-ATPases are believed to be the proteins responsible for generating such phospholipid asymmetry in biological membranes. The Drs2p/ATPase II subfamilies of P-type ATPases have been implicated as the enzymes that catalyze this activity.

The yeast P4–ATPase, Drs2p, is an integral membrane protein possessing 10 transmembrane segments (C. Y. Chen et al., 1999; Hua et al., 2002). There are four additional members of the P4–ATPase family in *S. cerevisiae*, namely Dnf1p, Dnf2p, Dnf3p and Neo1p (Catty, de Kerchove d'Exaerde, & Goffeau, 1997; Graham, 2004; Hua et al., 2002). Drs2p, along with Dnf1p, Dnf2p and Dnf3p, forms a group of essential genes. This means that presence of any one of these genes will allow for cell viability but deletion of all four of these genes will be fatal to the cell (Hua & Graham, 2003). Such a relationship suggests a certain degree of functional redundancy between these P4–ATPases. These proteins are typically associated with a β subunit (Cdc50p for Drs2p, Lem3p for both Dnf1p and Dnf2p) and form a heterodimeric complex. The association of the β subunit to the P4–ATPase (α subunit) is required for the ER export of this α–β subcomplex and proper localization. While Drs2p is normally localized to the TGN of a cell, it is thought to cycle between the TGN and the early endosomes, as well as to the plasma membrane, early endosomes and back to the TGN. Drs2p facilitates the formation of clathrin–coated vesicles from the TGN and early endosomes (Liu et al., 2008).

Clathrin–coated vesicles are found in all nucleated cells, from yeast to humans. These vesicles enable the trafficking of various proteins and lipids between organelles, especially between the plasma membrane and the endosomes, and between the TGN and the early endosome (Liu et al., 2008). For clathrin–coated vesicles (CCVs) to form, a variety of adaptor proteins and associated proteins are essential. The heterotetrameric adaptor protein, AP-1, is involved in CCV formation at the TGN while AP-2 functions in endocytosis at the plasma membrane. Initiation of vesicle formation, at the TGN, occurs when Arf1–GTP (ARF1, ADP–ribosylation factor 1) is recruited to the membrane. Arf1-GTP then proceeds to recruit AP-1 which recognizes and binds a variety of cargo proteins (Kirchhausen & Harrison, 1981; Ungewickell & Branton, 1981). Cytosolic clathrin is then recruited to the bound adaptor proteins. Clathrin organizes itself into hexagons and pentagons which enable it to enlarge the budding vesicle (Kirchhausen & Harrison, 1981). Membrane deformation increases as more coat proteins are assembled onto the vesicle. The protein amphiphysin then binds clathrin and acts as a receptor for dynamin which works to pinch off the fully formed vesicle at the bud neck. Hsc70–ATP and auxilin are responsible for driving the disassembly of the clathrin coat, once the vesicle has been formed (Ahle & Ungewickell, 1989).

As described in the Introduction (see section on "Membrane Asymmetry and Membrane Curvature"), there are several hypotheses about how membrane curvature is captured and the proteins responsible for creating this curvature. In the Graham lab, we favor the model that Drs2p, by its unidirectional flippase activity, is responsible for creating positive membrane curvature at sites of vesicle budding. Our lab has been able to show

that in the absence of Drs2p, there is no AP-1/CCV function even though the coat is recruited to the TGN (Liu et al., 2008). By electron microscopy, these Golgi membranes in *drs2*Δ cells are enlarged, cup-shaped structures with much less curvature than the tubular-vesicular structure of Golgi cisternae in wild-type cells. We hypothesize that Drs2p contributes to membrane curvature based on the appearance of Golgi cisternae in *drs2*Δ cells and predications based on the bilayer-couple hypothesis. Drs2p, we hypothesize, flips phospholipids from one leaflet to the other, expands the outer leaflet causing the creation membrane curvature which is captured by curvature-sensing proteins that are able to recruit AP-1 and clathrin onto the membrane (Graham & Kozlov, 2010). However we have no direct evidence that Drs2p activity causes membrane bending.

While phospholipid translocase activity had previously been observed in erythrocyte membranes, there had been no work correlating this activity to a particular class of proteins. The first indication that phospholipid translocase activity was due to the action of P4-ATPases, came when Paramasivam Natarajan (of the Graham lab) published his work looking at flippase activities in purified *trans*-Golgi membranes from the yeast, *S. cerevisiae*. Natarajan was able to show that activating these TGN membranes resulted in the translocation of spin-labeled analogs of phosphatidylserine (PS). Furthermore, he was able to demonstrate a Drs2p substrate specificity for PS over PC (phosphatidylcholine) (Natarajan et al., 2004).

Finally, it was in 2009, when independent publications from the Graham and Molday groups, showing the purification, reconstitution and *in vitro* flippase activities of P4-ATPases, that this work was directly tested (Coleman et al., 2009; Zhou & Graham, 2009). This was some of the first work demonstrating, in a reconstituted system, that flippases were able to flip a phospholipid across a membrane bilayer. Prior to this, several groups had been successful in purifying ATPase II/Atp8a1, but not in reconstituting it or demonstrating flippase activity (Ding et al., 2000; Moriyama & Nelson, 1988; Paterson et al., 2006; Xie, Stone, & Racker, 1989). The Graham lab was able to show flippase activity for Drs2p, while the Molday lab demonstrated this in ATP8A2. Initially there was much genetic evidence to suggest that these P4-ATPases were flippases but these observations could just as easily have been attributed to secondary transport mechanisms. It was the detection of flippase activity at the TGN (Natarajan et al., 2004), as well as the plasma membrane and secretory vesicles (Alder-Baerens et al., 2006; Pomorski et al., 2003; Riekhof & Voelker, 2006; Stevens, Malone, & Nichols, 2008) that gave convincing evidence that these proteins were indeed flippases. The work by these groups, coupled with the biochemical evidence presented by the Graham and Molday labs have further cemented the notion that P4-ATPases are phospholipid flippases.

While this work brought considerable progress to the field, the question remained – what influence, if any, does the flippase activity of P4-ATPases have on membrane morphology? To answer this question, I used a combination of purified Golgi membranes and negative stain EM to observe changes in membrane morphology. Golgi membrane purification was a technique developed by Paramasivam Natarajan

(Natarajan & Graham, 2006). TGN membranes were purified from strains which lacked four of the five yeast P4-ATPases (Drs2p, Dnf1p, Dnf2p, and Dnf3p), which are the four flippases that form an essential gene family. These strains were kept alive with either a wild-type or temperature-sensitive form of Drs2p (*DRS2* or *drs2-ts*). The advantage of using these strains was that changes in membrane morphology, due to the flippase activity of the protein, could be primarily attributed to the function of Drs2p. I found that late Golgi membranes, purified from these strains (which are extremely slow-growing), were very heterogeneous in size (Fig. 3-1A and B). It suggested that the Golgi membrane was fragmenting during purification. However, Drs2p was considerably enriched in the Golgi membranes when compared to whole-cell extracts (Fig 3-1D).

Since these samples (due to the heterogeneity in size of the membranes) were not ideal for further assays, I purified membranes from wild-type and *kes1*Δ cells. The hope was that, by using *kes1*Δ membranes, there would be greater amounts of flippase activity detectable since Drs2p-dependent PS flippase activity is hyperactive in these strains (Muthusamy, Raychaudhuri, et al., 2009). Late Golgi membranes from these strains yielded membranes which were larger, and easier to visualize using EM (Fig. 3-2A), with average membrane diameters around 150nm (compared to ~70nm for the quadruple mutant strains) (Fig. 3-2B). After addition of ATP, via an ATP regeneration system, and incubation for 15min at 37°C, wild-type membranes showed some tubulation and elongation (Fig. 3-4A). When these experiments were repeated with the three other strains (*kes1*Δ, *DRS2*, and *drs2-ts*), obvious tubulation and elongation were not apparent. What was apparent, was that it looked like there was fusion of smaller

membranes to form larger membranes (Fig. 3-4 C-E). Looking over the wild-type membrane data seems to suggest the same phenomenon.

Ultimately, while tubulation and elongation of the membrane (i.e. the creation of membrane curvature), cannot be ruled out since it was present in such a small percentage of the membranes, it is just as likely that activation of the membranes by ATP is causing vesicular fusion. This fusion, as it occurs, gives the appearance of tubulation and elongation. Finally, these experiments were designed to determine the influence of flippase activity on membrane morphology. Since these are native Golgi membranes which have many integral proteins present in the membrane, and cytosolic proteins that may be associated with the membrane, we cannot rule out the possibility that the changes in membrane morphology are due, either directly or indirectly, to the function of any number of these proteins. If it is possible to detect Drs2p on these membranes, by either immunogold labeling or affinity purifying these membranes against Drs2p antibodies so that all the membranes assayed possess at least one molecule of Drs2p, we will be much closer to determining whether the tubulation/elongation morphology or the membrane fusion, is in fact due to the activity of Drs2p phospholipid translocation.

To tie the influence of flippase activity to the generation of membrane curvature, as well as a potential role in the formation of transport vesicles, I attempted to recapitulate clathrin-coated vesicle budding using purified cytosol preps and Golgi membranes from my various strains. The cytosol preps were chock full of small vesicles that contained Drs2p (Fig. 3-5B). Attempts at purifying away these vesicles and obtaining a sample

containing only cytosolic proteins were unsuccessful (Fig. 3-5E). Initial experiments where late Golgi membranes were incubated with ATP and cytosol were also not conclusive. Improving cytosol purification conditions or purifying cytosolic proteins (involved in formation of transport vesicles) and adding them back into the reaction may alleviate this problem.

Furthermore, at the time of these experiments, the role of the C-terminal tail of Drs2p was not very clear. Perhaps using Drs2p strains lacking the C-tail or enzymatically removing the C-tail will ensure that most of the Golgi membranes will possess active Drs2p (Zhou et al., 2013). This change will, hopefully, increase the amount of flippase activity at the membrane and make changes in membrane morphology more apparent.

Since a major flaw with the Golgi membrane experiments was their complexity and our inability to control membrane composition, I transitioned to working with the reconstituted system in the hopes of gaining clearer results. Although learning the purification and reconstitution techniques was expected to be fairly straightforward – these protocols had been previously published from our lab – it was anything but. I was able to purify the protein and, in my hands, Drs2p had ATPase activity values similar to our previously published results. The major issue faced with these techniques was that reconstitution of Drs2p into properly sealed proteoliposomes was unsuccessful. This was a major setback and was one that was faced by Xiaoming Zhou as well (he developed these techniques). As a result, considerable amounts of time were spent trying to fix the "leaky liposome" problem. This included experiments tweaking every

aspect of the purification and reconstitution protocols (this work is detailed in the beginning of the Chapter 3, Section 2). Finally, it was switching detergents, from C12E9 to C12E8 (Fig. 3-6 versus Fig. 3-11), that enabled the formation of properly sealed proteoliposomes.

This single change improved the purification and reconstitution protocols considerably. In single-step purified Drs2p samples, the concentration of protein jumped from 25ng/μL to almost 55ng/μL (Fig. 3-11B). Furthermore, the ATPase activity of the samples increased 10-fold (Fig. 3-11E and F). Finally, while Drs2p reconstituted in the presence of C12E9 had 3-5% resistance to quenching by dithionite, Drs2p reconstituted in the presence of C12E8 was 25 – 30% resistant to dithionite quenching (Fig. 3-11D). This means that 50 – 60% of the proteoliposomes were sealed. This improvement in seal now allowed me to move forward with performing flippase assays and preparing proteoliposomes for electroformation into giant unilamellar vesicles. Best of all, these results were consistently reproducible and other graduate students in the lab were able to successfully reproduce these results.

During the attempts at improving proteoliposome seal, I attempted to purify and reconstitute Drs2p using a protocol developed by the lab of Robert Molday (Coleman et al., 2009). In their protocol, the detergents that were used included CHAPS and n-octyl-β-D-glucopyranoside. Furthermore, the protein was purified in the presence of lipids. Purifying Drs2p in this manner produced high yields of Drs2p that had significantly higher specific activities than samples produced either prior to or since. In fact, the

activity was almost 100-fold higher than what was published by Xiaoming (Fig. 3-9E). Although these Drs2p samples did not reconstitute into proteoliposomes, the foundations exist for creating protocols to purify and reconstitute very active protein. Furthermore, if future experiments require active, non-reconstituted protein, this would be an ideal technique to purify highly active Drs2p.

Since formation of properly sealed proteoliposomes containing active Drs2p was successful, I worked to visualize changes in membrane morphology due to Drs2p flippase activity. A growing field exists for the study of artificial membranes and protein association to these membranes. Some of these membranes, called giant unilamellar vesicles (GUV's) are particularly useful for these types of experiments since they are large (10-200μm), and can easily be visualized using fluorescence microscopy. Furthermore, these structures can be observed and imaged in real-time, which is a distinct advantage over EM experiments.

The trouble faced was that Drs2p is a 10-pass transmembrane protein and not much literature exists on the reconstitution of such large proteins into giant unilamellar vesicles. Purified Drs2p degrades rapidly so it was essential that Drs2p be able to maintain its structure and activity during the electroformation process. Through much trial-and-error, as well as successful collaborations with various labs (including Charles Day (Kenworthy lab), Sarah Veatch lab, and Thomas Günther-Pomorski lab), protocols were developed for electroforming Drs2p into GUVs. Initial attempts at making proteo-GUVs yielded preps with detectable levels of Drs2p (as assayed by Coomassie staining

of SDS-PAGE gels and Western blots, Fig. 3-12A and B). Furthermore, these preps had detectable levels of ATPase activity, although the sample needed to be added to the assay in 5-fold excess (Fig. 3-12C). Finally, when these proteoliposomes containing Drs2p and NBD-phospholipids were electroformed in the presence of a lipid film containing Rhodamine-PE, we could detect incorporation of both the NBD-PS and the Rho-PE into the GUV structures. This suggests that the proteoliposomes and the lipid film is fusing to form the GUVs (Fig. 3-12F). However, it can be argued that the NBD-lipids are dissociating from the proteoliposomes, or free NBD-lipids from the mixture, are incorporating into the GUVs and this is the fluorescence is being detected. Ultimately, using these techniques, we have no way of knowing whether, and how much, Drs2p is incorporating into the GUVs.

In collaboration with Lisa Theorin in the Pomorski lab, I generated preliminary videos showing tubes forming from proteo-GUVs, upon ATP addition (Fig. 3-14). This suggests that Drs2p proteoliposomes are in fact incorporating into the GUVs. Additionally, this is the first time we are able to show the effect of Drs2p on membrane morphology. Furthermore, this tubulation is surprisingly different from anything we had expected to see. Our initial hypothesis, based upon observations by the groups of Thomas Günther-Pomorski and Andreas Herrmann showed that, when phospholipids are added exogenously to a GUV, the entire body of GUV undergoes a shape change as large tubules form and extend outward (Papadopulos et al., 2007). The addition of the phospholipids to the outer leaflet would cause an expansion in the outer leaflet when compared to the inner leaflet. This is the reason for the formation of such tubules. This

manner of tubulation (similar to the images shown in Fig. 3-15C) was what I expected to see during ATP addition. The difference in the type of tubulation observed indicates that, in addition to flipping phospholipids, Drs2p is also working to stabilize the membrane at the site of increasing curvature. The conviction that this tubulation is due to the flippase activity of Drs2p is further cemented by the observation that these changes to GUVs are observed only upon addition of ATP.

However, many questions (as detailed in the Future Directions section of the Chapter 3, Section "Electroformation of Giant Unilamellar Vesicles") remain concerning the localization of Drs2p along the growing tubes and the presence of Drs2p in the GUV structures. Since labeling of the Drs2p yielded protein which, in spite of ATP addition and analysis of over 50 membranes possessing Alexa-488 labeled-Drs2p, was inactive (Fig. 3-16E), the only option was to find alternative methods to labeling Drs2p.

Experimentally addressing these questions will enable us to have clearer understanding about the role that Drs2p plays on membrane morphology (especially in the proteo-GUVs). Some ways to achieve this is by cloning GFP onto Drs2p which will enable detection of Drs2p in the GUVs and allow the experimenter to target GUVs that contain Drs2p. Other suggestions by leading scientists in the field include using SNAP tag systems to achieve labeled, active protein. This assay, once set up and optimized, will be very useful in addressing questions that go beyond the role of Drs2p in membrane curvature. For instance, it will now be possible to test the influence of specific proteins (especially regulators of flippases) on Drs2p flippase activity since we can purify and

add these proteins into the proteo-GUV system. Furthermore, GUVs of different phospholipid compositions can be created and the influence and effect of these molecules can be tested, both in regards to Drs2p and to the membrane as a whole. For instance, such systems will be significant in the field of microdomain and lipid raft formation. We can also ask questions that will help identify the major players and the sequence of steps involved in the budding of mature transport vesicles from a membrane.

I was able to use my optimized purification and reconstitution techniques to complete experiments looking at the influence of the C-terminal tail of Drs2p on regulating Drs2p activity (Zhou et al., 2013). The observation, initially made by Xiaoming, that C-terminally TAP-tagged Drs2p was enzymatically dead when compared to N-terminally tagged Drs2p (Fig. 2-1) spurred the exploration of whether the C-tail of Drs2p functions as an R domain to regulate Drs2p activity. Several P-type ATPases have regulatory domains in either their N-terminus or C-terminus. These domains serve to auto-regulate the activity of the ATPase and can also serve as sites of interaction with other proteins. Several examples of these are given in the Introduction to Chapter 2 (Au, 1987; P. James et al., 1988; Palmgren et al., 1990; Portillo et al., 1989; Rasi-Caldogno et al., 1992, 1993, 1995). Previous work from the Graham lab had shown that the Drs2p C-tail has motifs that can bind phosphatidylinositol 4-phosphate (PI(4)P) and Gea2p (a yeast Arf-GEF). The presence of PI(4)P or the addition of Gea2p to purified Golgi membranes also activated Drs2p flippase activity (Natarajan et al., 2009). Coupled with Xiaoming's

observations, we hypothesized that the C-terminal tail of Drs2p plays a major role in the self-regulating flippase activity.

In our experiments, enzymatically removing the C-terminal tail of Drs2p conferred higher levels of ATPase activity to the protein (Fig. 2-4). Drs2p activity, which is stimulated by the presence of PI(4)P was considerably increased in samples that possessed the full-length C-tail (Fig. 2-7D and E). When the C-tail was removed, PI(4)P had no influence on Drs2p activity (Fig. 2-7F). Moreover, the flippase activity of tail-less Drs2p had similar values to full-length Drs2p activated by the presence of PI(4)P.

Thus, we surmise that, within cells, the C-tail of Drs2p is responsible for auto-inhibition, and this inhibition is removed when the tail comes in contact with PI(4)P. This is the first evidence that PI(4)P directly interacts with Drs2p to regulate its activity. It is still unclear whether clipped Drs2p is found *in vivo*, although Western blots show no sign of such a moiety (Fig. 2-5). The Sec7 domain of Gea2p, which was shown to be a regulator of Drs2p in TGN membranes, was shown to have very little effect on Drs2p activity in the reconstituted system (Fig. 2-6). It is likely that this is due to the absence of Arl1-GTP, as proposed by the work of Fang-Jen Lee's lab (Tsai et al.). The Lee group was able to show that three proteins – Drs2p, Arl1p and Gea2p – form a stable ternary complex at the TGN. Additionally, these proteins directly interact with each other. It is possible that Arl1p is associated and co-purifies with Golgi membranes. This may serve to explain why, in purified late Golgi membranes, addition of exogenous Gea2p stimulates

Drs2p activity while it doesn't in the reconstituted system (Natarajan et al., 2009; Zhou et al., 2013).

In conclusion, the work presented in this thesis provides support for the model of how Drs2p creates membrane curvature and works to create transport vesicles. A new role for the C-terminal tail, in regulating Drs2p activity at the membrane, has been identified. Strong preliminary data showing the creation of membrane curvature and tubulation, upon ATP addition to Drs2p proteo-GUVs, has been detailed. I have also improved and re-established the purification and reconstitution methods for Drs2p. Furthermore, new insight has been gained on how to improve these purification conditions. A novel technique for electroformation of large integral membrane proteins has been developed and the foundations for answering an important question in the protein trafficking field – i.e. what role do flippases play in the creation of membrane curvature and how do they affect the formation of transport vesicles – has been presented. These tools will provide the foundation for further exploration of many important questions in the trafficking field. Finally, new roles for Drs2p regulators have been defined, which will aid in future experiments by allowing researchers to improve the conditions for testing flippase activities.

APPENDIX

PROTOCOLS FOR PURIFICATION AND IMAGING OF LATE GOLGI MEMBRANES

Yeast Strains used

Information about strain backgrounds can be found in the following papers:

Quadruple mutants: (Natarajan et al., 2004)

*kes1*Δ: (Muthusamy, Raychaudhuri, et al., 2009)

Negative Staining and Electron microscopy

Protocols for Preparation of Carbon grids and Negative staining can be found in my lab notebook. Melanie Ohi graciously provided these protocols as well as access to an electron microscope. More details about these protocols can be found in her paper (Ohi, Li, Cheng, & Walz, 2004).

Differential Centrifugation Assays:

** Protocols for Kex2 and GDPase assays can be found in the original paper (Natarajan & Graham, 2006).

** Bicinchoninic Acid (BCA) Assay protocol is provided with the BCA kit (Sigma).

Cell Fractionation (late-Golgi membrane prep)

* This protocol is modified from Natarajan, et al. (2006)

1. Inoculate the appropriate amount of cells into 1000mL or 2000mL of YPD and allow it to grow, overnight at 30°C (or 27°C for *ts*-strains), to an OD_{600} of 0.4 – 0.45 OD/mL. RECORD the OD_{600} of the culture in the morning.

2. Temperature shift all or part of the culture if needed for the experiment. If a temperature shift is not needed, allow the culture to grow to an approximate OD_{600} of 0.5 – 0.65 OD/mL. RECORD the OD_{600} of the culture.

3. Harvest the cells by centrifugation at 6000rpm for 10 minutes (Sorvall GS-3 rotor).

4. Wash the pellet with 10mM Na Azide. Spin at 6000rpm for 5 minutes (Sorvall SS-34 rotor). Pour off supernatant.

   500µL 1M Na Azide (NaN3) **Total volume: 50mL**
   45mL ddH_2O

   ** For 1 Liter of cells use 100mL.*

5. Resuspend the cells in softening buffer at 10 OD/mL. Incubate the cells, on ice, for 10 minutes. Spin at 6000rpm for 5 minutes. Pour off supernatant.

   Softening Buffer = 0.1M Tris-Cl, pH 9.4 + 40mM 2- (or β-) mercaptoethanol + 10mM Na Azide

   5mL 1M Tris-Cl, pH 9.4 **Total volume: 50mL**
   500µL 1M Na Azide
   44.36mL ddH_2O
   140µL 100% β-mercaptoethanol

6. Resuspend the cells in spheroplasting buffer at 50 OD/mL.

   Spheroplasting Buffer = 1M Sorbitol + 20mM Tris-Cl, pH 7.5 + 10mM Na Azide

   3.75mL 4M Sorbitol **Total volume: 15mL**
   300µL 1M Tris-Cl, pH 7.5
   150µL 1M Na Azide
   10.8mL ddH2O

   ** Combine the cells from all of the 50mL spun tubes into one spin tube (per strain) with buffer.*

7. Take 10µL of sample and dilute it to 1mL with water. Mix well and measure the OD_{600}. RECORD the value obtained.

8. Add to the cells, 1µL per 5 OD's of cells, a 10mg/mL solution of Zymolyase.

   ** This amount can be between 100 – 250µL of 10mg/mL Zymolyase per strain.*

9. Incubate the tubes at 30°C for 20 minutes. Measure the OD_{600} again. It should be ~5% of the starting value. If not, add more enzyme and continue to incubate the cells until it reaches this value. RECORD the final OD_{600} value obtained.

Spin at 6000rpm for 5 minutes. Pour off the supernatant.

10. Wash the cells in spheroplasting buffer at 10 OD/mL. Spin at 6000rpm for 5 minutes. Pour off supernatant.

    Spheroplasting Buffer = 1M Sorbitol + 20mM Tris-Cl, pH 7.5 + 10mM Na Azide

    12.5mL 4M Sorbitol **Total volume: 50mL**
    1mL 1M Tris-Cl, pH 7.5
    500µL 1M Na Azide
    36mL ddH2O

    ** Turn on the ultracentrifuge at this time and allow the vacuum to cool it down to 4°C. Place the Ti270 rotor in the refrigerator to cool.*

11. Resuspend the cells in cell lysis buffer at 15-20 OD/mL. Resuspend the pellet completely. Incubate the cells, on ice, for 15 minutes. Dounce homogenize using 10 – 15 strokes.

    Cell Lysis Buffer = 0.1M Sorbitol + 10mM TEA, pH 7.5 + 1mM EDTA + 1mM YPIC + 1mM PMSF

    1.25mL 4M Sorbitol **Total volume: 50mL**
    2mL 250mM TEA, pH 7.5
    500µL 500mM EDTA
    300 – 400µL Yeast Protease Inhibitor Cocktail (YPIC)
    100µL 500mM PMSF *(Prepare this in DMSO)*
    ~46.8mL ddH2O

    ** Use approximately 20mL of cell lysis buffer per strain. The excess can be used to top off the centrifuge tubes in step 13.*

12. Pour the cells into 50mL centrifuge tubes and centrifuge the lysate at 2800rpm (1000 x g) for 6 minutes in order to clear unbroken cells (Sorvall SS-34 rotor).

13. Transfer the supernatant into an ultracentrifuge tube. Spin, in the ultracentrifuge, at 40,500rpm (130,000 x g) for 1 hour at 4°C (T1270 rotor).

14. Carefully remove the supernatant from the ultracentrifuge tubes after the spin. Don't disturb the pellet. Resuspend the pellet in 200 – 400µL gradient buffer. Use a mini dounce homogenizer to resuspend the membrane pellet well, then add enough 60% sucrose to bring the volume up to 2mL.

    Gradient Buffer = 10mM Hepes, pH 7.5 + 1mM Na Azide

    500µL 1M Hepes, pH 7.5 **Total volume: 50mL**
    50µL 1M Na Azide
    ~49.5mL ddH2O

All sucrose solutions are prepared weight/weight in Gradient Buffer.

15. Layer a sucrose step gradient above the sample (in 60% sucrose) consisting of:

47.5% sucrose	1.5mL
45% sucrose	1.0mL
42% sucrose	2.0mL
40% sucrose	2.0mL
38% sucrose	1.0mL
36% sucrose	1.0mL
32% sucrose	1.5mL

16. Spin the tubes in the Beckman SW41Ti (or Sorvall TH-641) swinging bucket rotor at 31,000 rpm for 17 hours at 4°C.

17. Collect sucrose fractions (1mL each) starting from the top.

    ** The top layer is considered fraction 1. There will be approximately 12 fractions total (for each strain).*

18. Measure the refractive index of each fraction. Measure the Kex2 activity and GDPase activity of each of the fractions. Also, measure the amount of protein in each fraction using the BCA Assay (Sigma kit).

19. Combine the peak Kex2 fractions for late Golgi membranes. Combine the peak GDPase fractions which is early Golgi membranes.

    ** To determine the peak Kex2 fractions, calculate the following for each fraction: Kex2 activity divided by protein concentration (from BCA Assay) -- Kex2/[protein]. Combine the **two fractions** (per strain) that have the highest value after this calculation.*

20. Mix the two fractions as well as 3 volumes of H-Buffer and transfer into ultracentrifuge tubes. Spin, in the ultracentrifuge, at 40,500rpm (130,000 x g) for 1 hour at 4°C (T1270 rotor).

    H-Buffer = 10mM Hepes, pH 7.5 + 150mM NaCl

    500µL 1M Hepes, pH 7.5 **Total volume: 50mL**
    1.5mL 5M NaCl
    48mL ddH2O

21. Resuspend the pellet in 300µL of H-Buffer + 20% glycerol and measure the protein concentration of 5µL of the membranes using the BCA Assay.

    ** Use 5µL of the resulting solution to determine the total amount of protein collected.*
    ** Use H-Buffer + 20% glycerol as a blank for this step. Prepare ddH2O blank as a control.*

22. Dilute the membranes to a final concentration of 0.5mg/mL using H-Buffer + 20% glycerol. Aliquot 100µL into sterile eppendorf tubes and store in a box in the –80°C freezer.

Cytosol preparation

* This protocol was modified from the method described for "Preparation of Cytosolic Extracts" from *In Vitro Reconstitution of Intercompartmental Protein Transport to the Yeast Vacuole*, by Thomas A. Vida, Todd R. Graham, and Scott D. Emr.

1. Inoculate the appropriate amount of cells into 1000mL of YPD and allow it to grow, overnight at 30°C (or 27°C for ts-strains), to an OD_{600} of 2.0 – 5.0 OD/mL. RECORD the OD_{600} of the culture in the morning.

2. Harvest the cells by centrifugation at 6000rpm for 10 minutes (Sorvall GS-3 rotor).

3. Wash the cells with ice–cold H-Buffer. Spin at 6000rpm for 10 minutes (Sorvall GS-3 rotor). Pour off supernatant.

   H-Buffer = 10mM Hepes, pH 7.5 + 150mM NaCl

   500µL 1M Hepes, pH 7.5 **Total volume**: 50mL
   1.5mL 5M NaCl
   48mL ddH2O

4. Resuspend the cells in H-Buffer + YPIC + PMSF at 200 OD/mL. Filter the cells through cheesecloth. Passage the cells 6 times through the Emulsiflex to ensure efficient lysis.

   ** Do not exceed 30,000psi on the Emulsiflex! Do not pass less than 10mL in the Emulsiflex!*

5. Pour the cells into 50mL centrifuge tubes and centrifuge the lysate at 12,000rpm (17,000 x g) for 15 minutes in order to clear unbroken cells (Sorvall SS-34 rotor).

6. Transfer the supernatant into an ultracentrifuge tube. Spin, in the ultracentrifuge, at 42,000rpm (162,000 x g) for 1 hour at 4°C (T1270 rotor).

7. Aliquot the resulting supernatant into sterile eppendorf tubes and store in a box in the –80°C freezer.

8. Do a BCA Assay to determine the concentration of protein in the cytosol.

PROTOCOLS FOR PURIFICATION, RECONSTITUTION AND ASSESSING ACTIVITY OF Drs2p

The protocols in this section include those involved in the purification of Drs2p using C12E9, which was previously published by the Graham lab. Modifications to that protocol, including the use of C12E8 as a detergent, or a new protocol using CHAPS and n-octyl-β-D-glucopyranoside have also been included. The ATPase, Coomassie, Pre-quenching, Flotation and Flippase Assays that have been used within Chapter 3 of this thesis have also been outlined.

Yeast Strains used

Information about strain backgrounds can be found in the following paper (Zhou & Graham, 2009):

Single-step purification of TAP_N-Drs2p with C12E9

* Adapted from Zhou and Graham (2009)

Lysis buffer (LB)

	10mL total (∫L)	Final (mM)
1M Tris, pH 7.5	400	40
5M NaCl	1mL	500
0.5M EDTA	10	0.5
1M Imidazole, pH 8	400	40
0.1M PMSF 100X (EtOH)	100	1 (1X)
100X pPIC (EtOH)	100	1X
dH_2O	7.99mL	

1K OD/1mL LB (20mL minimum); EF-C3, 25K psi, 6 pass (lysis efficiency > 95%);
15K X g for 12 min at 4°C; Keep supernatant (S15);

Wash buffer (WB)

	10mL total (µL)	Final (mM)
1M Tris, pH 7.5	400	40
5M NaCl	1mL	500
1M Imidazole, pH 8	400	40
10% C12E9	100	0.1%
dH_2O	8.1mL	

Pre-wash Ni-NTA-beads w/ 10mL WB at 4°C and transfer into S15;
Add in 1/9 vol of total S15 of 10% C12E9 (containing 100µL new pPIC & PMSF);
Rock for 2hr at 4°C;
Spin down Ni-NTA-beads at 4°C and aspirate off most of supernatant;
Transfer the rest to column and flow thru at 4°C;
Wash Ni-NTA-beads w/ 100mL WB at 4°C;

Ni-NTA elution buffer (NEB)

	1mL total (µL)	Final (mM)
1M Tris, pH 7.5	40	40
5M NaCl	30	150
10% C12E9	10	0.1%
1M Imidazole, pH 8	200	200
dH_2O	720	

Incubate protein-Ni-NTA w/ two 0.5mL NEB for 5min at 4°C w/ periodical resuspension;
Elute and combine to 1mL eluate; Reconstitute.

Two-step purification of TAP_N-Drs2p with C12E9

* Adapted from Zhou and Graham (2009)

Lysis buffer (LB)

	10mL total (µL)	Final (mM)
1M Tris, pH 7.5	400	40
5M NaCl	300	150
0.5M EDTA	40	2
50% Glycerol	2mL	10%
0.1M PMSF 100X (EtOH)	100	1 (1X)
100X pPIC (EtOH)	100	1X
dH_2O	7.06mL	

1K OD/1mL LB (20mL minimum); EF-C3, 25K psi, 6 pass (lysis efficiency > 95%);
5K X g for 6 min at 4°C; Keep supernatant (S5);

Wash buffer a (WBa)

	10mL total (µL)	Final (mM)
1M Tris, pH 7.5	400	40
5M NaCl	300	150
50% Glycerol	2mL	10%
10% C12E9	100	0.1%
dH_2O	7.2mL	

Pre-wash IgG-beads w/ 10mL WBa at 4°C and transfer into S5;
Add in 1/9 vol of total S5 of 10% C12E9 (containing 100µL new pPIC & PMSF);
Rock for 2hr at 4°C;
Spin down IgG-beads at 4°C and aspirate off most of supernatant;
Transfer the rest to column and flow thru at 4°C;
Wash IgG-beads w/ 10mL WBa at 4°C;

TEV cleavage buffer (TCB)

	1mL total (µL)	Final (mM)
1M Tris, pH 7.5	40	40
5M NaCl	30	150
50% Glycerol	200	10%
10% C12E9	10	0.1%
100% *2-ME*	1.4	20
0.5M EDTA	1	0.5
dH_2O	717.6	

Add in 1mL TCB w/ 100U TEV; Incubate for 2hr at 16°C;

Wash buffer b (WBb)

	10mL total (µL)	Final (mM)
1M Tris, pH 7.5	400	40
5M NaCl	600	300
50% Glycerol	2mL	10%
10% C12E9	100	0.1%
1M Imidazole, pH 8	200	20
dH_2O	6.7mL	

Pre-wash Ni-NTA-beads w/ 10mL WBb at RT;

Ni-NTA binding buffer (NBB)

	10mL total (µL)	Final (mM)
1M Tris, pH 7.5	400	40
5M NaCl	600	300
50% Glycerol	2mL	10%
10% C12E9	100	0.1%
1M Imidazole pH 8	200	20
100% *2-ME*	7	10
dH_2O	6.693mL	

Elute 1mL TEV action at 4°C to a 15mL conical tube;
Add in 20µL 1M Imidazole pH 8 and 5µL 1M $MgCl_2$/mL TEV eluate;
Wash IgG-beads w/ 4mL NBB at 4°C and combine wash with TEV eluate;
Add eluate in Ni-NTA-beads and incubate in column for 1hr at 4°C;
Elute and discard flow-thru;
Wash Ni-NTA beads w/ 2x 10mL WBb at 4°C;

Ni-NTA elution buffer (NEB)

	1mL total (µL)	Final (mM)
1M Tris, pH 7.5	40	40
5M NaCl	60	300
50% Glycerol	200	10%
10% C12E9	10	0.1%
1M Imidazole, pH 8	200	200
dH_2O	490	

Incubate protein-Ni-NTA w/ 0.5mL NEB for 5min at 4°C w/ periodical resuspension;
Elute;
Add in 1vol 80% glycerol in H_2O and store at -20°C.

Reconstitution of purified TAP_N-Drs2p with C12E9

* Adapted from Zhou and Graham (2009)

1. Prepare lipid mixture as follows in chloroform:

   2umol egg PC + 20nmol NBD-PS

   Evaporate organic solvent under N_2 stream;

2. Put lipid sample in a vacuum desiccator for 1hr at RT;
3. Add in 375µL dH_2O, 50µL 10X RB and 75µL 10% C12E9;
4. Gently vortex for 10min at room temp and dissolve lipids completely;
5. Add in 500µL protein solution and incubate for 10min at 4°C;
6. Pre-wash BioBeads SM2 w/ 2x 10mL methanol (5min for the first), 3x 10mL water and 10mL 1x RB and keep it moist at 4°C;
7. Add 100mg wet pre-washed SM2 in proteoliposome sample and incubate for 6 hr at 4°C w/ end-to-end rotating;
8. Add another 200mg wet pre-washed SM2 in proteoliposome sample and incubate overnight at 4°C w/ end-over-end rotating;
9. Pipette off carefully and keep turbid supernatant; Store at 4°C.

10X RB: 400mM Tris 7.5 + 1.5M NaCl

1X RB: 40mM Tris 7.5 + 150mM NaCl

Liposomes were created as follows:

- Instead of adding 500µL protein solution (as indicated in step 5 above), add a 500µL buffer solution similar to the solution with which your protein will be eluted.

- All of the other steps are done exactly as written above.

Prequenching a sample

Mix 200 µL of each proteoliposome sample with 10mM dithionite (sodium hydrosulfite). Incubate the sample for 5 min on ice. Proceed with flotation protocol.

Flotation and Removal of Fractions

* Adapted from Zhou and Graham (2009)

On the bottom of the centrifuge tube, place 1:1 sample: 80% glycerol (mixed). This should be 400µL in volume.

Above that create a layer of 600µL volume of 10% glycerol.

Spin this sample at 50,000rpm in a TLS55 (spinning bucket) rotor for 3 hours at 4°C.

Remove 5 fractions in 200µL aliquots from the top.
The top fraction is F5 and the bottom is F1.

Time trace for samples

Mix 10µL of proteoliposome sample and 1mL of 1X RB in a disposable cuvette by inverting.
Measure the total fluorescence in the sample for 30 sec. λ_{ex} = 467nm and λ_{em} = 534nm.

Add in 10µL of 1M dithionite and mix by inverting several times.
Measure the amount of fluorescence quenched for 120 sec.

Add in 50µL of 10% Triton X-100 (from Anatrace) and mix by inverting 3 or 4 times.
Measure fluorescence for 30 sec.

** 1X RB = 40mM Tris 7.5 + 150mM NaCl

Coomassie Staining of Gels

Life Technologies pre-cast 10% Bis-Tris SDS-PAGE gels were used with MES running buffer. The microwave protocol for Simply Blue SafeStain by Invitrogen was used to stain the gels.

The following BSA Standards were prepared and 10µL each were loaded onto the gels:

2 ng/µL, 10 ng/µL and 50 ng/µL.

Gels were scanned using the Odyssey system.

ATPase Assay (and colorimetric determination)

* Adapted from Zhou and Graham (2009)

Setup for Assay:

Master mix:

	Per sample
100mM Na-ATP	2µL
0.5M HEPES, pH 7.5	5µL
1M NaCl	5µL
500mM KCl	5µL
100mM $MgCl_2$	5µL
dH_2O	18µL

Add 40µL of master mix to 10µL of sample (50µL total volume).
Incubate at 37°C for 60min.
Add 150µL dH_2O to stop the reaction (total vol is now 200µL).

Proceed to colorimetric determination.
** 5µL of 10% C12E8 (or other detergent) can also be added to the Master mix (decrease the amount of water to 13µL) if necessary.

Colorimetric Determination:

Add 150µL of PiA solution and mix; Wait 15s
Add 150µL of PiB solution and mix; Wait 2min
Add 500µL of PiC solution and mix; Transfer sample to cuvette
After 30min, read A_{625}.

PiA solution: 2 vol of 7.8% (v/v) H_2SO_4 + 1 vol 0.1M Na_2MoO_4

PiB solution: 37.16mg malachite green in 100mL 1% (w/v) polyvinyl alcohol (PVA; dissolves at 80°C); [0.4mM malachite green]

PiC solution: 7.8% (v/v) H_2SO_4

Measure nmol of Pi released against a KH_2PO_4 (0 nmol to 6 nmol) standard curve.

Single-step purification of TAP_N-Drs2p with CHAPS, n-octyl-β-D-glucopyronoside

* Adapted from Coleman, et al, 2009

Lysis buffer (LB)

	10mL total (µL)	Final (mM)
1M HEPES, pH 7.5	500	50
5M NaCl	300	150
1M $MgCl_2$	50	5
1M Imidazole pH 8	400	40
0.1M DTT	100	1
0.1M PMSF 100X (EtOH)	100	1X
100X pPIC (EtOH)	100	1X
dH_2O	8.45mL	

1K OD/1mL LB (20mL minimum); EF-C3, 25K psi, 6 pass (lysis efficiency > 95%);
Spin samples at 15K x g (11,400rpm in SS-34) for 12min at 4°C; Keep supernatant (S15);
Spin S15 at 23K x g (14,000rpm in SS-34) again for 12min, 4°C; Keep supernatant (S15-2);
Transfer S23 to ultracentrifuge tube and spin at 130K x g (40,500rpm in T-1270) for 60min;

Solubilizing buffer (SB)

	5mL total (µL)	Final (mM)
1M HEPES, pH 7.5	250	50
5M NaCl	150	150
1M $MgCl_2$	25	5
0.1M DTT	50	1
dH_2O	4.525mL	

Resuspend pellet with 1mL SB + 10µL new pPIC & PMSF and dounce homogenize (P130);
Mix 0.5mg DOPC (20µL) in 4mL SB + 550µL 200mM CHAPS (final:20mM) + 40µL pPIC & PMSF; Add to the resuspended pellet (P130);

Wash buffer a (WBa)

	5mL total (µL)	Final (mM)
1M HEPES, pH 7.5	250	50
5M NaCl	150	150
1M $MgCl_2$	25	5
0.1M DTT	50	1
200mM CHAPS	250	10
dH_2O	4.275mL	

Pre-wash Ni-NTA-beads w/ 5mL WBa at 4°C and transfer beads into P130;
Rock for 2hr at 4°C;
Transfer sample to column and flow thru at 4°C;

Wash buffer b (WBb)

	5mL total (∫L)	Final (mM)
1M HEPES, pH 7.5	250	50
5M NaCl	150	150
1M $MgCl_2$	25	5
1M Imidazole pH 8	200	40
10% n-octyl-β-D-glucopyranoside	375	0.75%
0.1M DTT	50	1
dH_2O	3.95mL	

Wash Ni-NTA-beads 6 times w/ 500µL WBb + 0.5mg/mL egg PC at 4°C; [3mL WBB + 1.5mg eggPC]

Ni-NTA elution buffer (NEB)

	1mL total (∫L)	Final (mM)
1M HEPES, pH 7.5	50	50
5M NaCl	30	150
1M $MgCl_2$	5	5
10% n-octyl-β-D-glucopyranoside	75	0.75%
0.1M DTT	10	1
1M Imidazole pH 8	200	200
dH_2O	630	

Incubate protein-Ni-NTA w/ two 400µL NEB for 10min at 4°C w/ periodical resuspension; Combine;

Reconstitution of purified protein (Dialysis method)

Reconstitution Buffer (RnB)

	0.5mL total (µL)	Final (mM)
1M HEPES, pH 7.5	25	50
5M NaCl	15	150
1M $MgCl_2$	2.5	5
10% n-octyl-β-D-glucopyranoside	50	1%
0.1M DTT	5	1
40% sucrose	125	10%
dH_2O	277.5	

Mix the purified protein 1:1 with reconstitution buffer + 5mg/mL egg PC; Rotate for 1h at 4°C;

Dialysis Buffer (DB)

	1L total (mL)	Final (mM)
1M HEPES, pH 7.5	50	10
5M NaCl	30	150
1M $MgCl_2$	5	5
0.1M DTT	10	1
dH_2O	905	

Dialyze the sample against 1L DB for ~20h with 2 changes to remove the detergent; Check seal.

Single-step purification of TAP_N-Drs2p with C12E9

* Modified from Coleman, et al, 2009

Lysis buffer (LB)

	10mL total (µL)	Final (mM)
1M HEPES, pH 7.5	500	50
5M NaCl	300	150
1M $MgCl_2$	50	5
1M Imidazole pH 8	400	40
1M DTT	10	1
0.1M PMSF 100X (EtOH)	100	1X
100X pPIC (EtOH)	100	1X
dH_2O	8. 45mL	

1K OD/1mL LB (20mL minimum); EF-C3, 25K psi, 6 pass (lysis efficiency > 95%);
Spin samples at 15K x g (11,400rpm in SS-34) for 12min at 4°C; Keep supernatant (S15);
Spin S15 at 23K x g (14,000rpm in SS-34) again for 12min, 4°C; Keep supernatant (S15-2);
Transfer S23 to ultracentrifuge tube and spin at 130K x g (40,500rpm in T-1270) for 60min;

Solubilizing buffer (SB)

	5mL total (µL)	Final (mM)
1M HEPES, pH 7.5	250	50
5M NaCl	150	150
1M $MgCl_2$	25	5
1M DTT	5	1
dH_2O	4.57mL	

Resuspend pellet with 1mL SB + 10µL new pPIC & PMSF and dounce homogenize (P130);
Mix 0.5mg DOPC (20µL) in 4mL SB + 1/9th total vol of 10%C12E9 (final: 1%) + 100µL pPIC & PMSF;
Add to the resuspended pellet (P130);

Wash buffer a (WBa)

	5mL total (µL)	Final (mM)
1M HEPES, pH 7.5	250	50
5M NaCl	150	150
1M $MgCl_2$	25	5
1M DTT	5	1
10% C12E9	50	0.1%
dH_2O	4.52mL	

Pre-wash Ni-NTA-beads w/ 5mL WBa at 4°C and transfer beads into P130; Rock for 2hr at 4°C;
Transfer sample to column and flow thru at 4°C;

Wash buffer b (WBb)

	10mL total (µL)	Final (mM)
1M HEPES, pH 7.5	500	50
5M NaCl	300	150
1M $MgCl_2$	50	5
1M Imidazole pH 8	400	40
10% C12E9	100	0.1%
1M DTT	10	1
dH_2O	8.64mL	

Wash Ni-NTA-beads 6 times w/ 500µL WBb + 0.5mg/mL egg PC at 4°C; [3mL WBB + 1.5mg eggPC]

Ni-NTA elution buffer (NEB)

	1mL total (µL)	Final (mM)
1M HEPES, pH 7.5	50	50
5M NaCl	30	150
1M $MgCl_2$	5	5
10% C12E9	10	0.1%
1M DTT	1	1
1M Imidazole pH 8	200	200
dH_2O	704	

Incubate protein-Ni-NTA w/ two 400µL NEB for 10min at 4°C w/ periodical resuspension; Combine;

Reconstitution of purified protein (Biobeads method)

Reconstitution Buffer (RnB)

	1mL total (µL)	Final (mM)
1M HEPES, pH 7.5	50	50
5M NaCl	30	150
1M $MgCl_2$	5	5
10% C12E9	150	1.5%
1M DTT	1	1
dH_2O	764	

Mix the purified protein 1:1 with reconstitution buffer + lipids (5mg/mL egg PC); Rotate for 30min at 4°C;

Dialysis Buffer (DB)

	1L total (mL)	Final (mM)
1M HEPES, pH 7.5	50	10
5M NaCl	30	150
1M $MgCl_2$	5	5
0.1M DTT	10	1
dH_2O	905	

Dialyze the sample against 1L DB for ~20h with 2 changes to remove the detergent; Add 200mg of activated Biobeads per 1L DB; Check seal.

Single-step purification of TAP_N-Drs2p with C12E8

* Modified from Zhou, X. et al (2009).

Lysis buffer (LB)

	10mL total (µL)	Final (mM)
1M HEPES, pH 7.5	400	40
5M NaCl	300	150
0.5M EDTA	10	0.5
1M Imidazole, pH 8	400	40
0.1M PMSF 100X (EtOH)	100	1 (1X)
100X pPIC (EtOH)	100	1X
dH_2O	8.69mL	

1K OD/1mL LB (20mL minimum); EF-C3, 25K psi, 7 pass (lysis efficiency > 95%);
15K X g for 15 min at 4°C; Keep supernatant (S15);

Wash buffer (WB)

	10mL total (µL)	Final (mM)
1M HEPES, pH 7.5	400	40
5M NaCl	300	150
1M Imidazole, pH 8	400	40
10% C12E8	100	0.1%
dH_2O	8.8mL	

Pre-wash Ni-NTA-beads w/ 10mL WB at 4°C and transfer into S15;
Add in 1/9 vol of total S15 of 10% C12E8 (containing 130µL new pPIC & PMSF);
Rock for 1hr at 4°C; Pour S15 into large chromatography column; allow the beads to settle to the bottom for 15min; flow thru the sample at 4°C;
Wash Ni-NTA-beads w/ 100mL WB at 4°C -- Split up into 10 washes (10mL each)

Ni-NTA elution buffer (NEB):

	1mL total (µL)	Final (mM)
1M HEPES, pH 7.5	40	40
5M NaCl	30	150
10% C12E8	10	0.1%
1M Imidazole, pH 8	200	200
dH_2O	720	

Incubate protein-Ni-NTA w/ three 0.5mL NEB for 10min at 4°C w/ periodical resuspension;
Elute and combine the first two elutions to 1mL eluate; Save the third eluate separately.
Store at 4°C or flash freeze and store at -20°C for longer storage.

Single-step purification of Drs2p-TAP$_C$ with C12E8

* Modified from Zhou, X. et al (2009).

Lysis buffer (LB)

	10mL total (µL)	Final (mM)
1M HEPES, pH 7.5	400	40
5M NaCl	300	150
0.5M EDTA	10	0.5
1M Imidazole, pH 8	10	1
0.1M PMSF 100X (EtOH)	100	1 (1X)
100X pPIC (EtOH)	100	1X
dH_2O	9.08mL	

1K OD/1mL LB (20mL minimum); EF-C3, 25K psi, 6 pass (lysis efficiency > 95%);
15K X g for 12 min at 4°C; Keep supernatant (S15);

Wash buffer (WB)

	10mL total (µL)	Final (mM)
1M HEPES, pH 7.5	400	40
5M NaCl	300	150
1M Imidazole, pH 8	10	1
10% C12E8	100	0.1%
100mM $CaCl_2$	200	2
dH_2O	8.99mL	

Pre-wash Ni-NTA-beads w/ 10mL WB at 4°C and transfer into S15;
Add in 1/9 vol of total S15 of 10% C12E8 (containing 100µL new pPIC & PMSF);
Rock for 2hr at 4°C;
Spin down Ni-NTA-beads at 4°C and aspirate off most of supernatant;
Transfer the rest to column and flow thru at 4°C;
Wash Ni-NTA-beads w/ 100mL WB at 4°C;

Calmodulin elution buffer (CEB):

	1mL total (µL)	Final (mM)
1M HEPES, pH 7.5	40	40
5M NaCl	30	150
10% C12E8	10	0.1%
30mM EGTA	200	6
dH_2O	720	

Incubate protein-Ni-NTA w/ three 0.5mL NEB for 10min at 4°C w/ periodical resuspension;
Elute and combine the first two elutions to 1mL eluate; Save the third eluate separately.
Store at 4°C or flash freeze and store at -20°C for longer storage.

Reconstitution of purified TAP_N-Drs2p and Drs2p-TAP_C (with C12E8)

* Adapted from Zhou and Graham (2009)

1. Prepare lipid mixture as follows in chloroform:

   2umol egg PC + 20nmol NBD-PS
   Evaporate organic solvent under N_2 stream;

2. Put lipid sample in a vacuum desiccator for 1hr 30min at RT;
3. Add in 375µL dH_2O, 50µL 10X RB and 75µL 10% C12E8;
4. Gently vortex for 10min at RT and dissolve lipids completely;
5. Add in 500µL protein solution and incubate for 10min at 4°C;
6. Pre-wash BioBeads SM2 w/ 3x 10mL methanol (5min for the first), 3x 10mL water and 20mL 1x RB and keep it moist at 4°C;
7. Add 150mg wet pre-washed SM2 in proteoliposome sample and incubate for 6 hr at 4°C w/ end-to-end rotating;
8. Add another 320mg wet pre-washed SM2 in proteoliposome sample and incubate overnight at 4°C w/ end-over-end rotating;
9. Pipette off carefully and keep turbid supernatant; Store at 4°C.

10X RB: 400mM Tris 7.5 + 1.5M NaCl

1X RB: 40mM Tris 7.5 + 150mM NaCl

Liposomes were created as follows:

- Instead of adding 500µL protein solution (as indicated in step 5 above), add a 500µL buffer solution similar to the solution with which your protein will be eluted.

- All of the other steps are done exactly as written above.

Flotation and Removal of Fractions

On the bottom of the centrifuge tube, place 1:1 sample: 80% glycerol (mixed). This should be 400µL in volume.

Above that create a layer of 600µL volume of 10% glycerol.

Spin this sample at 50,000rpm in a TLS55 (spinning bucket) rotor for 6 hours at 4°C.

Remove 5 fractions in 200µL aliquots from the top. The top fraction is F5 and the bottom is F1.

Flotations can also be done for half the volume, but spin times must be reduced.

Flippase Assay

1. For each reading, 40µL proteoliposome is used;
2. Add in 10µL 1X RB;
3. Add in 1µL 0.5M Na-ATP and 1µL 1M $MgCl_2$ per sample and incubate at 37°C for your designated experimental time

   Final 5mM Na-ATP and 10mM $MgCl_2$; Controls skip $MgCl_2$ and add ATPγS
4. At time points, take aliquots out and mix w/ 1mL 1X RB;

   I commonly use two time points for my assays – 0min and 40min. I use 20µL aliquots.
5. Total fluorescence (F_T) is recorded at λ_{ex}=460nm and λ_{em}=534nm by time trace for stable line (30s);
6. Add in 10µL 1M dithionite (prepared fresh in 1M Tris, pH 9.4) and mix gently;
7. Fluorescence after dithionite quenching (F_D) is recorded for new stable line (120s);
8. Add in 50µL of 20% TX100 to completely permeabilize liposome;
9. Background fluorescence (F_0) is read for another 30s.

1X RB: 40mM Tris 7.5 + 150mM NaCl

PROTOCOLS FOR ELECTROFORMATION OF GIANT UNILAMELLAR VESICLES

Several basic protocols for GUV formation were initially developed by Xiaoming Zhou, based on the classic GUV methods paper from the Bassereau lab (Girard et al, 2004), and are presented in the beginning of the protocols section. Charles A. Day, our collaborator and a Vanderbilt graduate student in the lab of Anne Kenworthy (Dept. of Molecular Physiology and Biophysics) visited the lab of Sarah Veatch (Univ. of Michigan) and learned her protocol for the formation of protein-free GUV's (Veatch, 2007). Additionally, our collaboration with the lab of Thomas Günther-Pomorski (Univ. of Copenhagen), provided access to their protocols. The Pomorski lab is working on the purification, reconstitution and GUV incorporation of the proton pump. Therefore, I've included their protocols for reconstitution and assays. Finally, I've included the protocol that I developed based on the techniques that I learned, as well as my experiences with GUV formation.

Formation of GUVs – Protocol #1

* from Xiaoming Zhou, Graham lab

1. Carefully deposit 2μL of lipids (2mg/ml DOPC), or 4μg of lipids on the conductive side of one ITO slide;
2. Air dry then dry in vacuum for 1hr at RT;
3. Assemble electroformation chamber (O-ring spacer) and fill w/ 120μL of electroformation buffer (EB);
4. Apply AC field at 1V/10Hz for 2hr at RT;
5. Apply AC field at 2V/5Hz for 1hr at RT (to detach GUVs from glass);
6. Collect GUVs w/ a pipetter using large tip opening;
7. Dilute 10x w/ GUV dilution buffer (GDB);
8. Store at 4°C.

EB (electroformation buffer): 1mM Tris, pH 7.5 + 100mM sucrose **+** 1% glycerol

GDB (GUV dilution buffer): 1mM Tris, pH 7.5 + 100mM glucose **+** 1% glycerol

Formation of GUVs – Protocol #2

* from Xiaoming Zhou, Graham lab

1. Carefully deposit 10μL of proteoliposomes (1mM, 99% DOPC+1% NBD-PS+0.1% Rho-PE, 1X RB) on the conductive side of one ITO slide;
2. Dry in a desiccator for 45min at RT;
3. Assemble electroformation chamber (O-ring spacer) and fill in w/ 100μL of electroformation buffer (EB);
4. Apply AC field at 1V/12Hz for 4-6hr at RT;
5. Apply AC field at 2V/4Hz for 30min at RT (to detach GUVs from glass);
6. Collect GUVs w/ a pipet using large tip opening;
7. (Optional) Dilute w/ GUV dilution buffer (GDB);
8. Store at 4°C.

1X RB: 40mM Tris, pH 7.5 **+** 150mM NaCl

EB (electroformation buffer): 2mM Tris, pH 7.5 **+** 200mM sucrose **+** 2% glycerol

GDB (GUV dilution buffer): 2mM Tris, pH 7.5 **+** 200mM glucose **+** 2% glycerol

Formation of GUVs – Protocol #3

* from Xiaoming Zhou, Graham lab

1. Carefully deposit 2μL of lipids (DOPC+Rho-DHPE), or 4μg of lipids on the conductive side of one ITO slide;
2. Air dry then dry in vacuum for 1hr at RT;
3. Assemble electroformation chamber (O-ring spacer) and fill w/ 120μL of electroformation buffer (EB);
4. Apply AC field at 1V/10Hz for 2hr at RT;
5. Apply AC field at 2V/5Hz for 1hr at RT (to detach GUVs from glass);
6. Collect GUVs w/ a pipetter using large tip opening;
7. Dilute 10x w/ GUV dilution buffer (GDB);
8. Store at 4°C.

EB (electroformation buffer): 2mM Tris, pH 7.5 **+** 200mM sucrose **+** 2% glycerol

GDB (GUV dilution buffer): 2mM Tris, pH 7.5 **+** 200mM glucose **+** 2% glycerol

Electroswelling Procedure for Giant Unilamellar Vesicles

* from the lab of Sarah Veatch (Univ. of Michigan)

Things to do in preparation for procedure:

1. Take out lipid stocks – let them warm up to room temperature (~45 min – 1 hr). Keep them covered in the dark box.

While lipids are equilibrating to room temperature perform steps 2-6

2. Wash caps with the holes at the top thoroughly with EtOH
3. Clean microscope slides (indium tin oxide (ITO)-coated microscope slides) with ethanol. Wet one kimwipe and wipe slide gently. Get a new kimwipe and wipe the cleaned slide dry. Use this kimwipe to clean the next slide. Repeat for all slides.
4. Use voltmeter and switch to the music note setting. Touch the red and black leads to the microscope slide. If the voltmeter, beeps the metal-coated side is up. Mark this side with your sample number (e.g. 1A, 1B, 2A, 2B, etc.) to test which side of slide is coated. If the voltmeter is silent, turn the slide over. Test this side to be sure. Mark the slide.
5. Set up vacuum
6. Turn on temperature block and set to 55 °C. Use the surface thermometer to check the temperature.

Mixing lipids:

7. Clean the appropriate Hamilton syringes with chloroform
8. Clean the screw cap with hole using acetone and chemwipe
9. Add 140 ml of choloform per sample to a single glass test tube (i.e. 140 ml for 1 sample, 280 ml for 2, 420 ml for 3 samples, etc.)
10. To that test tube add the appropriate amount of lipid and probe. Typically 350 mg of total lipid per sample is used. The probe is not included in the total mass of the lipid.
11. Place the microscope slides on the heat block at 55°C. Use 250 µl syringe and withdraw 80 µl of lipid mixture.
12. Deposit the lipid mixture in syringe to a microscope slide, near the top 1/3 of the slide.
13. Take the glass pipet and gently spread the liquid onto the slide, keeping to the top 1/3 of slide. For even coverage hold the pipet just off the slide surface and then pull the slide forward and backward. Try not to rub the pipet against the slide as it may damage the slide. Watch the lipid between the pipet and the slide to make sure that the lipid is deposited uniformly from right to left. Also stop spreading shortly before all chloroform has evaporated. This will prevent streaking.
14. Repeat on all slides.
15. When finished place both slides in dessicator.

Vacuum pump:

Connect the dessicator containing the slides to the vacuum pump. Cover dessicator with black cloth. Leave on pump for ~1 hr. While dessicator is on pump, should be able to achieve pressure of ~100 torr.

Procedures to do when desiccator is on vacuum pump:

16. Take out 100mM sucrose solution from fridge and fill a clean test tube 3/4 full.
17. Clean rubber o-rings: Clean large viton o-rings with EtOH. Rinse with H_2O. (The # of large o-rings you need = the number of samples you are making.) Place these in a kimwipe and put them on the heating block. Put another heating block over it to ensure o-rings are flat.

    Count out the number of small buna o-rings that you need. (the number of small o-rings = 4x the number of samples). Rinse with EtOH. These don't have to be thoroughly cleaned. They only act as spacers.

Sandwiching:

18. Place the large o-ring on slide 1A above the lipid. Using a spare slide press the o-ring into the lipid. This should cause it to adhere to slide 1A and seal it. If the o-ring is not round it can be heated on the heating stage with a heavy object on top to flatten it.

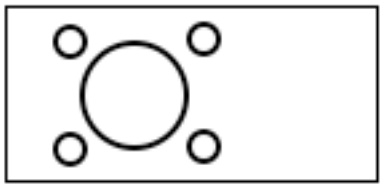

19. Take 700 µL of sucrose solution. Have your pipet at the ready with one hand and have slide 1B in your other hand, with lipid film facing down. Deposit the 700 µL sucrose into the large o-ring on 1A and quickly place slide 1B on top. Pick up the sandwiched slides by sliding the two slides off of the edge of the table (move them by sliding the kimwipe). Be sure to have a firm grip of both slides (thumb and index finger)
20. Place alligator clips on the either side of the slides
21. Take a kimwipe and wipe off excess sucrose by inserting kimwipe tip in between the slides.
22. Slide the sandwiched slides into the metal GUV block. Once it is in, use a binder clip to hold together the slides and release your grip.

You have now finished one sample. Repeat for all samples.

Electroswelling:

23. Turn on the pulse/function generator. Make sure oscilloscope is set correctly.
    10 ± 1 Hz, ± 1V ; Sinusoidal function
24. Connect the slide to the bus bars using alligator clips. Up to 4 slides can be on each bus bar before there is any effect on GUV production.
25. Connect the leads onto the bus bars.
26. Check to make sure none of the leads are contacting slides opposite to them.
27. Apply current for 40 minutes to 2 hours. Remove the samples from the leads and then turn off the wave generators.

Harvesting and washing GUV's:

28. Preheat the 100 mM Glucose media to 55°C.
29. Deposit 2-4 ml of Glucose media in a glass cuvette
30. Remove the alligator clips
31. Press the slides between your thumb and pointer finger. Move your thumb in a circular pattern until the seal begins to break.
32. Place the slide on the table top with slide having the unbroken seal on the bottom. Gently slide the top slide off.
33. Using a 1 ml pipeter (clip the tip), suction up the GUV's.
34. Drop the GUV's in the Glucose in small droplet just above the surface of the glucose media
35. Without making bubbles, gently pipet solution at the bottom and deposit it at the top of the liquid. Repeat 4 more times.
36. Give 10-20 minutes for the larger vesicles to settle to the bottom of the solution.

Making the Grease chamber:

37. Stick the end of a glass pipet into the vacuum grease.
38. Being careful not to touch the center of the cover slip, deposit grease around the edges of the coverslip using the glass pipet.
39. Deposit 4 ml of GUV's suspension on to the center of the glass coverslide using a pipet with the tip clipped. Try to avoid making contact between the grease and the GUV's. The best GUV's will be at the very bottom of the test tube. Therefore for checking the GUV's before the final experiment, take from near the bottom but leave the solution at the very bottom of the actual experiment.
40. Place a second coverslip on top of the first and gently press the two together. Here you are trying to seal the chamber without crushing the GUVs.

Reconstitution into small vesicles

* provided by the lab of Thomas Pomorski, Univ of Copenhagen

Reconstitution buffer:
10 mM Mes/KOH, pH 6.5 + 50 mM K_2SO_4 + 20% glycerol

- K_2SO_4 is not stable in 1 M solution, so I add the salt as a powder to the other components.
- Reconstitution buffer is stable for ca. 3 months, but has to be kept in the fridge so one can make ca. 500 mL-1 L depending on projected use.
- Purified proton pump in GMEKD (as at the end of general purification protocol)
- 30 mg/mL Asolectin in reconstitution buffer or other lipid of choice
- Detergent: 1 M Octylglucoside (Sigma) (OG) or 10% Deoxycholate (DOC)

Reconstitution:

Protein/lipid/buffer/detergent mix:

- 78 µL 30 mg/ml lipids,
- 11.5 µL of 1M OG/15 µL 10% DOC
- 12 µg (~115 pmol AHA2) of purified protein or 106 µg of membrane proteins.
- final volume of 220 µl in reconstitution buffer

- Prepare 2 g Sephadex g-50 fine in 50mL Reconst. Buffer (enough for 6-8 reconstitutions, can be kept in fridge for ca. 1 month) the day before, let swell in fridge
- Insert 2 ml syringes into 15 ml falcon tubes, and put glass wool at the bottom
- Fill the syringes with gel to the top with a Pasteur pipette; repeat adding gel until the syringe is full
- Centrifuge 5 min at 180g /1200 rpm at RT
- Transfer the syringes to new 15 ml falcon tubes
- Make the protein/lipid/buffer mixture; add detergent and vortex for 5 seconds
- Apply the samples (220 µl) to the top of the columns, and let stand for 5 minutes
- Centrifuge 7.5 minutes at 180 g at RT
- Recover the proteoliposomes, and transfer each of them to an Eppendorf tube containing 100 mg Biobeads (from BioRad); Shake gently for 30 min at RT
- Insert Eppendorf tube into spin column, inserted into a second Eppendorf tube. Pierce hole in the Eppendorf tube containing the vesicles (this step can also be performed without spin column, by simply inserting the Eppendorf tube with the sample in another Eppendorf tube and piercing hole).
- Centrifuge ensemble a few seconds at 1000 rpm, and collect the vesicles in the bottom Eppendorf tube. Measure the volume obtained (typically 150 µl).

Analysis of Reconstitution – ACMA assay

* provided by the lab of Thomas Pomorski, Univ of Copenhagen

Activity assay (based on quenching of ACMA dye):

ACMA buffer (20 ml)
20 mM MOPS-KOH, pH 7.0 (400 µL 1M)
40 mM K_2SO_4 (139 mg)
25 mM KNO_3 (0.5 ml 1 M)
2 mM ATP (80 µL ATP 0.5 M, pH 7.0)
1 µM ACMA (2 µl 10 mM in DMSO)
60 nM Valinomycin (1 µl 1.25 mM in ethanol)

Can be stored without ATP, ACMA, and Valinomycin, up to 6 months

Always run an emission and excitation scan to ensure your settings and buffers are OK:

ACMA:	Excitation	412 nm scan	350-450 nm
	Emission	480 nm scan	450-500 nm

The signal should be around 10^5-10^6
Time scan: Ex 412 nm, Em 480 nm, 1 point/s, 600 s duration
(all these settings are saved on the fluorometer computer in Gerdi/templates)

Running the assay:

1. Add 10 µl of reconstituted vesicles to 2 mL of ACMA buffer w ATP
2. Put cuvette in fluorometer (remember to include the stirring bar).
3. Let equilibrate for 1-2 min
4. Start time scan
5. If signal stable/after ca. 100 s Add $MgSO_4$ to start the reaction (6 µl 1 M)
6. Optional: Dissipate membrane potential by addition of 2 µl of 5 mM CCCP when the flourescence has stabilized.

ACMA: 9-amino-6-chloro-2-metoxyacridine, in DMSO
CCCP: m-chlorophenylhydrazon, in Ethanol

Evaluation:
Upon addition of Mg, there should be a visible drop. Fluorescence does not have to go to 0, but close to and stabilize to a more or less straight line (parallel to the time-axis). Depending on the activity, the drop will be steeper or flatter. Upon addition of CCCP, the fluorescence should go back (or almost) to the initial level.

*** An alternative method used by the Pomorski lab to analyze their reconstitutions is an ATPase assay based on the Baginsky method.**

Labeling of the Proton pump

* provided by the lab of Thomas Pomorski, Univ of Copenhagen

Purified proton pump:

- Stored in GMEKD supplemented with DDM (GMEKD: 20% Glycerol, 50 mM Mes/KOH pH 6.5, 50 mM KCl, 1mM EDTA, 1 mM DTT, ca. 2 µL/mL DDM) frozen in liq. Nitrogen, stored at -80 °C
- Concentration ca. 1-5 mg/mL

Labelling of the protein:

Material:

- Purified proton pump in GMEKD (as at the end of general purification protocol)
  Dye: Alexa Fluor ® 555 Microscale Protein Labeling Kit (A30007)

Dialysis of the protein:

- in GMEKD with 2 µL/mL DDM
- 3 times 1 hr in 200 mL buffer

Labelling: Exactly as described in the manual of the dye, except for the changes below

- pH change when 1M bicarbonate is added does not sufficiently alkalize the solution, instead of 1:10 we need 3:10 dilution of the 1 mg/mL protein solution (step 1.2)

Example: to 100 µL dialysed sample, added 1.78 µL reactive dye solution, resulting in deg of labeling ca. 1.5 as determined by Nanodrop

Preparation of Proteo-GUVs

* provided by the lab of Thomas Pomorski, Univ of Copenhagen

(adapted from Girard P, *et al.* (2004). *A new method for the reconstitution of membrane proteins into giant unilamellar vesicles*)

- 0.8 mg/mL lipid (16 µL BR recon or 6 µL AHA2 recon, 0% Glycerol) in 80 µL, diluted with water, addition of 0.25 mM Glucose (according to Poolman 0.1 g sugar/1g lipid)
- under vacuum for not more than 5 min, w/o any salt solution or special pressure
- swelling buffer: 0.1 M sucrose, 1 mM Mops-Tris, pH 7, 2 mM KCl, 10 µM Pyranine if needed (same buffer for both proteins, evt. change pH 6.5 for ATPase)
- Electroformation conditions: 6 min increment, 20 mV to 1.1 V, 12 Hz, 4-6 h
- Then 2 V, 4 Hz, 30 min
- Observe in microscopy buffer (0.1 M glucose, 5 mM Mops-Tris, pH 7, 5 mM KCl), dilution ca. 1:1

Even better results are obtained when the ready proteoliposomes are harvested by ultracentrifugation (40 min, 160 000 g) and resuspended in low ionic strength buffer (5 mM Mes/KOH, pH 6.5).

Immobilization of GUVs using Streptavidin

* provided by the lab of Thomas Pomorski, Univ of Copenhagen

Clean glass slides (stored in methanol dried under nitrogen)

Incubate with 50 µl of a 9:1 mix of BSA and BSA-Biotin (each 1g/L), in microscopy buffer, 20min

Wash 10 times by addition and removal of 200 µl buffer

Add 50 µl 1 g/l streptavidin, incubate 20 min

Wash 10 times

Add around 50 µl of GUVs and 50 µL microscopy buffer

5 minutes incubation to bind to the surface

Optional: wash with microscopy buffer

Electroswelling Procedure for Giant Unilamellar Vesicles

* adapted from the Veatch lab protocol (Univ. of Michigan), by Tessy Sebastian

Delta Technologies: ITO Slides #CG-90IN-S115
Marco Rubber: O-rings #V1000-016, #B1000-004

Spot your liposome or proteoliposome solution onto the ITO slides in 0.5 – 2μL aliquots.
Place the ITO slides in a vacuum chamber and dry the drops till they are just dry.
Clean rubber o-rings

Sandwiching:

1. Place the large o-ring on slide 1A above the lipid. Using a spare slide press the o-ring into the lipid. This should cause it to adhere to slide 1A and seal it. If the o-ring is not round it can be heated on the heating stage with a heavy object on top to flatten it.

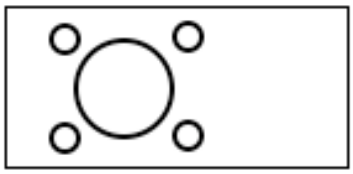

2. Take 700 μL of 100mM sucrose solution. Have your pipet at the ready with one hand and have slide 1B in your other hand, with lipid film facing down. Deposit the 700 μL sucrose into the large o-ring on 1A and quickly place slide 1B on top. Pick up the sandwiched slides by sliding the two slides off of the edge of the table (move them by sliding the kimwipe). Be sure to have a firm grip of both slides (thumb and index finger)
3. Place alligator clips on the either side of the slides
4. Take a kimwipe and wipe off excess sucrose by inserting kimwipe tip in between the slides.
5. Use a binder clip to hold together the slides and release your grip.

Electroswelling:

6. Turn on the pulse/function generator.
   10 ± 1 Hz, ± 1V ; Sinusoidal function
7. Connect the alligator clips and leads to the function generator.
8. Check to make sure none of the leads are contacting slides opposite to them.
9. Apply current for 40 minutes to 2 hours. Remove the samples from the leads and then turn off the generator.

Harvesting and Washing GUV's:

10. Remove the alligator clips
11. Press the slides between your thumb and pointer finger. Move your thumb in a circular pattern until the seal begins to break.
12. Place the slide on the table top with slide having the unbroken seal on the bottom. Gently slide the top slide off.
13. Using a 1 ml pipeter (clip the tip), suction up the GUV's.
14. Store in a microfuge tube at 4°C.

REFERENCES

Ahle, S., & Ungewickell, E. (1989). Identification of a clathrin binding subunit in the HA2 adaptor protein complex. *J Biol Chem, 264*(33), 20089-20093.

Albers, R. W., Fahn, S., & Koval, G. J. (1963). The Role of Sodium Ions in the Activation of Electrophorus Electric Organ Adenosine Triphosphatase. *Proc Natl Acad Sci U S A, 50*, 474-481.

Alder-Baerens, N., Lisman, Q., Luong, L., Pomorski, T., & Holthuis, J. C. (2006). Loss of P4 ATPases Drs2p and Dnf3p disrupts aminophospholipid transport and asymmetry in yeast post-Golgi secretory vesicles. *Mol Biol Cell, 17*(4), 1632-1642.

Alfaro, G., Johansen, J., Dighe, S. A., Duamel, G., Kozminski, K. G., & Beh, C. T. (2011). The sterol-binding protein Kes1/Osh4p is a regulator of polarized exocytosis. *Traffic, 12*(11), 1521-1536.

Au, K. S. (1987). Activation of erythrocyte membrane Ca2+-ATPase by calpain. *Biochim Biophys Acta, 905*(2), 273-278.

Axelsen, K. B., & Palmgren, M. G. (1998). Evolution of substrate specificities in the P-type ATPase superfamily. *J Mol Evol, 46*(1), 84-101.

Baldridge, R. D., & Graham, T. R. (2012) Identification of residues defining phospholipid flippase substrate specificity of type IV P-type ATPases. *Proc Natl Acad Sci U S A, 109*(6), E290-298.

Baldridge, R. D., & Graham, T. R. (2013) Two-gate mechanism for phospholipid selection and transport by type IV P-type ATPases. *Proc Natl Acad Sci U S A, 110*(5), E358-367.

Baldridge, R. D., Xu, P., & Graham, T. R. (2013). Type IV P-type ATPases distinguish mono- versus diacyl phosphatidylserine using a cytofacial exit gate in the membrane domain. *J Biol Chem, 288*(27), 19516-19527.

Balhadere, P. V., & Talbot, N. J. (2001). PDE1 encodes a P-type ATPase involved in appressorium-mediated plant infection by the rice blast fungus Magnaporthe grisea. *Plant Cell, 13*(9), 1987-2004.

Beck, R., Prinz, S., Diestelkotter-Bachert, P., Rohling, S., Adolf, F., Hoehner, K., . . . Wieland, F. (2011). Coatomer and dimeric ADP ribosylation factor 1 promote distinct steps in membrane scission. *J Cell Biol, 194*(5), 765-777.

Beck, R., Sun, Z., Adolf, F., Rutz, C., Bassler, J., Wild, K., . . . Wieland, F. (2008). Membrane curvature induced by Arf1-GTP is essential for vesicle formation. *Proc Natl Acad Sci U S A, 105*(33), 11731-11736.

Bonifacino, J. S., & Glick, B. S. (2004). The mechanisms of vesicle budding and fusion. *Cell, 116*(2), 153-166.

Bryde, S., Hennrich, H., Verhulst, P. M., Devaux, P. F., Lenoir, G., & Holthuis, J. C. (2010). CDC50 proteins are critical components of the human class-1 P4-ATPase transport machinery. *J Biol Chem, 285*(52), 40562-40572.

Bull, L. N., van Eijk, M. J., Pawlikowska, L., DeYoung, J. A., Juijn, J. A., Liao, M., . . . Freimer, N. B. (1998). A gene encoding a P-type ATPase mutated in two forms of hereditary cholestasis. *Nat Genet, 18*(3), 219-224.

Cacciagli, P., Haddad, M. R., Mignon-Ravix, C., El-Waly, B., Moncla, A., Missirian, C., . . . Villard, L. (2010). Disruption of the ATP8A2 gene in a patient with a t(10;13) de novo balanced translocation and a severe neurological phenotype. *Eur J Hum Genet, 18*(12), 1360-1363.

Carafoli, E. (1994). Biogenesis: plasma membrane calcium ATPase: 15 years of work on the purified enzyme. *FASEB J, 8*(13), 993-1002.

Caroni, P., & Carafoli, E. (1981). Regulation of Ca2+-pumping ATPase of heart sarcolemma by a phosphorylation-dephosphorylation Process. *J Biol Chem, 256*(18), 9371-9373.

Carter, S. G., & Karl, D. W. (1982). Inorganic phosphate assay with malachite green: an improvement and evaluation. *J Biochem Biophys Methods, 7*(1), 7-13.

Castoldi, E., Collins, P. W., Williamson, P. L., & Bevers, E. M. (2011). Compound heterozygosity for 2 novel TMEM16F mutations in a patient with Scott syndrome. *Blood, 117*(16), 4399-4400.

Catty, P., de Kerchove d'Exaerde, A., & Goffeau, A. (1997). The complete inventory of the yeast Saccharomyces cerevisiae P-type transport ATPases. *FEBS Lett, 409*(3), 325-332.

Chantalat, S., Park, S. K., Hua, Z., Liu, K., Gobin, R., Peyroche, A., . . . Jackson, C. L. (2004). The Arf activator Gea2p and the P-type ATPase Drs2p interact at the Golgi in Saccharomyces cerevisiae. *J Cell Sci, 117*(Pt 5), 711-722.

Charnock, J. S., & Post, R. L. (1963). Studies of the Mechanism of Cation Transport. I. The Preparation and Properties of a Cation-Stimulated Adenosine-Triphosphatase from Guinea Pig Kidney Cortex. *Aust J Exp Biol Med Sci, 41*, 547-560.

Chen, B., Jiang, Y., Zeng, S., Yan, J., Li, X., Zhang, Y., . . . Wang, X. (2010). Endocytic sorting and recycling require membrane phosphatidylserine asymmetry maintained by TAT-1/CHAT-1. *PLoS Genet, 6*(12), e1001235.

Chen, C. Y., & Graham, T. R. (1998). An arf1Delta synthetic lethal screen identifies a new clathrin heavy chain conditional allele that perturbs vacuolar protein transport in Saccharomyces cerevisiae. *Genetics, 150*(2), 577-589.

Chen, C. Y., Ingram, M. F., Rosal, P. H., & Graham, T. R. (1999). Role for Drs2p, a P-type ATPase and potential aminophospholipid translocase, in yeast late Golgi function. *J Cell Biol, 147*(6), 1223-1236.

Chen, S., Wang, J., Muthusamy, B. P., Liu, K., Zare, S., Andersen, R. J., & Graham, T. R. (2006). Roles for the Drs2p-Cdc50p complex in protein transport and phosphatidylserine asymmetry of the yeast plasma membrane. *Traffic, 7*(11), 1503-1517.

Chen, S. H., Shah, A. H., & Segev, N. (2011). Ypt31/32 GTPases and their F-Box effector Rcy1 regulate ubiquitination of recycling proteins. *Cell Logist, 1*(1), 21-31.

Coleman, J. A., Kwok, M. C., & Molday, R. S. (2009). Localization, purification, and functional reconstitution of the P4-ATPase Atp8a2, a phosphatidylserine flippase in photoreceptor disc membranes. *J Biol Chem, 284*(47), 32670-32679.

Coleman, J. A., & Molday, R. S. (2011). Critical role of the beta-subunit CDC50A in the stable expression, assembly, subcellular localization, and lipid transport activity of the P4-ATPase ATP8A2. *J Biol Chem, 286*(19), 17205-17216.

Coleman, J. A., Vestergaard, A. L., Molday, R. S., Vilsen, B., & Andersen, J. P. (2012). Critical role of a transmembrane lysine in aminophospholipid transport by mammalian photoreceptor P4-ATPase ATP8A2. *Proc Natl Acad Sci U S A, 109*(5), 1449-1454.

Cornelius, F., Mahmmoud, Y. A., Meischke, L., & Cramb, G. (2005). Functional significance of the shark Na,K-ATPase N-terminal domain. Is the structurally variable N-Terminus involved in tissue-specific regulation by FXYD proteins? *Biochemistry, 44*(39), 13051-13062.

Criado, M., & Keller, B. U. (1987). A membrane fusion strategy for single-channel recordings of membranes usually non-accessible to patch-clamp pipette electrodes. *FEBS Lett, 224*(1), 172-176.

Daleke, D. L. (2003). Regulation of transbilayer plasma membrane phospholipid asymmetry. *J Lipid Res, 44*(2), 233-242.

Daleke, D. L., & Huestis, W. H. (1985). Incorporation and translocation of aminophospholipids in human erythrocytes. *Biochemistry, 24*(20), 5406-5416.

Darland-Ransom, M., Wang, X., Sun, C. L., Mapes, J., Gengyo-Ando, K., Mitani, S., & Xue, D. (2008). Role of C. elegans TAT-1 protein in maintaining plasma membrane phosphatidylserine asymmetry. *Science, 320*(5875), 528-531.

Dean, M., & Annilo, T. (2005). Evolution of the ATP-binding cassette (ABC) transporter superfamily in vertebrates. *Annu Rev Genomics Hum Genet, 6*, 123-142.

Deloche, O., de la Cruz, J., Kressler, D., Doere, M., & Linder, P. (2004). A membrane transport defect leads to a rapid attenuation of translation initiation in Saccharomyces cerevisiae. *Mol Cell, 13*(3), 357-366.

Devaux, P. F. (1992). Protein involvement in transmembrane lipid asymmetry. *Annu Rev Biophys Biomol Struct, 21*, 417-439.

Dhar, M., Webb, L. S., Smith, L., Hauser, L., Johnson, D., & West, D. B. (2000). A novel ATPase on mouse chromosome 7 is a candidate gene for increased body fat. *Physiol Genomics, 4*(1), 93-100.

Dhar, M. S., Sommardahl, C. S., Kirkland, T., Nelson, S., Donnell, R., Johnson, D. K., & Castellani, L. W. (2004). Mice heterozygous for Atp10c, a putative amphipath, represent a novel model of obesity and type 2 diabetes. *J Nutr, 134*(4), 799-805.

Ding, J., Wu, Z., Crider, B. P., Ma, Y., Li, X., Slaughter, C., . . . Xie, X. S. (2000). Identification and functional expression of four isoforms of ATPase II, the putative aminophospholipid translocase. Effect of isoform variation on the ATPase activity and phospholipid specificity. *J Biol Chem, 275*(30), 23378-23386.

Doerrler, W. T., & Raetz, C. R. (2002). ATPase activity of the MsbA lipid flippase of Escherichia coli. *J Biol Chem, 277*(39), 36697-36705.

Dolis, D., Moreau, C., Zachowski, A., & Devaux, P. F. (1997). Aminophospholipid translocase and proteins involved in transmembrane phospholipid traffic. *Biophys Chem, 68*(1-3), 221-231.

Dong, J., Yang, G., & McHaourab, H. S. (2005). Structural basis of energy transduction in the transport cycle of MsbA. *Science, 308*(5724), 1023-1028.

Eastman, S. J., Hope, M. J., & Cullis, P. R. (1991). Transbilayer transport of phosphatidic acid in response to transmembrane pH gradients. *Biochemistry, 30*(7), 1740-1745.

Ekberg, K., Palmgren, M. G., Veierskov, B., & Buch-Pedersen, M. J. (2010). A novel mechanism of P-type ATPase autoinhibition involving both termini of the protein. *J Biol Chem, 285*(10), 7344-7350.

Emoto, K., Kobayashi, T., Yamaji, A., Aizawa, H., Yahara, I., Inoue, K., & Umeda, M. (1996). Redistribution of phosphatidylethanolamine at the cleavage furrow of dividing cells during cytokinesis. *Proc Natl Acad Sci U S A, 93*(23), 12867-12872.

Farge, E., & Devaux, P. F. (1992). Shape changes of giant liposomes induced by an asymmetric transmembrane distribution of phospholipids. *Biophys J, 61*(2), 347-357.

Flamant, S., Pescher, P., Lemercier, B., Clement-Ziza, M., Kepes, F., Fellous, M., . . . Besmond, C. (2003). Characterization of a putative type IV aminophospholipid transporter P-type ATPase. *Mamm Genome, 14*(1), 21-30.

Folmer, D. E., Elferink, R. P., & Paulusma, C. C. (2009). P4 ATPases - lipid flippases and their role in disease. *Biochim Biophys Acta, 1791*(7), 628-635.

Ford, M. G., Mills, I. G., Peter, B. J., Vallis, Y., Praefcke, G. J., Evans, P. R., & McMahon, H. T. (2002). Curvature of clathrin-coated pits driven by epsin. *Nature, 419*(6905), 361-366.

Fuglsang, A. T., Visconti, S., Drumm, K., Jahn, T., Stensballe, A., Mattei, B., . . . Palmgren, M. G. (1999). Binding of 14-3-3 protein to the plasma membrane H(+)-ATPase AHA2 involves the three C-terminal residues Tyr(946)-Thr-Val and requires phosphorylation of Thr(947). *J Biol Chem, 274*(51), 36774-36780.

Furuta, N., Fujimura-Kamada, K., Saito, K., Yamamoto, T., & Tanaka, K. (2007). Endocytic recycling in yeast is regulated by putative phospholipid translocases and the Ypt31p/32p-Rcy1p pathway. *Mol Biol Cell, 18*(1), 295-312.

Galan, J. M., Wiederkehr, A., Seol, J. H., Haguenauer-Tsapis, R., Deshaies, R. J., Riezman, H., & Peter, M. (2001). Skp1p and the F-box protein Rcy1p form a non-SCF complex involved in recycling of the SNARE Snc1p in yeast. *Mol Cell Biol, 21*(9), 3105-3117.

Gall, W. E., Geething, N. C., Hua, Z., Ingram, M. F., Liu, K., Chen, S. I., & Graham, T. R. (2002). Drs2p-dependent formation of exocytic clathrin-coated vesicles in vivo. *Curr Biol, 12*(18), 1623-1627.

Gall, W. E., Higginbotham, M. A., Chen, C., Ingram, M. F., Cyr, D. M., & Graham, T. R. (2000). The auxilin-like phosphoprotein Swa2p is required for clathrin function in yeast. *Curr Biol, 10*(21), 1349-1358.

Geering, K. (2001). The functional role of beta subunits in oligomeric P-type ATPases. *J Bioenerg Biomembr, 33*(5), 425-438.

Girard, P., Pecreaux, J., Lenoir, G., Falson, P., Rigaud, J. L., & Bassereau, P. (2004). A new method for the reconstitution of membrane proteins into giant unilamellar vesicles. *Biophys J, 87*(1), 419-429.

Gomes, E., Jakobsen, M. K., Axelsen, K. B., Geisler, M., & Palmgren, M. G. (2000). Chilling tolerance in Arabidopsis involves ALA1, a member of a new family of putative aminophospholipid translocases. *Plant Cell, 12*(12), 2441-2454.

Gourdon, P., Liu, X. Y., Skjorringe, T., Morth, J. P., Moller, L. B., Pedersen, B. P., & Nissen, P. (2011). Crystal structure of a copper-transporting PIB-type ATPase. *Nature, 475*(7354), 59-64.

Graham, T. R. (2004). Flippases and vesicle-mediated protein transport. *Trends Cell Biol, 14*(12), 670-677.

Graham, T. R., & Kozlov, M. M. (2010). Interplay of proteins and lipids in generating membrane curvature. *Curr Opin Cell Biol*. doi: S0955-0674(10)00065-7 [pii] 10.1016/j.ceb.2010.05.002

Harsay, E., & Bretscher, A. (1995). Parallel secretory pathways to the cell surface in yeast. *J Cell Biol, 131*(2), 297-310.

Hettema, E. H., Lewis, M. J., Black, M. W., & Pelham, H. R. (2003). Retromer and the sorting nexins Snx4/41/42 mediate distinct retrieval pathways from yeast endosomes. *Embo J, 22*(3), 548-557.

Hicks, A. A., Pramstaller, P. P., Johansson, A., Vitart, V., Rudan, I., Ugocsai, P., . . . Campbell, H. (2009). Genetic determinants of circulating sphingolipid concentrations in European populations. *PLoS Genet, 5*(10), e1000672.

Hinrichsen, L., Meyerholz, A., Groos, S., & Ungewickell, E. J. (2006). Bending a membrane: how clathrin affects budding. *Proc Natl Acad Sci U S A, 103*(23), 8715-8720.

Hua, Z., Fatheddin, P., & Graham, T. R. (2002). An essential subfamily of Drs2p-related P-type ATPases is required for protein trafficking between Golgi complex and endosomal/vacuolar system. *Mol Biol Cell, 13*(9), 3162-3177.

Hua, Z., & Graham, T. R. (2003). Requirement for neo1p in retrograde transport from the Golgi complex to the endoplasmic reticulum. *Mol Biol Cell, 14*(12), 4971-4983.

Hwang, I., Harper, J. F., Liang, F., & Sze, H. (2000). Calmodulin activation of an endoplasmic reticulum-located calcium pump involves an interaction with the N-terminal autoinhibitory domain. *Plant Physiol, 122*(1), 157-168.

Itoh, T., & De Camilli, P. (2006). BAR, F-BAR (EFC) and ENTH/ANTH domains in the regulation of membrane-cytosol interfaces and membrane curvature. *Biochim Biophys Acta, 1761*(8), 897-912.

Jacquot, A., Montigny, C., Hennrich, H., Barry, R., le Maire, M., Jaxel, C., . . . Lenoir, G. (2012). Phosphatidylserine stimulation of Drs2p.Cdc50p lipid translocase dephosphorylation is controlled by phosphatidylinositol-4-phosphate. *J Biol Chem, 287*(16), 13249-13261.

James, P., Maeda, M., Fischer, R., Verma, A. K., Krebs, J., Penniston, J. T., & Carafoli, E. (1988). Identification and primary structure of a calmodulin binding domain of the Ca2+ pump of human erythrocytes. *J Biol Chem, 263*(6), 2905-2910.

James, P. H., Pruschy, M., Vorherr, T. E., Penniston, J. T., & Carafoli, E. (1989). Primary structure of the cAMP-dependent phosphorylation site of the plasma membrane calcium pump. *Biochemistry, 28*(10), 4253-4258.

Juliano, R. L., & Ling, V. (1976). A surface glycoprotein modulating drug permeability in Chinese hamster ovary cell mutants. *Biochim Biophys Acta, 455*(1), 152-162.

Kato, U., Inadome, H., Yamamoto, M., Emoto, K., Kobayashi, T., & Umeda, M. (2013). Role for phospholipid flippase complex of ATP8A1 and CDC50A proteins in cell migration. *J Biol Chem, 288*(7), 4922-4934.

Kinuta, M., Yamada, H., Abe, T., Watanabe, M., Li, S. A., Kamitani, A., . . . Takei, K. (2002). Phosphatidylinositol 4,5-bisphosphate stimulates vesicle formation from liposomes by brain cytosol. *Proc Natl Acad Sci U S A, 99*(5), 2842-2847.

Kirchhausen, T. (2000a). Clathrin. *Annu Rev Biochem, 69*, 699-727.

Kirchhausen, T. (2000b). Three ways to make a vesicle. *Nat Rev Mol Cell Biol, 1*(3), 187-198.

Kirchhausen, T., & Harrison, S. C. (1981). Protein organization in clathrin trimers. *Cell, 23*(3), 755-761.

Kishimoto, T., Yamamoto, T., & Tanaka, K. (2005). Defects in structural integrity of ergosterol and the Cdc50p-Drs2p putative phospholipid translocase cause accumulation of endocytic membranes, onto which actin patches are assembled in yeast. *Mol Biol Cell, 16*(12), 5592-5609.

Kornberg, R. D., & McConnell, H. M. (1971). Inside-outside transitions of phospholipids in vesicle membranes. *Biochemistry, 10*(7), 1111-1120.

Kuhlbrandt, W. (2004). Biology, structure and mechanism of P-type ATPases. *Nat Rev Mol Cell Biol, 5*(4), 282-295.

Kus, B. M., Caldon, C. E., Andorn-Broza, R., & Edwards, A. M. (2004). Functional interaction of 13 yeast SCF complexes with a set of yeast E2 enzymes in vitro. *Proteins, 54*(3), 455-467.

Levano, K., Punia, V., Raghunath, M., Debata, P. R., Curcio, G. M., Mogha, A., . . . Banerjee, P. (2012). Atp8a1 deficiency is associated with phosphatidylserine externalization in hippocampus and delayed hippocampus-dependent learning. *J Neurochem, 120*(2), 302-313.

Lewis, M. J., Nichols, B. J., Prescianotto-Baschong, C., Riezman, H., & Pelham, H. R. (2000). Specific retrieval of the exocytic SNARE Snc1p from early yeast endosomes. *Mol Biol Cell, 11*(1), 23-38.

Li, Y., Moir, R. D., Sethy-Coraci, I. K., Warner, J. R., & Willis, I. M. (2000). Repression of ribosome and tRNA synthesis in secretion-defective cells is signaled by a novel branch of the cell integrity pathway. *Mol Cell Biol, 20*(11), 3843-3851.

Liu, K., Hua, Z., Nepute, J. A., & Graham, T. R. (2007). Yeast P4-ATPases Drs2p and Dnf1p are essential cargos of the NPFXD/Sla1p endocytic pathway. *Mol Biol Cell, 18*(2), 487-500.

Liu, K., Surendhran, K., Nothwehr, S. F., & Graham, T. R. (2008). P4-ATPase requirement for AP-1/clathrin function in protein transport from the trans-Golgi network and early endosomes. *Mol Biol Cell, 19*(8), 3526-3535.

Lopez-Marques, R. L., Poulsen, L. R., Hanisch, S., Meffert, K., Buch-Pedersen, M. J., Jakobsen, M. K., . . . Palmgren, M. G. (2010). Intracellular targeting signals and lipid specificity determinants of the ALA/ALIS P4-ATPase complex reside in the catalytic ALA alpha-subunit. *Mol Biol Cell, 21*(5), 791-801.

Lyssenko, N. N., Miteva, Y., Gilroy, S., Hanna-Rose, W., & Schlegel, R. A. (2008). An unexpectedly high degree of specialization and a widespread involvement in sterol

metabolism among the C. elegans putative aminophospholipid translocases. *BMC Dev Biol, 8*, 96.

Maeda, K., Anand, K., Chiapparino, A., Kumar, A., Poletto, M., Kaksonen, M., & Gavin, A. C. (2013). Interactome map uncovers phosphatidylserine transport by oxysterol-binding proteins. *Nature, 501*(7466), 257-261.

Malvezzi, M., Chalat, M., Janjusevic, R., Picollo, A., Terashima, H., Menon, A. K., & Accardi, A. (2013). Ca2+-dependent phospholipid scrambling by a reconstituted TMEM16 ion channel. *Nat Commun, 4*, 2367.

Manley, S., & Gordon, V. D. (2008). Making giant unilamellar vesicles via hydration of a lipid film. *Curr Protoc Cell Biol, Chapter 24*, Unit 24 23.

Marx, U., Polakowski, T., Pomorski, T., Lang, C., Nelson, H., Nelson, N., & Herrmann, A. (1999). Rapid transbilayer movement of fluorescent phospholipid analogues in the plasma membrane of endocytosis-deficient yeast cells does not require the Drs2 protein. *Eur J Biochem, 263*(1), 254-263.

Mathivet, L., Cribier, S., & Devaux, P. F. (1996). Shape change and physical properties of giant phospholipid vesicles prepared in the presence of an AC electric field. *Biophys J, 70*(3), 1112-1121.

Matsuoka, K., Orci, L., Amherdt, M., Bednarek, S. Y., Hamamoto, S., Schekman, R., & Yeung, T. (1998). COPII-coated vesicle formation reconstituted with purified coat proteins and chemically defined liposomes. *Cell, 93*(2), 263-275.

Maudoux, O., Batoko, H., Oecking, C., Gevaert, K., Vandekerckhove, J., Boutry, M., & Morsomme, P. (2000). A plant plasma membrane H+-ATPase expressed in yeast is activated by phosphorylation at its penultimate residue and binding of 14-3-3 regulatory proteins in the absence of fusicoccin. *J Biol Chem, 275*(23), 17762-17770.

McIntyre, J. C., & Sleight, R. G. (1991). Fluorescence assay for phospholipid membrane asymmetry. *Biochemistry, 30*(51), 11819-11827.

Menon, A. K. (1995). Flippases. *Trends Cell Biol, 5*(9), 355-360.

Mercer, J., & Helenius, A. (2008). Vaccinia virus uses macropinocytosis and apoptotic mimicry to enter host cells. *Science, 320*(5875), 531-535.

Moriyama, Y., & Nelson, N. (1988). Purification and properties of a vanadate- and N-ethylmaleimide-sensitive ATPase from chromaffin granule membranes. *J Biol Chem, 263*(17), 8521-8527.

Morth, J. P., Pedersen, B. P., Toustrup-Jensen, M. S., Sorensen, T. L., Petersen, J., Andersen, J. P., . . . Nissen, P. (2007). Crystal structure of the sodium-potassium pump. *Nature, 450*(7172), 1043-1049.

Muthusamy, B. P., Natarajan, P., Zhou, X., & Graham, T. R. (2009). Linking phospholipid flippases to vesicle-mediated protein transport. *Biochim Biophys Acta, 1791*(7), 612-619.

Muthusamy, B. P., Raychaudhuri, S., Natarajan, P., Abe, F., Liu, K., Prinz, W. A., & Graham, T. R. (2009). Control of protein and sterol trafficking by antagonistic activities of a type IV P-type ATPase and oxysterol binding protein homologue. *Mol Biol Cell, 20*(12), 2920-2931.

Nakano, K., Yamamoto, T., Kishimoto, T., Noji, T., & Tanaka, K. (2008). Protein kinases Fpk1p and Fpk2p are novel regulators of phospholipid asymmetry. *Mol Biol Cell, 19*(4), 1783-1797.

Natarajan, P., & Graham, T. R. (2006). Measuring translocation of fluorescent lipid derivatives across yeast Golgi membranes. *Methods, 39*(2), 163-168.

Natarajan, P., Liu, K., Patil, D. V., Sciorra, V. A., Jackson, C. L., & Graham, T. R. (2009). Regulation of a Golgi flippase by phosphoinositides and an ArfGEF. *Nat Cell Biol, 11*(12), 1421-1426.

Natarajan, P., Wang, J., Hua, Z., & Graham, T. R. (2004). Drs2p-coupled aminophospholipid translocase activity in yeast Golgi membranes and relationship to in vivo function. *Proc Natl Acad Sci U S A, 101*(29), 10614-10619.

Nossal, R. (2001). Energetics of clathrin basket assembly. *Traffic, 2*(2), 138-147.

Ohi, M., Li, Y., Cheng, Y., & Walz, T. (2004). Negative Staining and Image Classification - Powerful Tools in Modern Electron Microscopy. *Biol Proced Online, 6*, 23-34.

Olsson, A., Svennelid, F., Ek, B., Sommarin, M., & Larsson, C. (1998). A phosphothreonine residue at the C-terminal end of the plasma membrane H+-ATPase is protected by fusicoccin-induced 14-3-3 binding. *Plant Physiol, 118*(2), 551-555.

Palmgren, M. G. (2001). PLANT PLASMA MEMBRANE H+-ATPases: Powerhouses for Nutrient Uptake. *Annu Rev Plant Physiol Plant Mol Biol, 52*, 817-845.

Palmgren, M. G., Larsson, C., & Sommarin, M. (1990). Proteolytic activation of the plant plasma membrane H(+)-ATPase by removal of a terminal segment. *J Biol Chem, 265*(23), 13423-13426.

Palmgren, M. G., Sommarin, M., Serrano, R., & Larsson, C. (1991). Identification of an autoinhibitory domain in the C-terminal region of the plant plasma membrane H(+)-ATPase. *J Biol Chem, 266*(30), 20470-20475.

Papadopulos, A., Vehring, S., Lopez-Montero, I., Kutschenko, L., Stockl, M., Devaux, P. F., . . . Herrmann, A. (2007). Flippase activity detected with unlabeled lipids by shape changes of giant unilamellar vesicles. *J Biol Chem, 282*(21), 15559-15568.

Paterson, J. K., Renkema, K., Burden, L., Halleck, M. S., Schlegel, R. A., Williamson, P., & Daleke, D. L. (2006). Lipid specific activation of the murine P4-ATPase Atp8a1 (ATPase II). *Biochemistry, 45*(16), 5367-5376.

Paulusma, C. C., Folmer, D. E., Ho-Mok, K. S., de Waart, D. R., Hilarius, P. M., Verhoeven, A. J., & Oude Elferink, R. P. (2008). ATP8B1 requires an accessory protein for endoplasmic reticulum exit and plasma membrane lipid flippase activity. *Hepatology, 47*(1), 268-278.

Pedersen, B. P., Buch-Pedersen, M. J., Morth, J. P., Palmgren, M. G., & Nissen, P. (2007). Crystal structure of the plasma membrane proton pump. *Nature, 450*(7172), 1111-1114.

Perez-Victoria, F. J., Sanchez-Canete, M. P., Castanys, S., & Gamarro, F. (2006). Phospholipid translocation and miltefosine potency require both L. donovani miltefosine transporter and the new protein LdRos3 in Leishmania parasites. *J Biol Chem, 281*(33), 23766-23775.

Peyroche, A., Courbeyrette, R., Rambourg, A., & Jackson, C. L. (2001). The ARF exchange factors Gea1p and Gea2p regulate Golgi structure and function in yeast. *J Cell Sci, 114*(Pt 12), 2241-2253.

Peyroche, A., Paris, S., & Jackson, C. L. (1996). Nucleotide exchange on ARF mediated by yeast Gea1 protein. *Nature, 384*(6608), 479-481.

Piotrowski, M., Morsomme, P., Boutry, M., & Oecking, C. (1998). Complementation of the Saccharomyces cerevisiae plasma membrane H+-ATPase by a plant H+-ATPase generates a highly abundant fusicoccin binding site. *J Biol Chem, 273*(45), 30018-30023.

Pomorski, T., Holthuis, J. C., Herrmann, A., & van Meer, G. (2004). Tracking down lipid flippases and their biological functions. *J Cell Sci, 117*(Pt 6), 805-813.

Pomorski, T., Lombardi, R., Riezman, H., Devaux, P. F., van Meer, G., & Holthuis, J. C. (2003). Drs2p-related P-type ATPases Dnf1p and Dnf2p are required for phospholipid translocation across the yeast plasma membrane and serve a role in endocytosis. *Mol Biol Cell, 14*(3), 1240-1254.

Portillo, F. (2000). Regulation of plasma membrane H(+)-ATPase in fungi and plants. *Biochim Biophys Acta, 1469*(1), 31-42.

Portillo, F., de Larrinoa, I. F., & Serrano, R. (1989). Deletion analysis of yeast plasma membrane H+-ATPase and identification of a regulatory domain at the carboxyl-terminus. *FEBS Lett, 247*(2), 381-385.

Post, R. L., Hegyvary, C., & Kume, S. (1972). Activation by adenosine triphosphate in the phosphorylation kinetics of sodium and potassium ion transport adenosine triphosphatase. *J Biol Chem, 247*(20), 6530-6540.

Post, R. L., & Jolly, P. C. (1957). The linkage of sodium, potassium, and ammonium active transport across the human erythrocyte membrane. *Biochim Biophys Acta, 25*(1), 118-128.

Post, R. L., & Sen, A. K. (1965). An Enzymatic Mechanism of Active Sodium and Potassium Transport. *J Histochem Cytochem, 13*, 105-112.

Post, R. L., Sen, A. K., & Rosenthal, A. S. (1965). A Phosphorylated Intermediate in Adenosine Triphosphate-Dependent Sodium and Potassium Transport across Kidney Membranes. *J Biol Chem, 240*, 1437-1445.

Poulsen, L. R., Lopez-Marques, R. L., McDowell, S. C., Okkeri, J., Licht, D., Schulz, A., . . . Palmgren, M. G. (2008). The Arabidopsis P4-ATPase ALA3 localizes to the golgi and requires a beta-subunit to function in lipid translocation and secretory vesicle formation. *Plant Cell, 20*(3), 658-676.

Radji, M., Kim, J. M., Togan, T., Yoshikawa, H., & Shirahige, K. (2001). The cloning and characterization of the CDC50 gene family in Saccharomyces cerevisiae. *Yeast, 18*(3), 195-205.

Rasi-Caldogno, F., Carnelli, A., & De Michelis, M. I. (1992). Plasma Membrane Ca-ATPase of Radish Seedlings : II. Regulation by Calmodulin. *Plant Physiol, 98*(3), 1202-1206.

Rasi-Caldogno, F., Carnelli, A., & De Michelis, M. I. (1993). Controlled Proteolysis Activates the Plasma Membrane Ca2+ Pump of Higher Plants (A Comparison with the Effect of Calmodulin in Plasma Membrane from Radish Seedlings). *Plant Physiol, 103*(2), 385-390.

Rasi-Caldogno, F., Carnelli, A., & De Michelis, M. I. (1995). Identification of the Plasma Membrane Ca2+-ATPase and of Its Autoinhibitory Domain. *Plant Physiol, 108*(1), 105-113.

Ren, G., Vajjhala, P., Lee, J. S., Winsor, B., & Munn, A. L. (2006). The BAR domain proteins: molding membranes in fission, fusion, and phagy. *Microbiol Mol Biol Rev, 70*(1), 37-120.

Riekhof, W. R., & Voelker, D. R. (2006). Uptake and utilization of lyso-phosphatidylethanolamine by Saccharomyces cerevisiae. *J Biol Chem, 281*(48), 36588-36596.

Ripmaster, T. L., Vaughn, G. P., & Woolford, J. L., Jr. (1993). DRS1 to DRS7, novel genes required for ribosome assembly and function in Saccharomyces cerevisiae. *Mol Cell Biol, 13*(12), 7901-7912.

Robinson, M., Poon, P. P., Schindler, C., Murray, L. E., Kama, R., Gabriely, G., . . . Gerst, J. E. (2006). The Gcs1 Arf-GAP mediates Snc1,2 v-SNARE retrieval to the Golgi in yeast. *Mol Biol Cell, 17*(4), 1845-1858.

Roelants, F. M., Baltz, A. G., Trott, A. E., Fereres, S., & Thorner, J. (2010). A protein kinase network regulates the function of aminophospholipid flippases. *Proc Natl Acad Sci U S A, 107*(1), 34-39.

Ruaud, A. F., Nilsson, L., Richard, F., Larsen, M. K., Bessereau, J. L., & Tuck, S. (2009). The C. elegans P4-ATPase TAT-1 regulates lysosome biogenesis and endocytosis. *Traffic, 10*(1), 88-100.

Saito, K., Fujimura-Kamada, K., Furuta, N., Kato, U., Umeda, M., & Tanaka, K. (2004). Cdc50p, a protein required for polarized growth, associates with the Drs2p P-type ATPase implicated in phospholipid translocation in Saccharomyces cerevisiae. *Mol Biol Cell, 15*(7), 3418-3432.

Saito, K., Fujimura-Kamada, K., Hanamatsu, H., Kato, U., Umeda, M., Kozminski, K. G., & Tanaka, K. (2007). Transbilayer phospholipid flipping regulates Cdc42p signaling during polarized cell growth via Rga GTPase-activating proteins. *Dev Cell, 13*(5), 743-751.

Sakane, H., Yamamoto, T., & Tanaka, K. (2006). The functional relationship between the Cdc50p-Drs2p putative aminophospholipid translocase and the Arf GAP Gcs1p in vesicle formation in the retrieval pathway from yeast early endosomes to the TGN. *Cell Struct Funct, 31*(2), 87-108.

Sato, K., Sato, M., & Nakano, A. (2001). Rer1p, a retrieval receptor for endoplasmic reticulum membrane proteins, is dynamically localized to the Golgi apparatus by coatomer. *J Cell Biol, 152*(5), 935-944.

Sciorra, V. A., Audhya, A., Parsons, A. B., Segev, N., Boone, C., & Emr, S. D. (2005). Synthetic genetic array analysis of the PtdIns 4-kinase Pik1p identifies components in a Golgi-specific Ypt31/rab-GTPase signaling pathway. *Mol Biol Cell, 16*(2), 776-793.

Sebastian, T. T., Baldridge, R. D., Xu, P., & Graham, T. R. (2012). Phospholipid flippases: building asymmetric membranes and transport vesicles. *Biochim Biophys Acta, 1821*(8), 1068-1077.

Seigneuret, M., & Devaux, P. F. (1984). ATP-dependent asymmetric distribution of spin-labeled phospholipids in the erythrocyte membrane: relation to shape changes. *Proc Natl Acad Sci U S A, 81*(12), 3751-3755.

Sheetz, M. P., & Singer, S. J. (1974). Biological membranes as bilayer couples. A molecular mechanism of drug-erythrocyte interactions. *Proc Natl Acad Sci U S A, 71*(11), 4457-4461.

Sherman, F. (1991). Getting started with yeast. *Methods Enzymol, 194*, 3-21.

Siegmund, A., Grant, A., Angeletti, C., Malone, L., Nichols, J. W., & Rudolph, H. K. (1998). Loss of Drs2p does not abolish transfer of fluorescence-labeled phospholipids across the plasma membrane of Saccharomyces cerevisiae. *J Biol Chem, 273*(51), 34399-34405.

Siggs, O. M., Arnold, C. N., Huber, C., Pirie, E., Xia, Y., Lin, P., . . . Beutler, B. (2011). The P4-type ATPase ATP11C is essential for B lymphopoiesis in adult bone marrow. *Nat Immunol, 12*(5), 434-440.

Singer-Kruger, B., Lasic, M., Burger, A. M., Hausser, A., Pipkorn, R., & Wang, Y. (2008). Yeast and human Ysl2p/hMon2 interact with Gga adaptors and mediate their subcellular distribution. *Embo J, 27*(10), 1423-1435.

Spang, A., Matsuoka, K., Hamamoto, S., Schekman, R., & Orci, L. (1998). Coatomer, Arf1p, and nucleotide are required to bud coat protein complex I-coated vesicles from large synthetic liposomes. *Proc Natl Acad Sci U S A, 95*(19), 11199-11204.

Stachowiak, J. C., Schmid, E. M., Ryan, C. J., Ann, H. S., Sasaki, D. Y., Sherman, M. B., . . . Hayden, C. C. (2012). Membrane bending by protein-protein crowding. *Nat Cell Biol, 14*(9), 944-949.

Stapelbroek, J. M., Peters, T. A., van Beurden, D. H., Curfs, J. H., Joosten, A., Beynon, A. J., . . . Houwen, R. H. (2009). ATP8B1 is essential for maintaining normal hearing. *Proc Natl Acad Sci U S A, 106*(24), 9709-9714.

Stevens, H. C., Malone, L., & Nichols, J. W. (2008). The Putative Aminophospholipid Translocases, DNF1 and DNF2, Are Not Required for 7-Nitrobenz-2-oxa-1,3-diazol-4-yl-phosphatidylserine Flip across the Plasma Membrane of Saccharomyces cerevisiae. *J Biol Chem, 283*(50), 35060-35069.

Suzuki, J., Fujii, T., Imao, T., Ishihara, K., Kuba, H., & Nagata, S. (2013). Calcium-dependent phospholipid scramblase activity of TMEM16 protein family members. *J Biol Chem, 288*(19), 13305-13316.

Suzuki, J., Umeda, M., Sims, P. J., & Nagata, S. (2010). Calcium-dependent phospholipid scrambling by TMEM16F. *Nature, 468*(7325), 834-838.

Sze, H., Liang, F., Hwang, I., Curran, A. C., & Harper, J. F. (2000). Diversity and regulation of plant Ca2+ pumps: insights from expression in yeast. *Annu Rev Plant Physiol Plant Mol Biol, 51*, 433-462.

Takahashi, Y., Fujimura-Kamada, K., Kondo, S., & Tanaka, K. (2011). Isolation and characterization of novel mutations in CDC50, the non-catalytic subunit of the Drs2p phospholipid flippase. *J Biochem, 149*(4), 423-432.

Takatsu, H., Baba, K., Shima, T., Umino, H., Kato, U., Umeda, M., . . . Shin, H. W. (2011). ATP9B, a P4-ATPase (a putative aminophospholipid translocase), localizes to the trans-Golgi network in a CDC50-independent manner. *J Biol Chem*. doi: 10.1074/jbc.M111.281006

Takei, K., Haucke, V., Slepnev, V., Farsad, K., Salazar, M., Chen, H., & De Camilli, P. (1998). Generation of coated intermediates of clathrin-mediated endocytosis on protein-free liposomes. *Cell, 94*(1), 131-141.

Tang, X., Halleck, M. S., Schlegel, R. A., & Williamson, P. (1996). A subfamily of P-type ATPases with aminophospholipid transporting activity. *Science, 272*(5267), 1495-1497.

Toyoshima, C. (2009). How Ca2+-ATPase pumps ions across the sarcoplasmic reticulum membrane. *Biochim Biophys Acta, 1793*(6), 941-946.

Toyoshima, C., & Mizutani, T. (2004). Crystal structure of the calcium pump with a bound ATP analogue. *Nature, 430*(6999), 529-535.

Toyoshima, C., Nakasako, M., Nomura, H., & Ogawa, H. (2000). Crystal structure of the calcium pump of sarcoplasmic reticulum at 2.6 A resolution. *Nature, 405*(6787), 647-655.

Toyoshima, C., & Nomura, H. (2002). Structural changes in the calcium pump accompanying the dissociation of calcium. *Nature, 418*(6898), 605-611.

Toyoshima, C., Nomura, H., & Tsuda, T. (2004). Lumenal gating mechanism revealed in calcium pump crystal structures with phosphate analogues. *Nature, 432*(7015), 361-368.

Tsai, P. C., Hsu, J. W., Liu, Y. W., Chen, K. Y., & Lee, F. J. (2013) Arl1p regulates spatial membrane organization at the trans-Golgi network through interaction with Arf-GEF Gea2p and flippase Drs2p. *Proc Natl Acad Sci U S A, 110*(8), E668-677.

Ungewickell, E., & Branton, D. (1981). Assembly units of clathrin coats. *Nature, 289*(5796), 420-422.

Valdivia, R. H., Baggott, D., Chuang, J. S., & Schekman, R. W. (2002). The yeast clathrin adaptor protein complex 1 is required for the efficient retention of a subset of late Golgi membrane proteins. *Dev Cell, 2*(3), 283-294.

van der Velden, L. M., Wichers, C. G., van Breevoort, A. E., Coleman, J. A., Molday, R. S., Berger, R., . . . van de Graaf, S. F. (2010). Heteromeric interactions required for abundance and subcellular localization of human CDC50 proteins and class 1 P4-ATPases. *J Biol Chem, 285*(51), 40088-40096.

Verhulst, P. M., van der Velden, L. M., Oorschot, V., van Faassen, E. E., Klumperman, J., Houwen, R. H., . . . Klomp, L. W. (2010). A flippase-independent function of ATP8B1, the protein affected in familial intrahepatic cholestasis type 1, is required for apical protein expression and microvillus formation in polarized epithelial cells. *Hepatology, 51*(6), 2049-2060.

Vida, T. A., Graham, T. R., & Emr, S. D. (1990). In vitro reconstitution of intercompartmental protein transport to the yeast vacuole. *J Cell Biol, 111*(6 Pt 2), 2871-2884.

Wehman, A. M., Poggioli, C., Schweinsberg, P., Grant, B. D., & Nance, J. (2011). The P4-ATPase TAT-5 inhibits the budding of extracellular vesicles in C. elegans embryos. *Curr Biol, 21*(23), 1951-1959.

Wicky, S., Schwarz, H., & Singer-Kruger, B. (2004). Molecular interactions of yeast Neo1p, an essential member of the Drs2 family of aminophospholipid translocases, and its role in membrane trafficking within the endomembrane system. *Mol Cell Biol, 24*(17), 7402-7418.

Williamson, P., & Schlegel, R. A. (2002). Transbilayer phospholipid movement and the clearance of apoptotic cells. *Biochim Biophys Acta, 1585*(2-3), 53-63.

Xiao, J., Kim, L. S., & Graham, T. R. (2006). Dissection of Swa2p/auxilin domain requirements for cochaperoning Hsp70 clathrin-uncoating activity in vivo. *Mol Biol Cell, 17*(7), 3281-3290.

Xie, X. S., Stone, D. K., & Racker, E. (1989). Purification of a vanadate-sensitive ATPase from clathrin-coated vesicles of bovine brain. *J Biol Chem, 264*(3), 1710-1714.

Xu, P., Baldridge, R. D., Chi, R. J., Burd, C. G., & Graham, T. R. (2013). Phosphatidylserine flipping enhances membrane curvature and negative charge required for vesicular transport. *J Cell Biol, 202*(6), 875-886.

Xu, P., Okkeri, J., Hanisch, S., Hu, R. Y., Xu, Q., Pomorski, T. G., & Ding, X. Y. (2009). Identification of a novel mouse P4-ATPase family member highly expressed during spermatogenesis. *J Cell Sci, 122*(Pt 16), 2866-2876.

Xu, Q., Yang, G. Y., Liu, N., Xu, P., Chen, Y. L., Zhou, Z., . . . Ding, X. (2012). P4-ATPase ATP8A2 acts in synergy with CDC50A to enhance neurite outgrowth. *FEBS Lett, 586*(13), 1803-1812.

Yabas, M., Teh, C. E., Frankenreiter, S., Lal, D., Roots, C. M., Whittle, B., . . . Enders, A. (2011). ATP11C is critical for the internalization of phosphatidylserine and differentiation of B lymphocytes. *Nat Immunol, 12*(5), 441-449.

Zachowski, A. (1993). Phospholipids in animal eukaryotic membranes: transverse asymmetry and movement. *Biochem J, 294 (Pt 1)*, 1-14.

Zhang, X., & Oppenheimer, D. G. (2009). IRREGULAR TRICHOME BRANCH 2 (ITB2) encodes a putative aminophospholipid translocase that regulates trichome branch elongation in Arabidopsis. *Plant J, 60*(2), 195-206.

Zhou, X., & Graham, T. R. (2009). Reconstitution of phospholipid translocase activity with purified Drs2p, a type-IV P-type ATPase from budding yeast. *Proc Natl Acad Sci U S A, 106*(39), 16586-16591.

Zhou, X., **Sebastian, T. T.**, & Graham, T. R. (2013). Auto-inhibition of Drs2p, a yeast phospholipid flippase, by its carboxyl-terminal tail. *J Biol Chem, 288*(44), 31807-31815.

Zimmerman, M. L., & Daleke, D. L. (1993). Regulation of a candidate aminophospholipid-transporting ATPase by lipid. *Biochemistry, 32*(45), 12257-12263.

Zwaal, R. F., Comfurius, P., & Bevers, E. M. (2005). Surface exposure of phosphatidylserine in pathological cells. *Cell Mol Life Sci, 62*(9), 971-988.

Zwaal, R. F., Comfurius, P., & van Deenen, L. L. (1977). Membrane asymmetry and blood coagulation. *Nature, 268*(5618), 358-360.

Zwaal, R. F., & Schroit, A. J. (1997). Pathophysiologic implications of membrane phospholipid asymmetry in blood cells. *Blood, 89*(4), 1121-1132.